Enhancing blood circulation time and performance of nano-drug delivery systems using nanoparticles and hydrogels

Jakub Kruk, B.Sc.

Thesis for the degree of M.Sc. (Chemistry), University of Galway

Submitted November 2023

OLLSCOIL NA GAILLIMHE
UNIVERSITY OF GALWAY

Research performed at:

The School of Biological and Chemical Sciences

University of Galway, Galway

Supervisor: Dr. Andrea Erxleben.

Head of School: Prof. Olivier Thomas

Contents

Acknowledgements

I wish to sincerely thank the following people for their patience, time, help and contribution to this project, as their role in the project was essential.

Dr. Andrea Erxleben for giving me the opportunity to participate in this project and work with her research group.

Lamis Alaa for her advice, guidance and expertise, and her help with operating the Perkin Elmer Spectrum 400 FTIR machine and operating the X-ray crystallography software Oscail.

Nazanin Fereidouni for her advice and help with operating the Cary Varian 50 UV/Vis spectrometer.

Prof. Patrick McArdle for his help in understanding X-ray crystallography and operating the X-ray crystallography software Oscail.

David Cheung for helping me understand the mechanics of molecular modelling using the Spartan molecular animation software.

A special thanks to Research Laboratory 5's technical staff James Donohue, Muriel Voisin, and Eddie Myers, for helping me understand in how a laboratory safety audit is performed, and instructions on the preventive measures to undertake in case of an emergency. A special thanks also to Carolina Righetti Grizotto and Koey Yu for lending a helping hand in the drug release study of 4-nitrophenol from a PF-127 based hydrogel and plotting the test substance's calibration curve.

Last, but not least, I wish to thank my parents for their unwavering support over the course of the project.

Abstract

Mesoporous silica nanoparticles (MSNs) and hydrogels are some of the most sought-after methods of nano-drug delivery systems. Properties such as high biocompatibility, selectivity and loading capacity are among the many reasons as to the myriad of research performed using them as nano-drug delivery systems in addition to the increasing demand for more effective and safer treatments of cancer and cardiovascular disease. The aim of this project is to enhance blood circulation to improve the delivery of nano-drug systems, with the desired result being the development of more effective, ergonomic, and safer anti-cancer drugs replacing cisplatin as the standard chemotherapy treatment, with great emphasis on the carriers of the drugs; mesoporous silica nanoparticles (MSNs) and hydrogels. The MSNs, although synthesized, successfully aminofunctionalised and separated from their template (CTAB), and coated with gelatin, were only partially crosslinked with aldehyde groups, meaning that reliable pH-responsive surface linkers for targeting tumour cells were incomplete. Hydrogels were later synthesised as alternative drug delivery systems for anti-cancer drugs: chitosan was initially used as the primary polymer and β-glycerophosphate as the crosslinking agent, but were generally irreversible: once solidified at physiological temperature (37 °C), they did not reliquefy. They released drugs at quicker rates than allowed for sustained release. Pluronic F-127-based hydrogels were reversible, solidifying at physiological temperature and reliquefying at room temperature, but had a relatively short shelf life, as they decomposed in the presence of water after 3 days at physiological temperature.

1. Introduction

1.0. Relevance of Drug Delivery Systems

Drug delivery systems is one of the fastest growing fields in science, due to the amount of development it has undergone in recent years, with greater innovations predicted for the near

future. Despite the quickening progress with each coming year, many treatments of diseases have unacceptable side effects, which occur due to the drugs that interact in areas outside of their site of action[1]. Technologies of drug delivery have significantly improved patient compliance, lowering the risk of toxicity, and efficacy, while also enabling treatments with novel therapeutic agents if tailored to be compatible with both the human body and the agents. Earliest forms of controlled drug delivery came in the form Spansule technology in 1952, evolving into cellulose derivatives and cross-linked poly(acrylic acid polymers), and biodegradable poly(lactic-co-glycolic acid) (PGLA) and poly (lactic acid) (PLA)[2]. Two crucial parameters control the drug delivery systems:

- 1. The rate at which the drug is released upon reaching the site of action.
- 2. The durability of the drug carrier's casing.

Controlling the two parameters of drug release is a vital and extremely delicate balancing act: if the drug carrier is not durable enough, then it might not even reach its site of action and release the therapeutic agent prematurely, causing potentially harmful effects on the recipient's body. If the carrier is too durable, the therapeutic effect will not be delivered even if the drug reaches the site of action and will be excreted as waste instead.

There are two main types of drug delivery systems: rate-programmed, and activation modulated.

1. Rate-programmed: semisynthetic membranes encapsulating the drug. Composed of scaffolding of substances that are non-immunogenic, non-toxic, biocompatible, of low tensile strength, of high drug retention and can facilitate controlled release and drug delivery on both the micro and the nano scale. A good example of a rate-programmed drug delivery system are nanoparticles; the drug is loaded into a reservoir space, and the reservoir's surface is coated with a rate-programmed membrane, which can be purposely modified as a controlled-release barrier[3].

2. Activation modulated: Drug release from drug delivery systems can occur either due to internal or external stimuli. e.g. pH or temperature. Examples of such system include

magnetic nanoparticles loaded with therapeutic agents and guided by an externally-applied magnetic field to specific organs or tissues and to release their payload in that particular area[4]. The relevance of drug delivery systems comes from various reasons: apart from the rapid nature of their development, such systems offer safer and more effective alternatives to conventional chemotherapy, radiotherapy, and tumour surgery, which are still relevant but do not guarantee complete removal of cancer cells or absence of post-treatment side effects.

1.1 Drug delivery systems for anti-cancer drugs.

Cancer is currently one of the deadliest diseases in the world, accounting for 30% of deaths in Ireland[5] and 10 million people worldwide every year[6]. One of the most successful methods of anti-cancer treatments developed was chemotherapy. The concept of chemotherapy began in 1908, with Paul Ehrlich's rabbit model testing arsenic-based drugs as syphilis treatments. Ehrlich then experimented with alkylating agents and aniline dyes, though chances of success were slim. Up until the late 1960s, radiotherapy and surgeries were the dominant methods of cancer therapy. But, as previously mentioned, the two methods had two major drawbacks:

- The excision of cancer tumours did not guarantee complete removal of cancer cells, allowing some of them to remain in the patients' bodies and multiply again.
- Radiotherapy, while an effective killer of cancer cells, always risked collateral damage of healthy cells, resulting in the weakening of the patients' body and immune system.

Soon, the necessity for combination chemotherapy became clear due to more radical local treatments plateauing at around 33%. This was caused by the presence of heretofore unappreciated micro-metastases which enabled advanced stages of cancer. The chemotherapy agents were arsenicals, nitrogen mustard in lymphomas, antifolates, thiopurines, 5-fluorouracil and methotrexate. These chemicals, though revolutionary, lacked efficacy as cancer treatments due to:

- Very brief and incomplete remissions in nitrogen mustard treatment of non-Hodgkin's lymphoma

- Increased uptake and use of uracil by tumours to counter treatments.
- Insufficient molecular targeting: targeting was mainly focused on biochemical pathways[7].

Cisplatin was one of the most revolutionary developments in modern medicine: first synthesized in 1844 by Italian chemist Michele Peyrone, with its anti-cancerous properties discovered by Barnett Rosenberg[8]. It was tested in vivo in a mouse with a rapidly growing sarcoma, which it was found to attack. The drug, however is non-specific, which causes harmful side effects[9]. Despite the toxicity, the systems of the mice did not reject cisplatin at low doses: the sarcomas stopped growing and were rapidly destroyed. Six months later, the mice showed no signs of relapse, which further cemented the drug's anti-cancerous properties[10].

Cisplatin was first FDA-approved in 1978. However, toxicity at high doses and resistance to the drug occurring in some cancer patients, led to the discovery of new derivatives of the drug. Side effects of cisplatin include, but are not limited to:

- Damage to the Corti organs and stria vascularis.
- Thrombocytopenia, leukopenia, anaemia.
- Excess transaminases and bilirubin, hepatic failure.
- Sinus bradycardia, tachyarrhythmia, paroxysmal ventricular tachycardia[11].

Examples of these derivative compounds are carboplatin (FDA-approved in 1989), oxaliplatin (FDA-approved in 2002), which proved to be successful in cancers such as ovarian cancer (carboplatin) and colorectal cancer (oxaliplatin)[12]. The use cisplatin in drug delivery is described in a review by Pavan, et al,[13] as a novel treatment for lung carcinomas.

1.2 Drug delivery involving cisplatin

- **Lipoplatin**: Cisplatin can be encapsulated into liposomes using soy phosphatidyl-choline (SPC-3), methoxy-polyethylene glycol-distearoyl phosphatidylethanolamine (mPEG 2000-DSPE), dipalmitoyl phosphatidyl glycerol (DPPG), and cholesterol. Boulikas et al. formed reverse micelles of DPPG and cisplatin are formed under

tissue-particular conditions of ionic strength and pH and aided by ethanol. The DPPG-cisplatin reverse micelles would undergo conversion to liposomes by interacting with neutral lipids[14].

- **Micelles**: They consist of diblock, triblock copolymers or copolymers outfitted with hydrophilic or hydrophobic functional groups commonly used in cancer therapy. Examples are hybrid micelles containing cisplatin and tocopherol polyethylene glycol succinate (TPGS) mixed in a 2:1 ratio[15].
- **Mesoporous silica**: An example of such a drug delivery system by Zhang et al. involves mesoporous silica nanoparticles (MSNs) are ones into which chlorine6 photosensitizer was encapsulated. This was done for monitoring and facilitating anti-cancer activity in the cisplatin-resistant carcinoma cells[16].
- **Hydrogels:** An example of such a drug delivery system, by Yang et al. used a semi-interpenetrating network hydrogel loaded with cisplatin for trans-portal vein chemoembolization in mouse liver cancer models[17].

1.3 Mesoporous silica nanoparticles

Many literatures mention mesoporous silica nanoparticles as novel drug delivery systems. These are silica nanoparticles with tubular pores ranging around 2-50 nm in diameter, arranged in an ordered structure, for example, the very first mesoporous silica nanoparticles MCM-41 have a hexagonal structure and a pore diameter ranging from 2.5 to 6 nm, but not all MSNs are in hexagonal configuration. Their structural shape can be influenced by either the starting precursors or reaction conditions, for example, MCM-48 has a cubic structural arrangement, and MCM-50's arrangement is lamella-like[18].

- ***History, synthesis, and use of mesoporous silica nanoparticles in drug delivery systems.***

  A compound that produced mesoporous silica was patented circa. 1970, in an experiment, which was considered an improvement of a synthesis of silica using tetraalkyl silicate and a technique conducting tetraalkyl silicate's hydrolysis with the aid of a cationic surface-active agent, whose purpose was to control the bulk density

of the resulting silica to be that between 96.1108 kg/m^3 and 368.4247 kg/m^3 [19]. Another procedure, patented in 1967, described preparing porous silica, which underwent partial crystallization via calcination of silica gel at a temperature ranging from 800-1200 °C. The silica gel contained alkali ions of 1-10% w/w[20]. It wasn't until 1990 that they were independently synthesized by Yanagisawa et al. at Waseda University in Tokyo. In their synthesis of mesoporous silica nanoparticles, Yanagisawa et al. used kanemite, prepared using a mixture of amorphous silica and NaOH, all dispersed in 100 mL of cooled methanol, dispersed in water, filtered using a vacuum pump and finally air-dried, with its structure confirmed using ^{29}Si-MAS NMR and X-ray powder diffraction: composition was identical to $NaHSi_2O_5.3H_2O$. This compound, called kanemite, was then used to prepare alkyltrimethylammonium-kanemite complexes. Once the stirring was complete, the product was vacuum filtered, repeating the entire procedure up until that point before washing the product in excess acetone and air-drying it again. Calcination of the complexes in air, using a thermal analyser set to 700 °C, resulted in the complete pyrolyzation of the alkyltrimethylammonium ions[21]. Synthesis of MSNs starts with Stober pioneering a network of chemical reactions for the synthesis of spherical, monodisperse micron-sized silica particles, with the synthesis named after him. However, Stober's synthesis underwent a series of modifications to create monodisperse, ordered (single-structure) nanosized particles which showed that MSNs could be synthesized in any pH level, whether acidic, basic or neutral.

The mechanism of forming MCM-41 particles[22] is given below:

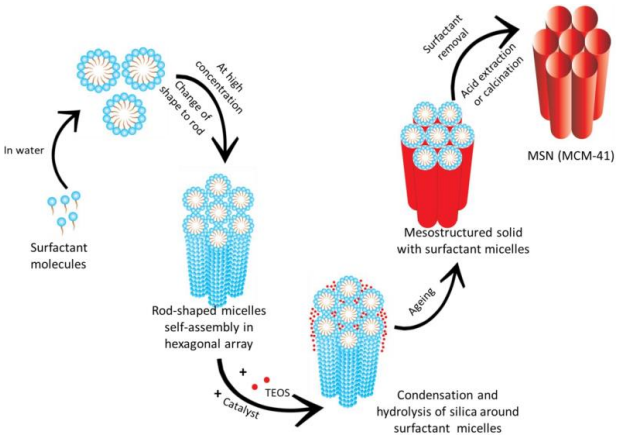

Fig.1: Synthesis of MCM-41 mesoporous silica nanoparticles.

Reprinted with permission from ref. 22. Copyright 2018 MDPI

In the initial hydrolysis of tetramethyl orthosilicate (TMOS) and the silica source, adsorption of silicate ions generally takes place around the micelles, along with the condensation of the precursor during the growth phase. This leads to charge reduction around the surfactant. With the reducing charge comes the reduction of intermicellar repulsion, which enables small silica aggregates to form. After approximately 400 seconds, the reaction mixture would show subtle, hexagonally arranged silica mesopores. Tetraethyl orthosilicate (TEOS) is used because it is an oil-like monomer and has shown phase separation in its static state, but once thoroughly and vigorously stirred, it showed an emulsion-like system. The initial micelle-builder is cetyltrimethylammonium bromide (CTAB), forming ellipsoidal micelles with an inner hydrophobic core, which both expands their size and changes their shape from ellipsoidal to spherical. Hydrolysis of tetraethyl orthosilicate hydrophilizes the monomers that are released into the aqueous environment. The hydrophilic (negatively charged) tetraethyl orthosilicate monomers adsorb onto the CTAB micelles due to electrostatic attraction. The micelles then contract once the orthosilicate is fully consumed within the hydrophobic core, and spontaneous hydrolysis and condensation occur, causing continuous shrinking of the micelles until all the orthosilicate is used up. A silica casing forms around the micelles and aggregation of neighbouring micelles grows the particles, thus creating a mesoporous

structure[23]. The idea of selecting MSNs as candidates for drug delivery stems has prerequisites: high potential loading capacity, high permeability by cancer cells, and ability to elude the mononuclear phagocytic system (MPS), endosomal escape and drug release. Other important factors are optimum accumulation in the tumour and intratumoural penetration. Sufficient biocompatibility is also important, which depends on the material used to create them, degradation, and excretion. Mesoporous silica nanoparticles, due to their adjustable pore and particle size, superior high specific surface area (which is highly functionisable), and biocompatibility are better candidates for drug delivery. Waterman, et al. describes the synthesis of nanoparticles using CTAB as the surfactant and TEOS as the condensation precursor, but also how their characteristics influence biological systems into which they are administered. High surface area is decreased due to modifications like coating or amination: a large surface area increases the MSNs' loading capacity for small molecule drugs. For efficient drug delivery, a low polydispersity index (PDI) is most suited. The MSNs' size, shape and charge influence particle uptake, and entry into cells hinges on applied targeting strategy, the most prominent of which is receptor-mediated endocytosis of targeted MSNs. The ligands or functional groups attached to the MSN micelles influence which cellular surface receptors they bond with, which in turn influences the rate of their endocytic process and their incorporation into endosomes, though there is an exception that proves the rule: untargeted MSNs are capable of bonding with plasma membranes by surface modifications allowing for non-specific binding interactions, which results in endocytosis. The best MSN shapes for endocytosis were spherical, cylindrical. rod, and cubic, when the particles were larger than 100 nm.

MSNs can be designed as passive or active targets with the ultimate goal of developing site-directed cancer therapy and lower toxic side effects:

Passive targeting: also known as the enhanced permeability and retention (EPR) effect, involving the favourable accumulation of drugs in the solid tumour tissue.

Enhancing effectiveness of passive targeting considers particle size, morphology and surface modifications: to avoid renal excretion, the particles must have a diameter of at least 10 nm and a size between 100 and 200 nm, helping them avoid the MPS. It influences the EPR effect as well. Surface modifications, like polyethylene glycol (PEG) lower opsonization also helps in MPS evasion. PEGylation of nanoparticles has been implied to decrease cellular uptake in cancer cells and macrophages, however experiment, carried out by Zhu, et al.[24], reported improved uptake of PEGylated hollow MSNs compared to the un-PEGylated ones acting on cervical cancer tumours, and mouse fibroblasts. Elevated interstitial fluid pressure may significantly impact passive targeting as it may be 10 to 40 times higher than standard interstitial fluid pressure in healthy cells. This likely leads to pressure gradients and heterogeneous interstitial flow, impacting the MSNs' distribution, and possible decreased concentrations in the tumour. However, necrotic tissues are common features of larger and metastatic tumours or hypovascular centres, due to angiogenesis being slower growth, hence why passive targeting is insufficient for MSNs to deliver their payloads at these sites of action, as they can barely get there. Another experiment, by Wilhelm et al. confirms this: only 0.4 ± 0.2% of the unmodified MSNs were found in tumours, along with 0.8 ± 0.5% of the modified MSNs.

Active targeting: conducted to membrane receptors, which are nigh-ubiquitous in tumours, vascular tissues or the nuclear membrane. Leukemic diseases call for modification of MSNs into targets as the EPR effect is insufficient here. Targeting moieties attached to MSNs can be various types of molecules, e.g., aptamers, antibody fragments/entire antibodies, and small molecules. Folate receptors are a prominent example, as many tumours feature excessive expression of it. This is proven by Qi et al's experiment, which targeted laryngeal carcinoma using MSNs fitted with folic-acid. MSNs successfully delivered commonly used anti-cancer payloads like cisplatin, paclitaxel, and 5-fluoruracil, along with siRNA targeting the

drug efflux pump ABCG2 responsible for multidrug resistance of tumours, present in laryngeal cancer cells. Earlier on, with the aid of folate-conjugated and cisplatin-loaded MSNs, results showed greater reduction in laryngeal tumour size in mice, than in untargeted MSNs[25].

1.4 Hydrogels

Hydrogels are essentially three-dimensional networks of hydrophilic polymers which can expand in the presence of water as well as store large amounts of water while retaining their structure as each individual polymer chain from which they are made is cross-linked to another[26].

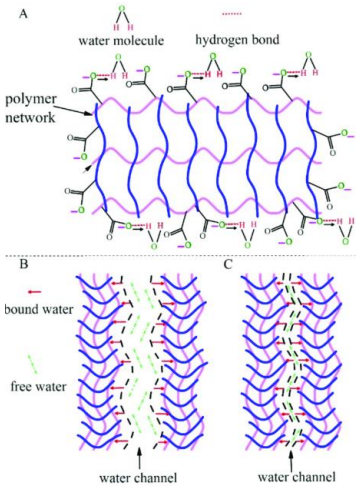

Fig.2: Cross-linking of polymer chains in hydrogels[27]. Reprinted with permission from ref. 27 with permission from Copyright 2017 MDPI

The polymer building blocks of hydrogels feature hydrophilic functional groups in their structures, like hydroxyl groups (-OH), amines ($-NH_2$), amides (-CONH, $-CONH_2$) and sulphates ($-SO_3H$). These enable the hydrogel's absorption of water and other fluids, resulting in its expansion and larger volume occupation, (a process known as swelling, during which the cross-linked hydrogel structure stops dissolution and fracturing of the cross-links). In polymeric hydrogels, water molecules exist in three forms: free, intermediate, and bound. Free water molecules freeze at their freezing points, due to no bond existing between water

and the functional groups in the polymers, however, the amount of free water molecules depends on the hydrogel structure, which directly affects the swelling ratio. Hence, a compact hydrogel structure has smaller amounts of free water. Polymers used to create hydrogels can either be synthetic or naturally-occurring, with the latter mainly in the form of polysaccharides or protein chains. Polysaccharides are the most preferable polymers for hydrogels due to their hydrophilic structures, which is one of the most imperative aspects of a hydrogels, and examples of such include, but are not limited to chitin, chitosan, hyaluronic acid, starch, alginate, cellulose, etc. Protein chains forming natural hydrogel lattices are silk, resilin, collagen, keratin, gelatin, and elastin. Synthetic polymers used in creating hydrogels include polyacrylamide, poly (ethylene oxide), poly (vinyl alcohol) and poly (ethylene glycol), but naturally occurring polymers are far preferable, as they are more biocompatible, due to them undergoing enzyme-facilitated biodegradation by enzymes found in the human body such as lysozyme, culminating in biocompatible by-products.

- ***History, synthesis, and use of hydrogels as drug delivery systems***

  The word "hydrogel" first came to be in 1894 as an explanation of a novel colloidal gel, but the earliest record of using hydrogels for medicinal purposes was a 1960 report by Wichterle and Lim[28]. Wichterle and Lim created the first cross-linked network material having typical hydrogel properties (one of them being high water affinity), a polyhydroxyethylmethacrylate (pHEMA) hydrogel, which inspired further studies for using hydrogels in biomedical applications in the 1970s. This made hydrogels the first synthesized materials used in patients. The first method of generating hydrogels was cross-linking chemically modified monomers or polymers using initiators. Hydrophobic interactions between chains or ionic interactions between long-chain polyanions and polycations were used to bind them together to create hydrogels[29]. The preparation of hydrogels primarily involves crosslinking of polymers, and this can be done chemically or physically, and the intermolecular forces involved are hydrogen bonds, ionic and hydrophobic interactions. This cross-linking is vital for hydrogels not just because this is a process that creates them, but

also because it improves the properties of polymers like chitosan, e.g., stability and durability to make them suitable drug carriers in drug delivery. One of the simpler ways of synthesizing hydrogels is preparing solutions of chitosan in acetic acid at pH 4. Once the solution has been stirred overnight and cooled, β-glycerophosphate would be added dropwise into the chitosan solution[30].

Another strategy of cross-linking is the covalent linking of chitosan macromers, culminating in irreversible bonds, described by Ahmadi, et al [31]. Many cross-linking agents have been used, including, but not limited to glutaraldehyde, palladium cation, genipine, diisocyante, and acrylic acid. The use of genipin, however, is worth a separate mention, especially in the experiment conducted by Domalik-Pyzik, et al., which not only warns about the cytotoxicity of certain agents used to make hydrogels, like beta-glycerophosphate, but also that physical crosslinking is reversible, while chemical crosslinking is not. Domalik-Pyzik, et al. describe that chemical crosslinking can form three main types of polymer networks: hybrid polymer networks (HPNs), semi-interpenetrating polymer networks (semi-IPNs), and interpenetrating polymer networks (IPNs), and that genipine is less cytotoxic than glutaraldehyde. It reacts with chitosan almost instantly and is extracted from *Gardenia jasminodes* fruit, delivering its cross-linking effect even at smaller molar ratios[32].

High-capacity cross-linking networks and water not being bound to their functional groups, are why hydrogels have found widespread clinical use. These structures allow both for spatial and temporal control of releasing different types of therapeutic agents, like macromolecule drugs and small-molecules drugs. Li and Mooney, in their review of hydrogels as drug delivery systems, firstly emphasize the importance of hydrogel size, as such delivery systems have three primary categories: macroscopic hydrogels, microgels, and nanogels, with their dimensions being reflected in their respective names, Macroscopic hydrogels are the easiest to synthesize and use[33].

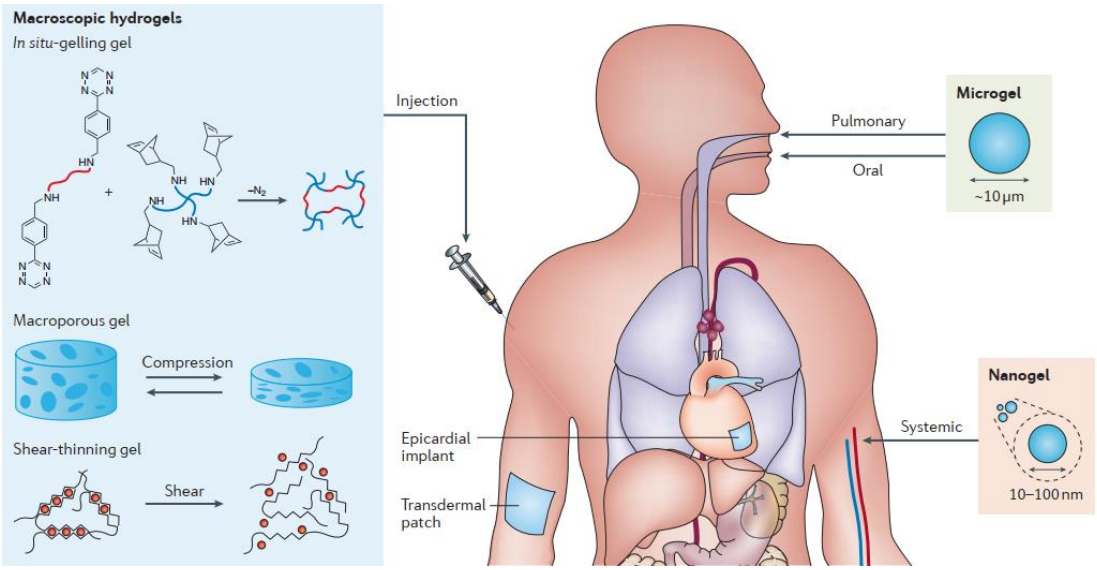

Fig.3: Types of hydrogels and their routes of administration. Reprinted from ref. 33 with permission. Copyright 2016 Springer Nature Group

Macroscopic hydrogels can be administered to the human body either via surgical implants, or by transepithelial drug delivery. An example of surgically-implanted hydrogels is INFUSE, a collagen type I-based gel, with a unique ability of releasing human bone morphogenetic protein BMP2 to treat long bone fractures and spinal fusions. Epithelial barriers, like the intestinal epithelium, mucosa and the human skin are impenetrable to the hydrogels themselves. They are very much permeable to the drugs released by hydrogels. Synthetic polymer and biopolymer-based hydrogels are widely used wound dressings. Their delivery of proteins like insulin and calcitonin and their physicochemical properties make them great candidates for transdermal drug delivery. An example are alginate hydrogels used to deliver potential therapeutics like substance P to accelerate wound healing. Recent clinical trials involving a hydrogel delivering the recombinant human granulocyte-macrophage colony stimulating factor for the treatment of second-degree burns. The invasive and risky nature of surgical implantation warrants the demand for injectable hydrogels. They can be designed to gelate within the body or outside the body but change into a flowable state when subjected to pre-injection shear stress. Examples of injectable hydrogels are in-situ gelling hydrogels: injected in liquid form, and undergoing sol-

gel transition within the body, assume the shape of the space at the injection site. The most basic strategy of these gels is creating slow-gelling systems, allowing for gelation outside the body. The slow speed of the process allows for injection of the hydrogels before solidification. Ideally, kinetics should be slow enough to prevent needle clotting, but rapid enough to prevent the pre-gel solution from diluting within the body. Many gelating mechanisms adopted this approach, including stereocomplexation, Michael addition and charge interaction. Charge interactions are found in systems like elastin-adjacent, cross-linked polypeptides through electrostatic interactions between their cationic lysine residues and anionic organophosphorus cross-linkers. Another example of an in-situ hydrogel system is a poly-electrolyte complex based hydrogel, which showed a sustained release of proteins over a two-week period. However, charge is not the only stimulus for gelation of these systems: thermo-responsive hydrogel systems gelating at body temperature (37 °C) are also considered for in-situ gelation. Naturally occurring polymers gelate as soon as the temperature lowers, warranting administration at supraphysiological temperatures. Synthetic polymers, on the other hand, like poly(ethylene oxide)-poly(propylene oxide)-poly(ethylene oxide) gelate reversely. They solidify at increased temperatures and are flowable at room temperature, allowing for easy injectability and reusability. Hydrophobic domains are often found in thermo-responsive polymers, allowing for structural incorporation of hydrophobic drugs like doxorubicin. Such systems have their drawbacks, like poor physical stability and low mechanical strength. Furthermore, polymers like poly(N-isopropylacrylamide) are not very biodegradable, but stability could be augmented via covalent cross-linking following initial gelation[34].

1.5 Objectives

In the first part of the project, the objective was the successful synthesis of aminofunctionalised MSNs and their coating with gelatin via a glutaraldehyde crosslinker. The gelatin served to create a tumour microenvironment (TME) responsive coating, enabling the opening of the pores of the MSNs at the tumour site, releasing the anti-cancer drug.

Gelatin is TME-responsive, because a TME environment is characterised by hypoxia, upregulated levels of enzymes, acidic pH and a redox environment[35]: gelatin can change its morphology if the pH is further from its isoelectric point and can facilitate controlled release of anti-cancer drugs from gelatin by thermal response[36], provided that its temperature range is adjusted to that of the tumours (roughly 37-40 °C) using imine linkages between amine and hydroxyl functional groups and gelatin[37].

In the second part of the project, the objectives were to synthesize and optimize thermo-responsive hydrogels based on chitosan and Pluronic F-127, to study their thermo-responsiveness, and the encapsulation and release of model drugs.

2. Mesoporous silica nanoparticles

Results and discussion

1. Synthesis of MSNs: Initially, the first nanoparticles were synthesized, using CTAB, as the template, 2M NaOH as the base catalyst, TEOS as the alkoxysilane precursor and ethyl acetate as a co-solvent using the two-phase system approach described in the literature[38]. However, this produced excess precipitate because of agglomeration. Hence why reaction conditions were modified by changing of the amount of co-solvent used, lowering of the reaction temperature, extending the reaction times, changing the substance used as co-solvent, changing the base catalyst, variation of the template and precursor concentration.

All reaction conditions are shown in Table 1:

Table 1. Reaction conditions of the attempted MSNs syntheses:

Method	Amount of CTAB (mg)	Vol. TEOS (mL)	Base catalyst	Vol. water (mL)	Co-solvent	Temperature (°C)	Reaction time (hr)	Yield after work-up (mg)
1	100	0.5	2M NaOH	50	ethyl acetate	80	2	38.3
2	100	0.5	2M NaOH	50	-	80	2	155.8

3	100	0.5	2M NaOH	50	ethyl acetate	80	2	-
4	100	0.5	2M NaOH	50	ethyl acetate	50	3	371.9
5	100	0.5	2M NaOH	50	ethyl acetate	50	3	-
6	100	0.5	2M NaOH	50	ethyl acetate	50	3	1090.9
7	1115	2.5	TEA	22	EtOH	60	2	1199.2

Method 2,3 and 4 often resulted in precipitate due to agglomeration. Methods 1, 5 and 6 did not give agglomeration, but often gave very low yields.

Method 7 seemed the best method that didn't give agglomeration, and gave a reasonable yield, but the yield was not reproducible. Method 7 was then selected for characterisation via FTIR spectroscopy

Method 3 did not produce any yields as excess precipitate formed on the surface of the solution, meaning that isolation of MSNs by centrifugation was not possible. Method 5 resulted in a solution that was milky, but separation of MSNs by centrifugation was not possible. Method 7 produced a high yield of MSNs with suspension, without significant agglomeration. This method was selected to prepare the MSNs for the next step, but was not repeatable, with a significantly lower amount of yield of MSNs on the repeat.

The verification of the MSNs was performed by FTIR analysis, illustrated by Fig.10. What confirmed the sample's identity as MSNs were the characteristic strong peaks at 1040.52 cm-1 corresponding to an Si-O-Si bend, at 788.6 cm-1 signifying an Si-O stretch. Other two peaks at 2920.63 cm-1, 2853.17 cm-1 correspond to the C-H bond of CTAB, and a medium peak at 3337.30 cm-1 shows an Si-OH stretch[39].

2. Aminofunctionalisation of MSNs:

The MSNs were initially aminated with APTES as the aminofunctionalising agent and ethanol as the solvent, as described on the literature[40], in a procedure known as post-synthetic grafting (labelled MSN_NH_2). This approach gave a reasonable yield (88.1 mg) resulted in a weak FTIR peak of NH_2 groups, which warranted the change of the method to con-condensation of the precursor (TEOS) with the aminofunctionalising agent (APTES). The IR spectrum showed a medium peak at 1637.22 cm-1, corresponding an N-H stretch and a very weak peak at 3424.60 cm-1, corresponding to an NH_2 stretch

The one-pot method initially dispersed CTAB in distilled water and 2M NaOH, before adding APTES and TEOS, which initially gave a good yield (98.1 mg), with its repetition resulting in excess agglomeration, which called for the following modifications: addition of co-solvent, increase in template (CTAB) concentration, increase in precursor concentration, increase in aminofunctionalising agent concentration, and decrease in reaction temperature. The modifications (labelled MSN-NH_2) resulted in a good yield (3263.7 mg) with no agglomeration. The IR spectrum showed a band at 3309.52 cm-1, an asymmetric NH2 stretch, and a medium peak at 1639.20 cm-1, showing an asymmetric N-H bend[41].

3. Removal of surfactant: Aminofunctionalised MSNs had the surfactant (template) removed via triplicate dispersion in a MeOH-NaCl solution, a solvent extraction, per the literature[42]. Generally produced a good yield, was repeatable and could be upscaled. To confirm repeatability of this method and repeatability, modifications of the conditions were as follows: increase in NaCl concentration and increase in solvent volume.

The absence of CTAB was verified by FTIR analysis, shown by Fig.14. Confirming this on the IR spectrum was the absence of strong peaks at 2920.63 cm-1 and 2853.17 cm-1, corresponding to C-H bond of CTAB.

4. Quantification of amino groups: To quantify the amino groups present in CTAB-free MSNs, the 4-nitrobenzaldehyde assay was used, as per the literature procedure[43]. The aminofunctionalised MSNs were dispersed in a 4-nitrobenzaldehyde-water solution.

Following the hydrolysis of the imine bonds, centrifugation, and washing, the concentration of 4-nitrobenzaldehyde in the supernatant by UV/Vis spectroscopy. ($1.0704\ x\ 10^{-6}$ $\mu mol/mg$ calc. from absorbance, 0.0513 $\mu mol/mg$ calc. from composition)

5. Redispersibility tests: The MSNs underwent a series of tests to test their redispersibility. The redispersibility was tested using PBS, water, basic solution, acidic solution, DMF and DMSO. DMF and DMSO were selected for the redispersibility test because these agents would likely be used as a co-solvent to test loading of water-insoluble drugs.

All reaction conditions are listed in Table 2:

Table 2. Samples types and solvents tested.

Sample type	**Solvent**	**Redispersibility after five days**
CTAB-MSNs	PBS	Precipitation after four days.
Aminofunctionalised MSNs		Milky suspension
CTAB-free MSNs		Slightly milky
CTAB-MSNs	Water	Milky
Aminofunctionalised MSNs		Milky
CTAB-free MSNs		Slightly milky
CTAB-MSNs	Water/2M NaOH	Colourless
Aminofunctionalised MSNs		Slightly milky
CTAB-free MSNs		Colourless
CTAB-free MSNs	Water/2M NaOH	Slightly milky

	Water/0.1M HCl	Milky
	DMF	Milky
	DMSO	Slightly milky

The results indicate that CTAB-free MSNs dissolve at alkaline conditions and agglomerate in BPS. The suspensions of PBS are stable over the course of five days.

6. Gelatin coating and aldehyde functionalisation:

Gelatin coating of the aminofunctionalised MSNs by post-synthetic grafting (MSN_NH_2) grafted serves to provide a tumour microenvironment (TME)-responsive coating, whose physiological conditions allow for the opening of the pores of the MSNs into which drugs can be loaded. To achieve this, a linker is required to attach the gelatin, and a suitable one is the dialdehyde glutaraldehyde which can link the gelatin to the MSNs by forming an imine bond. Or, as an alternative approach, the aminofunctionalised MSNs can be coated with gelatin by electrostatic interactions, which, once crosslinked with glutaraldehyde, will link gelatin molecules to one another.

7. Aldehyde functionalisation:

(a) Direct aldehyde functionalisation (gelatin coating by adding a dialdehyde linker)

The aminofunctionalised MSNs (MSN_NH_2) (sans gelatin) needed a linker to attach the gelatin to the surface. A suitable linker is the dialdehyde that can link the gelation to the MSNs via imine formation. Following the literature procedure[44], the MSNs were dispersed in a water-glutaradehyde solution. This reaction was unsuccessful because the MSNs (aminofunctionalised by post-synthetic grafting) did not exhibit functionalisation by aldehyde groups, possibly for two main reasons: the low number of amino groups present in them, meaning that there was an insufficient number to form reactions with aldehydes (like imine

bonds), and because their FTIR spectrum showed no characteristic peak of aldehyde groups in MSNs at 1716 cm-1. This clearly indicated that the MSNs' aldehyde functionalisation[45] was unsuccessful.

(b) Gelatin crosslinking with aldehyde (Gelatin coating by electrostatic attraction, followed by linking the attached molecules to each other via a dialdehyde linker):

As direct aldehyde functionalisation was unsuccessful, this warranted coating the MSNs via electrostatic interaction, and then attempting to cross-link the gelatin with aldehyde functional groups via an imine bond and determining the feasibility of this approach. Based on the literature experiment[46] this coating can be created by electrostatic forces generated by dispersing MSNs in a water-gelatin solution for 5 hours before immersing the mixture in an ice bath and separating the mixture by centrifugation twice. The gelatin-coated MSNs were dispersed in a water-glutaraldehyde solution before centrifugation and triplicate washing with water. Overall, the method is only partially feasible and not repeatable, as samples only showed partial crosslinking between gelatin and glutaraldehyde.

Gelatin coating of the MSNs was verified by the pronounced peak at 1536.12 cm-1, corresponding to the gelatin's N-H stretching vibration, seen on Fig.3. The less-pronounced signals of 2936.50 cm-1 and 2884.92 cm-1 correspond to the gelatin's C-H stretching[47] vibrations. FTIR data showed the successful coating of the MSNs and crosslinking was partially successful with the slight peak at 1472.68 cm-1, corresponding to the aldimine linkage ($N=CH-(CH_2)_3-CH=N$) with gelatin chains, while lacking a strong peak 1244 cm-1, which corresponds to a strong C-O vibration[48], characteristic of aldehydes.

8. Drug loading

The loading of acetazolamide into the MSNs was studied. Acetazolamide is a carbonic anhydrase inhibitor. Carbonic anhydrase inhibitors have recently caught interest as cancer treatments, due to their ability to "sensitize" cancer cells to changes in pH, caused by inhibition of carbonic anhydrase (during which the amount of bicarbonate and H^+ ions is

altered)[49]. Drug loading can be studied by introducing the MSNs to an acetazolamide solution and, determining the concentration of non-encapsulated acetazolamide in the supernatant after centrifugation using UV/Vis spectroscopy. First, the UV/Vis spectrum of acetazolamide was measured at different pH values to find the best buffer for the analysis.

MSNs can interfere with UV/Vis spectra. Their critical wavelength is below 370 nm[50], which allows them to scatter UV/Vis light, albeit marginally. As residual nanoparticles can interfere with UV/Vis spectra after being left in solution after centrifugation, a 'blank' loading experiment was carried out. The CTAB-free MSNs were dispersed in acetone and centrifuged. The supernatant (50 µL) was diluted to 5 mL with pH buffer 8, which was then UV/Vis analysed. In a second test, known concentrations of acetazolamide were added to the supernatant, and the concentration determined by UV/Vis analysis was compared with the known concentration using the calibration plot:

Table 4. Analyte components of the samples for testing MSNs for UV/Vis interference with corresponding absorbance values.

Sample	Analyte components	pH buffer 8 volume (mL)	Absorbance @ 320 nm	Conc. calcd. from analyte composition	Conc. calcd. from absorbance (mg/ml)
1	Supernatant/Acetazolamide	4.4	0.24694	0.0126	0.0393
2	Acetone	4.9	0.040382	0.1333	6.4253×10^{-3}
3	Supernatant	4.9	0.095352	2.52×10^{-3}	0.0153
4	Acetazolamide	4.5	0.089376	0.0126	0.0142
5	Supernatant/Acetazolamide	4.4	0.245675	0.0126	0.0391
6	Supernatant/Acetazolamide	3.9	0.284481	0.0252	0.0453

The concentration values obtained using the absorbance values were much different than those calculated using the composition of the analyte, meaning that MSNs did interfere with the UV/Vis spectrum This test was repeated in acetone/buffer and methanol/buffer solutions.

Table 5. Acetone-acetazolamide sample proportions and calculated masses of acetazolamide (mg)

Sample	Weight acetazolamide (mg)	Absorbance @ 320 nm	Conc. calcd. from analyte composition (mg/mL)	Conc. calcd. from absorbance (mg/mL)	Weight of acetazolamide (calc.) (mg)
1	30.1	0.335197	0.0602	0.0564	28.2584
2	30.1	0.381133	0.0602	0.0606	30.3216
3	30.1	0.348472	0.0602	0.0554	27.7234
4	30.5	0.382067	0.061	0.0608	30.3964
5	30.6	0.302086	0.0612	0.0481	24.0331
6	30.4	0.27895	0.0608	0.0442	22.1244

Table 6. Methanol-acetazolamide sample proportions and calculated masses of acetazolamide (mg)

Sample	Weight acetazolamide (mg)	Absorbance @ 320 nm	Conc. calcd. from analyte composition (mg/mL)	Conc. calcd. from absorbance (mg/mL)	Weight of acetazolamide (calc.) (mg)
1	30.78	0.137605	0.0308	0.0219	21.8949
2	30.8	0.16864	0.0308	0.0268	26.833
3	30.53	0.177359	0.0305	0.0282	28.2203

(The same results are for methanol, the measured value fell short of the weighed out value).

The data in Tables 5 and 6 show that UV/Vis spectroscopy is not suitable to analyse drug

loading. HPLC would be a more accurate and feasible method of drug loading analysis but could not be performed due to time constraints.

Experimental section

1. Materials and methods

- *Chemicals*: Hexadecyltrimethylammonium bromide (CTAB) (*TCI Chemicals*), Tetraethyl orthosilicate (TEOS) (*Millipore Corporation (Merck)*), ethanol (absolute, 99%, EtOH) (*Fisher Scientific*), triethanolamine (TEA) (*Sigma-Aldrich*), 3-aminopropyltriethoxysilane (APTES) (*TCI Chemicals*), methanol (99.9%, MeOH) (*Fisher Scientific*), dimethylformamide (DMF) (*TCI Chemicals*), dimethyl sulfoxide (DMSO) (*TCI Chemicals*), glutaraldehyde (*TCI Chemicals*), porcine gelatin (*Sigma-Aldrich*), 4-nitrobenzaldehyde (*TCI Chemicals*), acetazolamide (50%) (*TCI Chemicals*), dibasic potassium phosphate (K_2HPO_4) (*Sigma-Aldrich*), N-hydroxysuccinimide (*TCI Chemicals*), 4-phenylbutyric acid (*TCI Chemicals*), (3-dimethylamino-propyl)-ethyl-carbodiimide hydrochloride (EDC HCl) (*TCI Chemicals*), saccharin (*Sigma-Aldrich*), acetone (*Fisher Scientific*).
- *UV/Vis spectroscopy*: The samples' UV/Vis spectra were recorded on a Cary-Varian 50 Scan UV/Vis spectrometer in the range 200-900 nm.
- *FTIR spectroscopy*: FTIR analysis of the samples performed with a Perkin-Elmer Spectrum 400 FT-IR/FT-NIR spectrometer in the range 4000.0-650.0 cm^{-1} at a resolution of 3 µm, seventeen scans were performed, window of operation was 4000 cm^{-1} (2.5 µm)-5x10^{-3} cm^{-1} (50 µm).
- *Separation of MSNs*: MSNs were separated by 5500 rpm centrifugations using a Thermo Scientific Heraeus Megafuge 16 centrifuge while 14400 rpm centrifugations were performed with a Sigma 1-14 microcentrifuge.

2. Preparation of MSNs

Different approaches were used, with the details of the reaction given in Table 7.

Method 1: MSNs were synthesized by dispersing CTAB in distilled water and subsequently adding 2M NaOH and heating the mixture to 80 °C. TEOS and ethyl acetate are then added to the mixture left to stir for 2 h at 80 °C before leaving the solution to cool to room temperature and separating the MSNs from the solvents by centrifugation at 5500 rpm. The MSNs were washed with EtOH and water, then left to oven-dry at 60°C overnight.

Method 2: This MSN synthesis followed the same procedure as *Method 1*, with the exception that the co-solvent was not added.

Method 3: This approach involved the dispersion of CTAB in distilled water and subsequent addition of 2M NaOH, heating the mixture to 80 °C, and adding TEOS (0.1 mL) and ethyl acetate, and leaving the mixture to stir at 80 °C for 2 h. This was to be cooled to room temperature, followed by centrifugation, washing with EtOH and water, and subsequent oven-drying overnight

Method 4: MSNs were synthesized using the same procedure as *Method 3*, except that the ethyl acetate was added in a larger dose (2 mL), and the solution was left to stir for 3 h at 50 °C before cooling to room temperature overnight.

Method 5: MSNs were synthesis using the same procedure for *Method 3*, except that TEOS and ETAC were combined with each other and added in one go, before stirring the mixture for 3 h at 50 °C and leaving it to cool to room temperature overnight. The MSNs were to be centrifuged, washed with EtOH and water, and oven-dried overnight.

Method 6: MSN synthesis used the same procedure as Method 3, except that the mixture which was stirred for 3 h at 50 °C.

Method 7: MSNs were synthesized by dispersing CTAB (1115 mg) in water and ethanol (6.6 mL) and stirring the mixture at room temperature for 10 min. TEA (5.7 mL) was added to the mixture, which was stirred for 30 min at room temperature. The solution was then heated to 60 °C, and dropwise addition of TEOS (2.5 mL), was stirred for 2 h at 60 °C, before the usual centrifugation, EtOH-water washing, and overnight oven-drying.

FTIR (cm^{-1}): 3337.30 m (asymmetric $\nu_{Si\text{-}OH}$), 2920.63 s (asymmetric $\nu_{C\text{-}H\ of\ CTAB}$) 2853.17 s (asymmetric $\nu_{C\text{-}H\ of\ CTAB}$), 1040.52 s ($\nu_{Si\text{-}O\text{-}Si}$), 788.6 s (asymmetric $\delta_{Si\text{-}OH}$)

The reaction parameters and reagent proportions are given in the table below:

Table 7. Reaction parameters, reagent proportions and yields for all methods of MSN synthesis used.

Method	Amount of CTAB (mg)	Vol. TEOS (mL)	Base catalyst	Vol. water (mL)	Co-solvent	Sequence of addition of TEOS and co-solvent	Temperature (°C)	Reaction time (h)	Yield (mg)
1	99.5	0.5	0.35 mL 2M NaOH	50	0.35 mL ethyl acetate	TEOS first, ethyl acetate second	80	2	38.3
2	100.4	0.5	0.35 mL NaOH	50	-	TEOS alone	80	2	155.8
3	99.8	0.5	0.35 mL NaOH	50	0.1 mL ethyl acetate	TEOS first, ethyl acetate second	80	2	-
4	99.8	0.5	0.35 mL NaOH	50	2 mL ethyl acetate	TEOS first, ethyl acetate second	50	3	371.9
5	100.7	0.5	0.35 mL 2M NaOH	50	2 mL ethyl acetate	Ethyl acetate added to TEOS, added in a single aliquot	50	3	-
6	100.8	0.5	0.35 mL 2M NaOH	50	2 mL ethyl acetate	TEOS first, after 5 min ethyl acetate second	50	3	1909.9
7	1115.2	2.5	5.7 mL TEA	22	6.6 mL EtOH	TEA added first, after 30 min TEOS added second, dropwise	60	2	1199.2

3. Aminofunctionalisation of MSNs by post-synthetic grafting

MSNs (100.4 mg) were dispersed in ethanol (10 mL) and heated to 80 °C before APTES (80 µL) was added and the mixture stirred for 3 h. The MSNs were then separated by centrifugation and oven-dried at 60 °C, giving a yield of 88.1 mg.

FTIR (cm^{-1}): 3424.60 m (asymmetric ν_{NH2}), 2948.4 w (asymmetric $\nu_{C\text{-}H\ of\ CTAB}$), 1637.22 m (asymmetric $\delta_{N\text{-}H}$), 1052.42 s ($\nu_{Si\text{-}O\text{-}Si}$), 790.74 s (asymmetric $\delta_{Si\text{-}OH}$)

4. Synthesis of aminofunctionalised of MSNs by co-condensation of TEOS and APTES

Method 1: MSNs synthesis involved dispersing CTAB (100 mg) in water and 2M NaOH (0.35 mL) and heating the mixture to 80 °C for 30 min. APTES (140 µL) and TEOS (0.5 mL) was subsequently added to the mixture, which was stirred for 2 h at 80 °C and left to cool to room temperature overnight. The nanoparticles were separated via centrifugation and oven-dried overnight. Yield: 98.1 mg

FTIR (cm^{-1}): 3309.52 s (asymmetric ν_{NH2}), 2920.63 m (asymmetric $\nu_{C\text{-}H\ of\ CTAB}$), 2853.17 m (asymmetric $\nu_{C\text{-}H\ of\ CTAB}$), 1639.20 m (asymmetric $\delta\nu_{N\text{-}H}$), 1022.68 s ($\nu_{Si\text{-}O\text{-}Si}$), 772.90 s (asymmetric $\delta_{Si\text{-}OH}$)

Method 2: MSN synthesis involved dispersing CTAB (1110.8 mL) in water (22 mL) and ethanol (6.6 mL), stirring the solution at room temperature for 10 min. TEA (5.7 mL) was subsequently added to the solution, which was stirred at room temperature for 30 min before adding APTES (0.7 mL). The mixture was heated to 60 °C and TEOS (2.5 mL) was added dropwise for 2-3 min. The solution was kept at 60 °C for 2 h before centrifugation and oven-drying overnight at 60 °C. Yield: 3263.7 mg

FTIR (cm^{-1}): 3309.52 s (asymmetric ν_{NH2}), 2920.63 m (asymmetric $\nu_{C\text{-}H\ of\ CTAB}$), 2853.17 m (asymmetric $\nu_{C\text{-}H\ of\ CTAB}$), 1639.20 m (asymmetric $\delta\nu_{N\text{-}H}$), 1022.68 s ($\nu_{Si\text{-}O\text{-}Si}$), 772.90 s (asymmetric $\delta_{Si\text{-}OH}$)

5. Removal of surfactant

Removal of the template from the MSNs involved dissolving NaCl (170 mg) in methanol (21 mL), before adding the aminofunctionalised MSNs (88.1 mg) and stirring the mixture at room temperature for 3 h. The MSNs were isolated by centrifugation before preparing a new NaCl-MeOH solution and repeating the procedure two more times, before oven-drying the MSNs at 60 °C. Yield: 46.3 mg

FTIR (cm^{-1}): 1637.86 m (asymmetric $\delta\nu_{N\text{-}H}$), 1043.06 s ($\nu_{Si\text{-}O\text{-}Si}$), 786.12 m (asymmetric $\delta_{Si\text{-}OH}$)

6. Quantification of the amino groups using the 4-nitrobenzaldehyde assay.

(a) Calibration plot of 4-nitrobenzaldehyde

4-nitrobenzaldehyde (100.8 mg) was dispersed in 2 mL of methanol before preparing the stock solution with PBS (30.5 mg 4-nitrobenzaldehyde in 250 mL). The stock was pipetted into seven sample vials and diluted with PBS per the proportions listed in Table 8:

Table 8. Proportions of 4-nitrobenzaldehyde stock solution and PBS per standard.

Standard no.	Vol. of stock	Vol. of PBS buffer
1	200 µL	4.8 mL
2	500 µL	4.5 mL
3	1 mL	4.0 mL
4	1.5 mL	3.5 mL
5	2 mL	3.0 mL
6	2.5 mL	2.5 mL
7	3 mL	2.0 mL

The standards were then UV/Vis analysed, and their absorbance values obtained at wavenumber 319.95 nm, and plotted against the concentration of 4-nitrobenzaldehyde, as listed below:

Table 9. Absorbance and concentration values of the standards

Standard no.	Conc. (mg/mL)	Absorbance @ 319.95 nm
1	4.88E-03	0.113432
2	0.0122	0.168584
3	0.0244	0.173015
4	0.0366	0.40617

5	0.0488	0.530541
6	0.061	0.669702
7	0.0732	0.768608

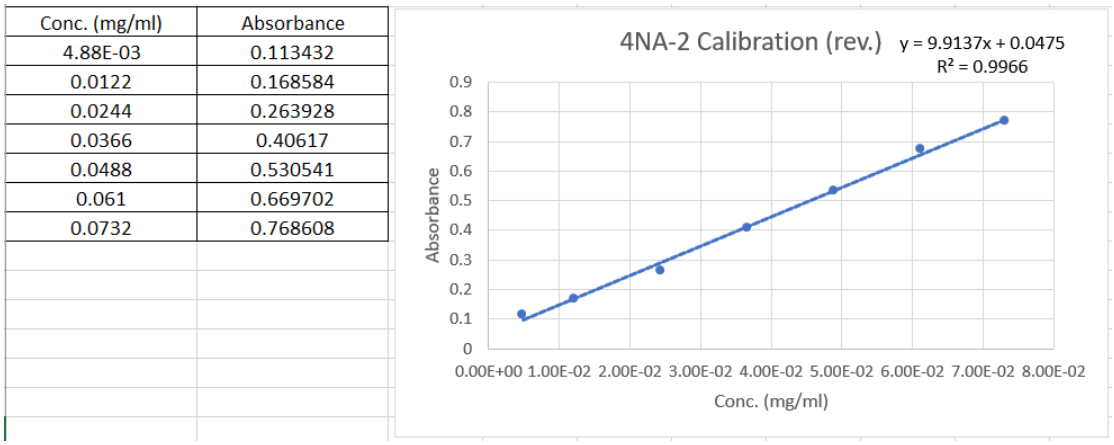

Fig.4: Calibration plot for 4-nitrobenzaldehyde

(b) Quantification of the amino groups

The CTAB-free MSNs (40.2 mg) were dispersed in methanol (20 mL), before adding at 4-nitrobenzaldehyde (1039.2 mg) and stirring the mixture at 45 °C overnight. The MSN were then centrifuged for 10 min, with the supernatant removed and kept. Subsequently, methanol (1 mL) was added to the Eppendorf microcentrifuge tube of MSNs, followed by a second 10-min centrifugation, and extraction of the supernatant. The centrifugation was repeated five times before redispersing the MSNs in water and ethanol (both 1 mL) and stirring the mixture at 45 °C overnight. The next day, three extractions of supernatants via centrifugation at 14400 rpm were performed (an hour-long stirring of the MSNs at 45 °C was performed before the final centrifugation), with the supernatants combined, diluted to 100 mL with PBS and UV/Vis analysed, its absorbance recorded and subbed into the equation. The absorbance of the supernatant was 0.93779 subbed in for y = 10.828x with the concentration calculated to be 0.089804 mg/ml. Another sample was prepared with 32.5 mg of 4-nitrobenzaldehyde dissolved in 2 ml of water and UV-Vis analysed and its absorbance was obtained as 0.011735

and first subbed into y = 9.9137x + 0.0475, and then into the refined equation with a set intercept of x at 0; y = 10.828x. Further calculations gave the amount of amino groups in the MSNs as 5.48814 μmol/mg.

7. Redispersibility tests

Method 1: Three types of MSNs: CTAB-MSNs, aminated MSNs and CTAB-free MSNs were dispersed in three test tubes, each containing 5 mL of PBS and left for 5 days.

Method 2: The procedure was the same as *Method 1*, except water was used as the solvent.

Method 3: The procedure was the same as *Method 1*, except that a mixture of water and 2M NaOH (100 μL) was used as the solvent.

Method 4: The procedure was the same as *Method 1*, except that 25 μL of 2M NaOH was added to the water solvent for CTAB-MSNs, 100 μL of 0.1M HCl was added to the water solvent for aminated MSNs, and 150 μL of 0.1M HCl was added to the water solvent for CTAB-free MSNs.

Method 5: The procedure was the same as *Method 1*, except that CTAB-MSNs were dispersed in 5 mL of DMF, and aminated MSNs and CTAB-free MSNs were dispersed in 5 mL of DMSO.

All MSN types, their amounts and solvent compositions are listed in Table 4:

Table 10. Types of MSNs, their proportions, composition of solvents and their appearances after MSNs were dispersed.

MSN type	Sample amount (mg)	Solvent	Color of solution after 5 days
CTAB-MSNs	25.1	5 mL PBS	Milky
Aminofunctionalised MSNs	25.2	5 mL PBS	Milky
CTAB-free MSNs	25.7	5 mL PBS	Slightly milky
CTAB-MSNs	25.5	5 mL water	Milky

Aminofunctionalised MSNs	25.0	5 mL water	Milky
CTAB-free MSNs	25.0	5 mL water	Slightly milky
CTAB-MSNs	25.4	5 mL water/100 µL 2M NaOH	Colourless
Aminofunctionalised MSNs	25.0	5 mL water/100 µL 2M NaOH	Slightly milky
CTAB-free MSNs	25.6	5 mL water/100 µL 2M NaOH	Colourless
CTAB-free MSNs	25.3	5 mL water/25 µL 2M NaOH	Slightly milky
CTAB-free MSNs	25.2	5 mL water/100 µL 0.1M HCl	Milky
CTAB-free MSNs	25.4	5 mL water/150 µL 0.1M HCl	Milky
CTAB-free MSNs	25.6	5 mL DMF	Slightly milky
CTAB-free MSNs	25.4	5 mL DMSO	Colourless
CTAB-free MSNs	25.5	5 mL DMSO	Colourless

8. Gelatin coating

The aminofunctionalised MSNs via post-synthetic grafting (19.8 mg) were dispersed in a water-gelatin (20.8 mg/1 mL) solution, whose pH was then adjusted to 5.92 via 5 µL additions of 0.05 HCl. The mixture was then stirred for 5 h at 50 °C before being quickly transferred to 8 mL of distilled water in a 4 °C ice bath, before being separated by centrifugation at 5500 rpm, and washed with water. The centrifugation and washing were repeated twice before the MSNs were oven-dried at 60 °C overnight. Yield: 16.8 mg

FTIR (cm^{-1}): 2936.50 w (asymmetric $\nu_{C\text{-}H\ of\ gelatin}$), 2884.92 w (asymmetric $\nu_{C\text{-}H\ of\ gelatin}$), 1645.15 m (asymmetric $\delta\nu_{N\text{-}H}$), 1536.12 m (asymmetric $\nu_{N\text{-}H\ of\ gelatin}$), 1040.52 s ($\nu_{Si\text{-}O\text{-}Si}$); 786.78 m (asymmetric $\delta_{Si\text{-}OH}$)

9. Aldehyde functionalisation

Method 1: Initially, direct aldehyde functionalisation of the aminofunctionalised MSNs with no gelatin coating was attempted. The aminofunctionalised MSNs by post-synthetic grafting (20.1 mg) were dispersed in water (1 mL), with glutaraldehyde (20 µL) added soon after. The mixture is then stirred at room temperature for 5 h. The MSNs were then extracted by centrifugation at 14400 rpm and oven-dried at 60 °C. Yield: 13.4 mg

FTIR (cm^{-1}): 1637.22 w (asymmetric $\delta\nu_{N\text{-}H}$); 1040.52 s ($\nu_{Si\text{-}O\text{-}Si}$); 788.76 m (asymmetric $\delta_{Si\text{-}OH}$)

Method 2: An alternative method was used to aldehyde functionalize the MSNs by crosslinking them with their gelatin coating. The gelatin-coated MSNs (20.8 mg) were dispersed in water (8 mL) and glutaraldehyde (30 µL) at room temperature before being centrifuged for 15 min, washed with water in triplicate and oven-dried at 60 °C. Yield: 15.6 mg

FTIR (cm^{-1}): 2940.47 w (asymmetric $\nu_{C\text{-}H\ of\ gelatin}$), 2884.92 w (asymmetric $\nu_{C\text{-}H\ of\ gelatin}$), 1637.22 m (asymmetric $\delta\nu_{N\text{-}H}$), 1543.07 m (asymmetric $\nu_{N\text{-}H\ of\ gelatin}$) 1472.68 w (symmetric $\nu_{(N=CH\text{-}(CH2)3\text{-}CH=N)\ with\ gelatin\ chains}$), 1044.49 s ($\nu_{Si\text{-}O\text{-}Si}$); 788.76 m (asymmetric $\delta_{Si\text{-}OH}$)

10. UV pH titration curve for loading analysis and calibration plot:

Part I - UV pH titration curve for loading analysis

An acetazolamide-KCl-water solution (25.3 mg acetazolamide, 4.6226g KCl/500 mL) was prepared, and half of the solution was transferred to a 250 mL Erlenmeyer flask, its pH increased to 9 with 0.1M NaOH and obtaining a UV/Vis spectrum with every major increase. The same procedure was performed on the second half, with pH decreased to 3.5 with 0.1M HCl. Initially produced distorted graph, but NaOH graphs were generally more linear than

those for HCl. After calibrating the pH meter with two 0.1M standards of NaOH and HCl, the pH of acetazolamide solution was measured as 5.64. The pH was then increased with 50 µL aliquots of 0.1M NaOH, with each substantial increase in pH being UV/Vis analysed, its absorbance obtained at 319.95 nm. This continued until the pH of the solution reached 9. The pH of other half of the acetazolamide-KCl-water soln. was measured as 5.64., before adding 50 µL aliquots of 0.1M HCl, until the pH reached 3.5. The samples were listed per Table 11:

Table 11. The first series of UV/Vis analysed acetazolamide samples with increasing and decreasing pH listed with absorbance.

Sample	Acid/Base used	Number of 50 µL aliquots	pH	Absorbance @ 319.95 nm
Standard 1	NaOH	0	5.64	-0.003
Standard 2	HCl	0	5.46	-0.00042
ACT-NAOH-1	NaOH	1	6.14	0.022622
ACT-NAOH-3	NaOH	3	6.52	0.079547
ACT-NAOH-4	NaOH	4	6.76	0.107974
ACT-NAOH-5	NaOH	5	6.96	0.159255
ACT-NAOH-8	NaOH	8	7.30	0.234481
ACT-NAOH-11	NaOH	11	7.68	0.317147
ACT-NAOH-13	NaOH	13	7.95	0.339804
ACT-NAOH-15	NaOH	15	8.16	0.35478
ACT-NAOH-17	NaOH	17	8.41	0.368067
ACT-NAOH-21	NaOH	21	8.74	0.348181
ACT-NAOH-25	NaOH	25	8.94	0.33039
ACT-NAOH-28	NaOH	28	8.99	0.321292

ACT-HCL-1	HCl	1	4.47	0.00025
ACT-HCL-2	HCl	2	4.23	0.00193
ACT-HCL-4	HCl	4	3.84	0.000813
ACT-HCL-5	HCl	5	3.72	0.010455
ACT-HCL-6	HCl	6	3.62	0.012798
ACT-HCL-7	HCl	7	3.54	0.009059

The procedure was repeated with the pH first half of the acetazolamide-KCl-water (25.0 mL/500 mL with 2.2553g of KCl added to the first half) solution measured as 5.49, before adding 50 µL aliquots of 0.1M HCl until the pH reached 3.5, obtaining a UV/Vis spectrum with every substantial decrease in pH. Five pH and absorbance values were obtained. The other half of the acetazolamide-water solution was given 2.2524 g of KCl, before its pH was measured as 5.79. Like in the previous method, adding 50 µL aliquots of 0.1M NaOH until the pH reached 9. Fourteen pH and absorbance values were obtained. The samples were listed per Table 12:

Table 12. The second series of UV/Vis analysed acetazolamide samples with increasing and decreasing pH plotted against absorbance.

Sample	**Acid/Base used**	**Number of 50 µL aliquots added**	**pH**	**Absorbance @ 319.95 nm**
ACT-Blank 1	HCl	0	5.49	2.75E-05
ACT-Blank 2	NaOH	0	5.71	2.75E-05
ACT-HCL-1	HCl	1	4.35	0.013331
ACT-HCL-2	HCl	2	3.93	-0.007
ACT-HCL-3	HCl	3	3.78	-0.00985
ACT-HCL-4	HCl	4	3.64	-0.00143
ACT-HCL-5	HCl	5	3.53	-0.00665
ACT-NAOH-1	NaOH	1	6.45	-0.00352
ACT-NAOH-2	NaOH	2	6.63	0.153613

ACT-NAOH-3	NaOH	3	6.97	0.220047
ACT-NAOH-4	NaOH	4	7.21	0.271507
ACT-NAOH-5	NaOH	5	7.45	0.317302
ACT-NAOH-6	NaOH	6	7.64	0.338568
ACT-NAOH-7	NaOH	7	7.85	0.345844
ACT-NAOH-8	NaOH	8	8.09	0.37486
ACT-NAOH-9	NaOH	9	8.30	0.397397
ACT-NAOH-10	NaOH	10	8.47	0.404326
ACT-NAOH-11	NaOH	11	8.63	0.405131
ACT-NAOH-12	NaOH	12	8.78	0.395432
ACT-NAOH-13	NaOH	13	8.92	0.38904
ACT-NAOH-14	NaOH	14	9.05	0.377575

Part II – Acetazolamide calibration plot

An acetazolamide-pH buffer 8 stock solution was prepared and pipetted into 7 sample vials, and diluted to 5 mL with pH buffer 8, per the proportions on Table 7. Each standard had its absorbance value obtained at 319.95 nm after UV/Vis analysis. Each of their concentrations was calculated in mg/ml and were listed along with absorbance values in Table 7:

Sample:	Conc. (mg/ml)	Absorbance
ACT-pH8-S1	5.04E-03	0.04439
ACT-pH8-S2	0.0126	0.090651
ACT-pH8-S3	0.0252	0.157033
ACT-pH8-S4	0.0378	0.249067
ACT-pH8-S5	0.0504	0.318133
ACT-pH8-S6	0.063	0.392285
ACT-pH8-S7	0.0756	0.469206

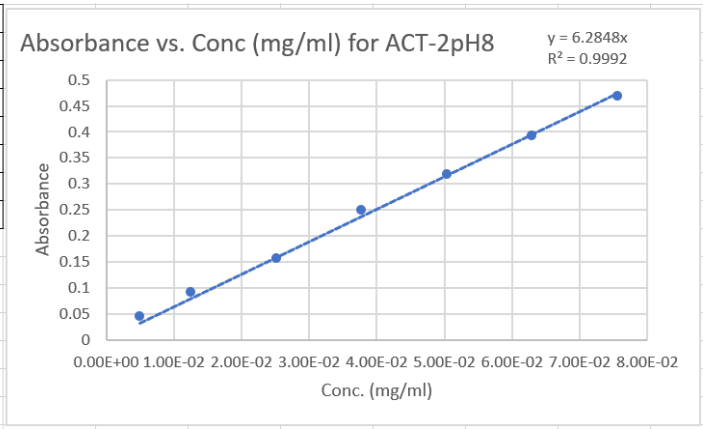

Fig.5: Calibration plot for acetazolamide (PBS pH 8)

11. Testing MSNs for interference with UV/Vis spectrum

CTAB-free MSN-NH_2 (20.6 mg) were dispersed in acetone (3 mL), sonicated for 10 minutes, then placed in an Eppendorf tube and centrifuged, the supernatant (centrifuged to ensure no

residual MSNs remain after centrifugation, which would interfere with the analysis) served as the blank, with 50 µL of it diluted to 5 mL with pH buffer 8. Subsequently, acetone supernatant (100 µL), acetazolamide stock solution (Conc. 0.126 mg/mL, 500 µL), and pH buffer 8 solution (4.4 mL) were transferred to a 10 ml sample vial: the mixture was shaken and tested for intervention via UV/Vis analysis (pH buffer 8 served as the blank). Five more samples were prepared, UV/Vis analysed had their absorbance values obtained at wavenumber 320 nm, which were subbed in to used to calculate the concentrations:

Table 13. Analyte and solvent proportions, absorbance values and concentrations of samples tested for MSN interference.

Sample	Analyte composition	PBS Buffer 8 volume (mL)	Absorbance @ 320 nm	Concentration calcd. from analyte composition	Concentration calcd. from absorbance (mg/mL)
1	Supernatant 100 µL/Acetazolamide 500 µL	4.4	0.24694	0.0126	0.0393
2	Acetone 100 µL	4.9	`0.040382	0.1333	6.4253×10^{-3}
3	Supernatant 100 µL	4.9	0.095352	2.52×10^{-3}	0.0153
4	Acetazolamide 500 µL	4.5	0.089376	0.0126	0.0142
5	Supernatant 100 µL/Acetazolamide 500 µL	4.4	0.245675	0.0126	0.0391
6	Supernatant 100 µL/Acetazolamide 1 mL	3.9	0.284481	0.0253	0.0453

12. Acetazolamide drug loading test:

Acetazolamide (30.1 mg) was dispersed in acetone (4 mL), and diluted to 5 mL with acetone in a volumetric flask, prepared alongside a blank (50 µL acetone in 4.950 mL pH buffer 8). A 50 µL aliquot of the solution was pipetted into a sample vial and diluted to 5 mL with pH buffer 8. After shaking, the mixture was UV/Vis analysed at 320 nm, with its absorbance collected and subbed into the equation $y = 6.2848x$ and used to calculate the weight of acetazolamide. The sample's absorbance was used to calculate its concentration and mass of

acetazolamide. The procedure was repeated in quintuplicate. The sample compositions, absorbance values and concentrations are given in the table below:

Table 14. Compositions and proportions of acetone-acetazolamide samples analysed at 320 nm

Sample	Weight acetazolamide (mg)	Vol. extracted (µL)	Vol. pH buffer 8 (mL)	Absorbance @ 320 nm	Conc. calcd. from analyte composition (mg/mL)	Conc. calcd. from absorbance (mg/mL)
1	30.1	50	4.950	0.335197	0.0602	0.0564
2	30.1	50	4.950	0.381133	0.0602	0.0606
3	30.1	50	4.950	0.348472	0.0602	0.0554
4	30.5	50	4.950	0.38207	0.061	0.0607
5	30.6	50	4.950	0.302086	0.0612	0.0481
6	30.4	50	4.950	0.27895	0.0608	0.0442

The procedure was later modified with methanol replacing acetone as the solvent for acetazolamide, and as the blank in UV/Vis analysis. The aliquots and dilution volumes were increased from 50 µL diluted to 5 mL to 100 µL diluted to 10 mL. This was performed to determine whether solvent change had any influence on the overall accuracy of this method. The sample compositions, absorbance values and concentrations are given in the table below:

Table 15. Compositions and proportions of methanol-acetazolamide samples analysed at 320 nm

Sample	Weight acetazolamide (mg)	Vol. extracted (µL)	Vol. pH buffer 8 (mL)	Absorbance @ 320 nm	Conc. calcd. from analyte composition (mg/mL)	Conc. calcd. from absorbance (mg/mL)
1	30.78	100	9.9	0.137605	0.0308	0.0219

2	30.8	100	9.9	0.16864	0.0308	0.0268
3	30.53	100	9.9	0.177359	0.0305	0.0282

13. Saccharin calibration curve:

Saccharin calibration plot

A saccharin-pH buffer 8 stock solution was prepared and was transferred to seven sample vials in increasing aliquots before being diluted to 5 mL with pH buffer 8. All were UV/Vis analysed at 260 nm, with their absorbance values plotted on Excel against concentration.

Table 16. Proportions of the standards' components, their concentrations and absorbance values

Standard	Vol. Stock (mL)	Vol. pH buffer 8 (mL)	Conc. (mg/ml)	Absorbance @ 260 nm
1	0.200	4.800	5.01E-03	0.0395412
2	0.500	4.500	0.01252	0.11494
3	1.000	4.000	0.02504	0.217163
4	1.500	3.500	0.03756	0.304519
5	2.000	3.000	0.05008	0.406526
6	2.500	2.500	0.0626	0.511405
7	3.000	2.000	0.07512	0.595898

Sample	Conc. (mg/ml)	Absorbance
2Saccharin+pH8-1	5.02E-03	0.0395412
2Saccharin+pH8-2	0.01256	0.11494
2Saccharin+pH8-3	0.02512	0.217163
2Saccharin+pH8-4	0.03768	0.304519
2Saccharin+pH8-5	0.05024	0.406526
2Saccharin+pH8-6	0.0626	0.511405
2Saccharin+pH8-7	0.07512	0.595898

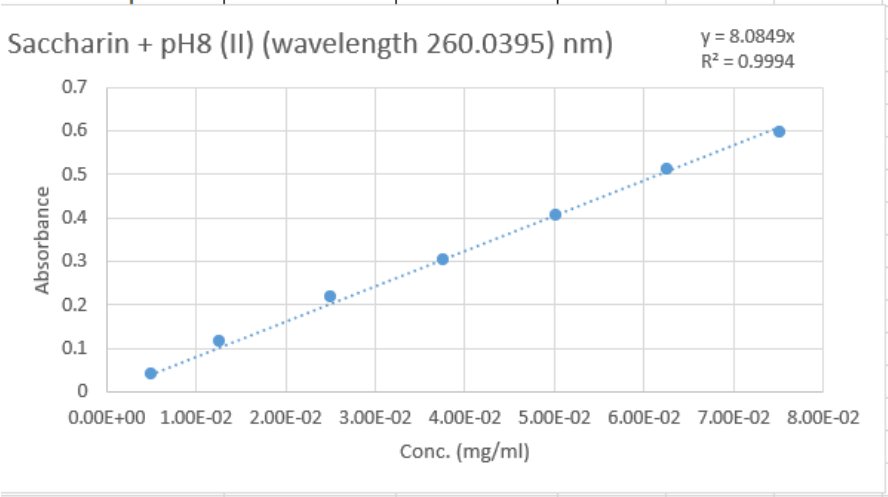

Fig.6: Saccharin calibration plot

3. Hydrogels

Results and discussion

Preparation of chitosan hydrogels.

Initially, the hydrogels were synthesized following the literature procedure, which involved dispersing chitosan (HMM) in 0.1M acetic acid (adjusted to pH 4 with 1M KOH) and adding 48% w/v β-glycerophosphate (the crosslinking agent) dropwise to the chitosan solutions while the solution is immersed in ice[51]. The very first trial took inspiration from the experiment by Ardhaoui and Cherif, studying viscosity of chitosan-based materials in DMSO/HCl[52]. This first attempt resulted in a prematurely solidified gel. Subsequently, various concentrations of crosslinker and chitosan were investigated. However, dispersal of chitosan in a solvent alone, like GP-water, HCl and water generally failed to produce solidified gels. Using HCl as the solvent only managed to solidify only two gels, meaning that this method is generally not reproducible.

Only the dropwise addition of a pH buffer (1M KOH) to the acetic acid, until the pH of the acid was 4, managed to consecutively solidify four gels. Sodium hydrogen carbonate $NaHCO_3$ was used as a co-crosslinking agent intended to stabilize and strengthen the chitosan (LMM)-based hydrogel and was selected because it allows for removal of water without raising the temperature, which would dissolve the polymeric region, and serves to support the crosslinked chain networks and prevent the collapse of pores during oven-drying[53], solidified gels successfully four consecutive times, with one premature solidification. Five more gels were solidified, but one of them solidified 2 h overdue, after oven-drying, and one was not solidified for injectability tests (CS-23).

Later, the first modification to the crosslinker/co-crosslinker configuration using $NaHCO_3$ as the solvent for seven β-GP solidified gels both at lower doses of chitosan/acetic acid: 45 mg/2 mL and at higher doses of at 90 mg/4 mL (numbered CS-30, CS-31, CS-32, CS-33, CS-34 and CS-38), which were all tested for injectability prior to and after oven-drying. One solidified at room temperature 4 min after oven-drying for 7 min, showing that when the concentration is too high, the gel solidifies at room temperature.

Later attempts to crosslink the chitosan chains in the solution with varying doses of the GP-water crosslinker ended only one premature solidification at room temperature. An attempt to strengthen the gel using porcine gelatin (46.0 mg) as the copolymer solidified the gel but was not reproducible.

Addition of methyl cellulose as a co-polymer (used as it is a widely-used organic polymer, allowing for better thermoresponsive behaviour of hydrogels[54]) resulted in three premature gelations, one full gelation and two partial gelations, indicating the lack of reproducibility of this method. Using a tertiary crosslinker $CaCl_2.2H_2O$ (used due to it being commonly used in the synthesis of poly(vinyl alcohol) (PVA)-based hydrogels[55], and has been found to enhance particle size, interfacial layer thickness,

apparent viscosity and viscoelastic behaviour of hydrogels[56]) resulted one full gelation and one non-solidification, indicating $CaCl_2.2H_2O$ is not an efficient crosslinker of chitosan-based hydrogels. Replacing β-GP-water with $C_{11}H_{22}CaO_{14}.H_2O$ as the primary crosslinker (used to protect the hydrogel from premature breakdown by enzymes due to its function as an enzyme inhibitor in the pathway of methyl glycosides[57]) resulted in one gelation, one partial gelation, and one non-solidification, meaning that this approach is not reproducible, and it is not an effective crosslinker in the chitosan-based system.

Characterisation of chitosan hydrogels.

The properties of the synthesized hydrogels (gelation time, reversibility of gel formation, injectability, stability in PBS and strength are summarized in Tables 17-19.

Table 17. Properties of chitosan-based hydrogels (HMM) using HCl as the solvent.

Hydrogel no.	Gelation time (min)	Reversibility of gel formation	Injectability	Stability in PBS	Strength
CS-5	-	-	Not tested	Not tested	No solidification
CS-46	10	Irreversible	Not tested	Stable in PBS	Medium-strength gel
CS-47	10	Irreversible	Not tested	Stable in PBS	Medium-strength-to-weak gel

Only the dropwise addition of a pH buffer (1M KOH) to the acetic acid, until the pH of the acid was 4, managed to produce hydrogels that were of acceptable strength. Overall this resulted in four gels that successfully solidified at 37 °C (three of medium strength, one weak) but were still not reversible and two gels prematurely

solidified at room temperature. They were stable in PBS, but were not tested for injectability. A lower molecular mass (LMM) of chitosan was used to improve compatibility of the chitosan with the proportions of the acetic acid solvent, investigated with varying doses of β-GP-water.

A lower molecular mass (LMM) of chitosan was used to improve compatibility of the chitosan with the proportions of the acetic acid solvent, investigated with varying doses of β-GP-water.

Table 18. Properties of the synthesized chitosan (LMM) β-GP hydrogels.

Hydrogel no.	Gelation time (min)	Reversibility of gel formation	Stability in PBS	Injectability	Strength
CS-12	-	-	-	-	No solidification
CS-13	10	Irreversible	Stable in PBS	-	Solidification at room temperature
CS-14	-	-	-	-	No solidification
CS-15	-	-	-	-	No solidification
CS-16	-	-	-	-	No solidification: chitosan did not dissolve
CS-17	8	Irreversible	Unstable in PBS	Not tested	Medium-strength gel

CS-23	-	-	-	-	No solidification, tested for injectability

The initial attempts to crosslink the chitosan chains in the solution with varying doses of the GP-water crosslinker ended only one premature solidification at room temperature, and an unstable solution in PBS. Adding porcine gelatin (46.0 mg) as the copolymer to CS-17, dissolved along with the chitosan, resulted in an 8-min gelation time, and a much stronger gel, but it was still irreversible and dispersed 5 min after being added to PBS. In water, the gel broke apart after 5 min, but did not dissolve until after 10 min. This indicates the gels are only stable as gels at low temperatures. Addition of sodium hydrogen carbonate $NaHCO_3$ to stabilize and strengthen the chitosan-based hydrogel generally resulted in decreased gelation times, and medium strength to strong gels that were stable in PBS, albeit still irreversible. Various concentrations of the chitosan and $NaHCO_3$ were tested. One of the gels did not receive the dose of co-crosslinker and was not oven-dried, being the first selected as a test substance for injectability (labelled CS-23, a chitosan (LMM)-acetic acid (90.8 mg/4 mL) solution, crosslinked with β-GP-water, with no co-crosslinking agent). The substance failed to fill the syringe when attempted to be drawn in, both with and without the needle. Later, the first modification to the crosslinker/co-crosslinker configuration using $NaHCO_3$ as the solvent for β-GP produced generally strong gels at lower doses of chitosan/acetic acid: 45 mg/2 mL, but weaker gels at 90 mg/4 mL, but both doses were tested for injectability. The inconsistency in gel strength was an indication that this modification is not reproducible.

Table 18. Properties of the synthesized chitosan β-GP-$NaHCO_3$ hydrogels (CS-28-CS-31 directly dissolved the β-GP in $NaHCO_3$ solution).

Hydrogel no.	Gelation time (min)	Stability in PBS	Reversibility of the gel formation	Injectability	Strength
CS-19	5	Stable in PBS	Irreversible	Not tested	Medium strength gel
CS-20	5	Stable in PBS	Irreversible	Not tested	Medium strength gel
CS-21	2	Stable in PBS	Irreversible	Not tested	Strong gel
CS-22	2	Not tested	Irreversible	Not tested	Solidification at room temperature
C-23	-	Not tested	-	Not injectable sans or via needle	No solidification, tested for injectability
C-24	120	Not tested	Irreversible	Not tested	Solidification at room temperature after 2 h at 37 °C
C-25	10	Stable in PBS	Irreversible	Not tested	Medium strength gel
C-26	7	Stable in PBS	Irreversible	Not tested	Strong gel
C-27	5	Stable in PBS	Irreversible	Not tested	Medium strength gel
CS-28	-	Irreversible	Not tested	Not tested	Solidification at room temperature
CS-29	10	Irreversible	Stable in PBS	Not tested	Medium-strength gel
CS-30	16	Irreversible	Not tested	Injectable sans needle, injectable via needle	Half gelated after 40 min at room temperature, the other tested for injectability before 10 min oven-drying

CS-31	20	Irreversible	Not tested	Injectable sans needle, injectable via needle	Half gelated at room temperature after 10 min in oven - tested for injectability, other half gelated after 10 min oven-drying

This generally resulted in decreased gelation times, and medium strength to strong gels that were stable in PBS, albeit still irreversible. These results indicate the efficiency of $NaHCO_3$ as a crosslinker of chitosan chains, but also the importance of the amount of solvent, as sub-optimal levels of solvent could jeopardize the reaction. When the reaction was modified for the $NaHCO_3$ to act as the solvent for the primary crosslinker, once it solidified at room temperature 4 min after oven-drying for 7 min, but mostly resulted in medium-strength gels, six of which were selected for injectability tests (labelled CS-30, CS-31, CS-32, CS-33, CS-34 and CS-38) prior to and after oven-drying. The second injectability test involved three chitosan-acetic acid hydrogels: CS-30, CS-31 (both ~90 mg/4 mL) and CS-32 (45.6 mg/2 mL). CS-30 and CS-31 were easily injectable sans needle but were difficult to draw in via needle. However, they were administrable via needle. CS-32 was easily injectable both sans and via needle. The third injectability test involved CS-33 and CS-34 (the same composition as previous gels, but with a 0.125 mL dose of 112.4 mg/0.25 mL) were both injectable sans and via needle before solidification in the oven, even after the latter was left for 2 h at room temperature. CS-38, a repetition of CS-33, with increased dose of $NaHCO_3$ 0.25 mL, showed that the stronger a hydrogel is, the less injectable it is.

The results show that when the concentration is too high, the gel solidifies at room temperature. A lower molecular mass (LMM) of chitosan was used to improve

compatibility of the chitosan with the proportions of the acetic acid solvent, investigated with varying doses of β-GP-water.

Table 19. Properties of the synthesized chitosan (LMM) β-GP hydrogels tested for injectability.

Hydrogel no.	Gelation time (min)	Reversibility of gel formation	Stability in PBS	Injectability	Strength
CS-23	-	-	-	-	No solidification, tested for injectability
CS-30	16	Irreversible	-	Injectable sans needle, not injectable via needle	One half gelated after 40 min at room temperature, the other tested for injectability before oven-drying for 10 min
CS-31	20	Irreversible	-	Injectable sans needle, not injectable via needle	One half gelated at room temperature after 10 min in oven and tested for injectability, other half gelated after 10 min in oven
CS-32	-	Irreversible	Stable in PBS	Injectable	Weak gel: Solidification at room temperature, after tested for injectability
CS-33	9	Irreversible	Stable in PBS	Injectable	Strong gel: Solidification after injectability test

CS-34	1440	Irreversible	Stable in PBS	Injectable	Medium strength gel: Solidification after injectability tests
CS-38	6	Irreversible	Stable in PBS	Injectable	Strong gel: Solidification after injectability test

Alternative methods include addition of methyl cellulose as a co-polymer resulted in three premature gelations, one strong gel and two weak gels, indicating the lack of reproducibility of this method.

Using a tertiary crosslinker $CaCl_2.2H_2O$ resulted in a medium gel and lack of gelation, indicating $CaCl_2.2H_2O$ is not an efficient crosslinker of chitosan-based hydrogels

Replacing β-GP-water with $C_{11}H_{22}CaO_{14}.H_2O$ as the primary crosslinker resulted in a very weak gel, a strong gel and lack of solidification, meaning that this approach is not reproducible, and it is not an effective crosslinker in the chitosan-based system.

Preparation of PF-127 hydrogels.

Pluronic PF-127 is a suitable polymer for hydrogels, as it is biocompatible, non-toxic, and biodegradable. Pluronic F-127 was also selected due to its thermosensitivity: this unique property allows it to carry encapsulated cells in its structure, favourable conditions for initial cell adhesion within defect sites[58]. Subsequently, various concentrations of PF-127 were tested, with hydroxypropyl cellulose as the co-polymer and crosslinker. PF-1 (using 200.6 mg of PF-127 and 20.4 mg of cellulose in 2 mL of water) failed to dissolve, while PF-2 (200.4 mg PF-127 and 20.5 mg hydroxypropyl cellulose), while PF-3 (500.9 mg PF-127 and 20.7 mg hydroxypropyl cellulose) solidified. The result was the same for PF-4 (400.5 mg PF-127 and 19.96 mg hydroxypropyl cellulose). PF-5 (300.5 mg PF-127 and 20.1 mg hydroxypropyl cellulose) failed to solidify. PF-6 (using 500.1 mg PF-127 and 40.1 mg

hydroxypropyl cellulose), and PF-7 yielded the same result as PF-3 and PF-4. PF-8 (300.8 mg PF-127 and 40.3 mg hydroxypropyl cellulose) partially solidified.

The next PF-127 hydrogels, PF-10 (500.9 mg PF-127, 40.0 mg hydroxypropyl cellulose), PF-11 (500.3 mg PF-127, 20.5 mg hydroxypropyl cellulose), PF-12 (500.3 mg PF-127, 40.3 mg hydroxypropyl cellulose), PF-14 (500.4 mg PF-127, 20.2 mg hydroxypropyl cellulose), and PF-15 (500.4 mg PF-127, 20.1 hydroxypropyl cellulose) were loaded with saccharin (62.5 mg in 25 mL water stock, 2 mL acting as solvent) and amoxicillin trihydrate (62.8 mg in 25 mL water stock, 2 mL acting as solvent) as test substances. Saccharin was used, as it is a carbonic anhydrase inhibitor. Amoxicillin trihydrate was used as a model compound due to it being a potent antibiotic used to treat bacterial infections e.g. pneumonia[59], and its higher resistance to being metabolized by gastric acid, which enables its high serum levels when administered orally[60].

Characterisation of PF-127 hydrogels.

In the case of PF-1, in which the PF-127-cellulose powder mixture failed to dissolve in 2 mL water (the volume and type of solvent used in all PF-127-based gels) indicated that cellulose is unsuitable as a co-crosslinker and co-polymer. PF-2, using 200.6 mg of PF-127 and 20.5 mg of hydroxypropyl cellulose dissolved the powders in water, but failed to solidify the gel, indicating that 200 mg of the main polymer is insufficient to create a PF-127-based gel. PF-3 (with 500.9 mg PF-127 and 20.7 mg hydroxypropyl cellulose) was the first successful PF-127-based gel, solidifying into a medium-strength gel after 8.5 min of oven-drying at 40 °C. It was then found to be stable in PBS, when a small portion of the gel was transferred via spatula into a PBS vial. More importantly, its reliquefication after 5 min at room temperature post-solidification, indicated this was the first reversible hydrogel. After easily filling the syringe via needle, and being retransferred back to the vial, it was confirmed to be injectable. PF-4 (using 400.5 mg PF-127 and 19.96 mg hydroxypropyl cellulose)

yielded the same results of gel strength, stability in PBS, injectability, and reversibility as PF-3, but solidifying in 6 min. PF-5 (using 300.5 mg PF-127 and 20.1 mg hydroxypropyl cellulose) failed to solidify indicating that 300 mg of the main polymer is insufficient for gelation. Subsequently, three more hydrogels, PF-6 (500.1 mg PF-127 and 40.1 mg hydroxypropyl cellulose), PF-7 (400.0 mg PF-127 and 20.1 mg hydroxypropyl cellulose) and PF-8 (300.8 mg PF-127 and 40.3 mg hydroxypropyl cellulose) were prepared. PF-6 and PF-7 had the same gel strength, stability in PBS, injectability, and reversibility as PF-3 and PF-4, but both gelating in under 4.5 min. PF-8 took 24 hours to gelate, resulting in a very weak gel, but nonetheless stable in PBS, and reversible. This was another indication that 300 mg of the main polymer did not give the gel the required gel strength.

Table 21. Proportions of PF-127-based hydrogels using cellulose and hydroxypropyl cellulose as the co-polymer and crosslinking

Hydrogel no.	Gelation time (min)	Reversibility of gel formation	Stability in PBS	Injectability	Strength
PF-1	-	-	-	-	Did not dissolve
PF-2	138	-	-	-	Did not solidify
PF-3	8.6	Reversible	Stable in PBS	Injectable	Medium-strength gel
PF-4	6.	Reversible	Stable in PBS	Injectable	Medium-strength gel
PF-5	-	-	-	-	Did not gelate
PF-6	4.2	Reversible	Stable in PBS	Injectable	Medium-strength gel
PF-7	4.5	Reversible	Stable in PBS	Injectable	Medium-strength gel
PF-8	1440	Reversible	Stable in PBS	Injectable	Weak gel

The next four, PF-10, PF-11, PF-12, PF-14, PF-15 loaded with saccharin, and amoxicillin trihydrate, respectively, into the water solvent also produced injectable hydrogels, both sans and via needle, were stable in PBS and all had a gelation time of 10 min. These particular gels were tested for the release of the substances in them.

Table 22. Proportions of PF-127-based hydrogels loaded with saccharin (PF-10-PF-12) and amoxicillin trihydrate (PF-14 and PF-14)

Hydrogel no.	Gelation time (min)	Reversibility of gel formation	Stability in PBS	Injectability	Strength
PF-10	10	Reversible	Stable in PBS	Injectable	Medium-strength gel
PF-11	10	Reversible	Stable in PBS	Injectable	Medium-strength gel
PF-12	10	Reversible	Stable in PBS	Injectable	Medium-strength gel
PF-14	10	Reversible	Stable in PBS	Injectable	Medium-strength gel
PF-15	10	Reversible	Stable in PBS	Injectable	Medium-strength gel

Release studies

Chitosan-based hydrogels: Release through a membrane

The first release test involved nicotinamide as a model compound and was performed as a control to determine the passage of 5 mL of a nicotinamide-PBS stock solution through the membrane of the dialysis tube, with no gel carrier.

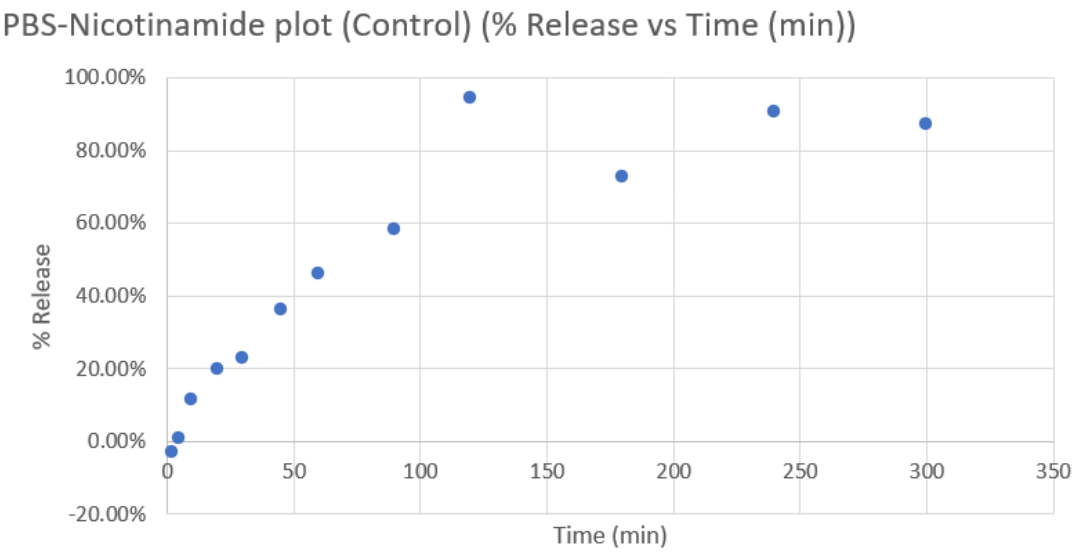

Fig.7: Nicotinamide release plot (control)

The highest release percentage calculated using the calibration plot's equation[61] was 94.42% after 2 h, and after 5 h, had dropped to 87.23%, indicating that almost all of the nicotinamide was released. A possible reason for the supposed lowering of the percentage released could be due to an error in extracting the sample using the automatic pipette. Overall, the fact that 45.95% was released in the span of 1 h indicates a very slow release through the membrane, showing that the membrane method is unsuitable release studies.

PF-127-based hydrogels: Release sans membrane

The first release experiment of PF-127-based hydrogels, second controlled experiment involved a PF-127-based hydrogel loaded with water to test if PF-127 based hydrogels interfere with UV/Vis spectra. The absorbance values ranged from -0.046 to 0.044, which is an indication of very little to no interference.

Saccharin was the first substance investigated for release from PF-127-based hydrogels. Three experiments were performed to determine if hydrogel composition had any impact on the rate of release of saccharin and the correct wavelength at which to measure the rate of release, using the following proportions: 500.9 mg of PF-127 & 40.0 mg of hydroxypropyl cellulose (PF-10, which was the gel into transferred to a centrifuge tube, with 35 mL of PBS added directly to the gel, with no dialysis tube), 500.3 mg of PF-127 & 20.5 mg of hydroxypropyl cellulose (PF-11), and 500.3 mg of PF-127 & 40.3 mg of hydroxypropyl cellulose (PF-12), respectively.

For PF-10 and PF-11, the % of saccharin released was higher for the first three hours in PF-10 (144.8% after 1 h, 202.5% after 2 h and 235.5% after 3 h) than in PF-11 (78.4% after 1 h, 169.8% after 2 h, and 200.2% after 3 h), with PF-12 showing slightly higher release rates (120.1% after 1 h, 197.2% after 2 h, and 236.0% after 3 h). The reason for abnormally high percentage results was likely the presence of contaminants in the PBS solution. This affirmed that a higher concentration of

hydroxypropyl cellulose (~20 mg/ml) means a faster rate of release of the model substance in PF-127 based gels. While the drug release was still fast, the better wavelength at which to measure the release of saccharin was 223 nm. To provide a standard aiding to assess how 2 mL of the saccharin-water analyte would behave if fully released in 50 mL of PBS, the stock (2 mL) was diluted with 50 mL of PBS, 0.5 mL of the diluted solution was diluted to 5 mL with PBS, which was UV/Vis analysed, gave an absorbance value of 0.663644.

The amoxicillin trihydrate (4 mL) was loaded into a PF-127 hydrogel (acting as the solvent) composed of 500.4 mg of PF-127 and 20.2 mg of hydroxypropyl cellulose (labelled PF-14), with absorbance values obtained at 225 nm The experiment was later repeated with the same parameters, resulting in the following graphs:

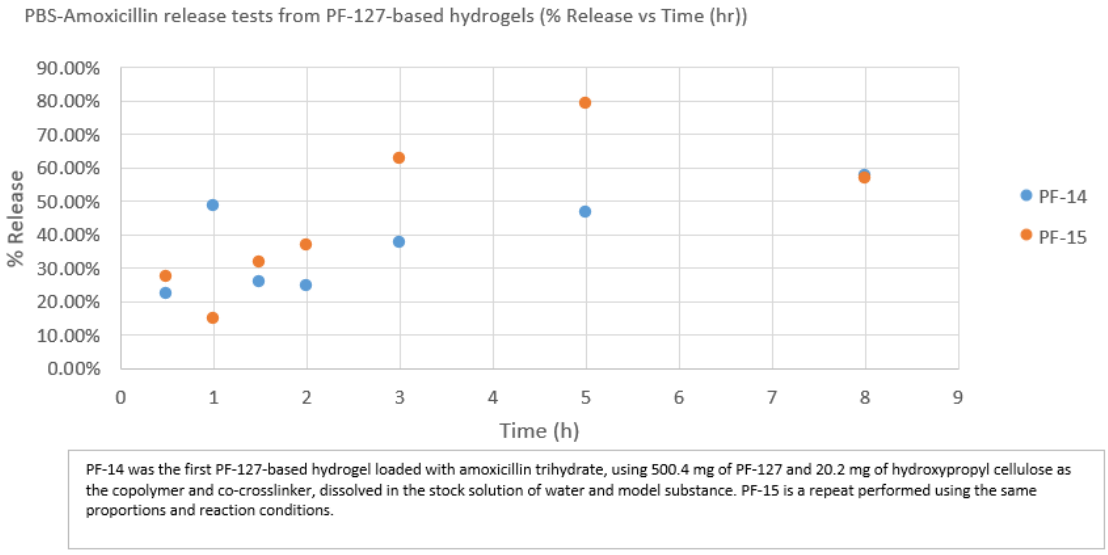

Fig.8: Amoxicillin trihydrate release tests from PF-127-based hydrogels

The fluctuations in the percentage of amoxicillin trihydrate, shown by the plots of the two tests are possibly due to error in extracting the samples using the automatic pipette. Overall, PF-127 based hydrogels have shown to release model substances at a quicker rate.

Experimental section

1. Materials and methods:

- Chemicals: Potassium hydroxide (KOH) (*Millipore Corporation (Merck)*), glacial acetic acid (*Fisher Scientific*), β-glycerophosphate (β-GP) (*Sigma-Aldrich*), chitosan (HMM: *Sigma-Aldrich*, LMM: *Glentham Life Sciences*), dimethylsulfoxide (DMSO) (*TCI Chemicals*), saccharin (*Sigma-Aldrich*), phosphate-buffered saline (PBS), sodium hydrogen carbonate ($NaHCO_3$) (*Fisher Scientific*), calcium chloride dihydrate $CaCl_2.2H_2O$ (*TCI Chemicals*), nicotinamide (*Sigma-Aldrich*), hyaluronic acid (TCI Chemicals), magnesium acetate ($Mg(CH_3COO)_2.4H_2O$) (Sigma-Aldrich), calcium gluconate monohydrate (TCI Chemicals), Pluronic F-127 (*Sigma-Aldrich*), methyl cellulose (*TCI Chemicals*), 4-nitrophenol (*Alfa Aesar*), amoxicillin trihydrate (*TCI Chemicals*).
- UV/Vis spectra recorded on a Cary-Varian UV/Vis spectrometer

2. Preparation of chitosan hydrogels

Chitosan (HMM) (59.5 mg) was initially dispersed in a β-GP-water (96.1 mg/2 mL) solution for 1 hr before DMSO (0.2 mL) was added dropwise (numbered CS-1). A larger dose of chitosan (96.4 mg) was subsequently dispersed in β-GP-water solution, before a higher-concentration β-GP (192.1 mg/2 mL) solution was used to disperse chitosan, with its dose lowered to 60 mg. The crosslinker's concentration was increased to 384.3 mg/2 mL, then lowered to 96.6 mg/1 mL, as per the table:

Table 23. Early chitosan (HMM)-based hydrogels crosslinked with β-GP-water

Hydrogel no.	Weight of chitosan (HMM) (mg)	Solvent	Primary crosslinker	Temperature (°C)
CS-2	96.4	β-GP/water (96.1 mg/2 mL)	β-GP/water (96.1 mg/2 mL)	37
CS-3	60.3	β-GP/water (192.1 mg/2 mL)	β-GP/water (192.1 mg/2 mL)	37

CS-4	60.3	β-GP/water (384.3 mg/2 mL)	β-GP/water (384.3/2 mL)	37
CS-5	60.9	β-GP/water (96.6 mg/1 mL)	β-GP/water (96.6 mg/1 mL)	37

As a change of solvent, another dose of chitosan (60.9 mg) (CS-3) was dispersed in a dispersed 0.1M HCl (3 mL), before adding β-GP dropwise (96.6 mg/0.5 mL) to the solution in ice and oven-drying it at 37 °C to solidify. Water was used to disperse two more chitosan (60 mg) (CS-4 and CS-5) portions in two volumes, first with 3 mL and then 6 mL, before the solutions were left at room temperature. Another dose of chitosan was dispersed in a 0.1M acetic acid solution (4.5 mL) buffered to pH 4 via dropwise addition of 1M KOH overnight before adding β-GP dropwise to the solution in ice and oven-drying it at 37 °C to solidify. The experiment was later repeated in duplicate in a higher concentration of crosslinker (450 mg/0.5 mL H_2O), with the proportions given in the table:

Table 24. Proportions of chitosan-based hydrogels featuring a pH buffer added to their solvent.

Hydrogel no.	**Weight of chitosan (HMM) (mg)**	**Solvent**	**pH buffer**	**Primary crosslinker**	**Temperature (°C)**
CS-9	60.9	0.1M Acetic acid (4.5 mL)	1M KOH	β-GP/water (96.5 mg/1 mL)	37
CS-10	90.7	0.1M Acetic acid (4 mL)	1M KOH	β-GP/water (450.5 mg/1 mL)	37
CS-11	90.5	0.1M Acetic acid (4 mL)	1M KOH	β-GP/water (450.6 mg/0.5 mL)	37

Another chitosan-acetic acid (lower molecular mass: LMM, used for all chitosan-based hydrogel onwards, except CS-47) (89.3 mg/4 mL) mix was sonicated for 5 min and stirred for 30 min in quadruplicate and then stirred and sonicated for 10 min. The mixture was then cooled in ice for 10 min before adding β-GP dropwise while stirring. Further stirring for 1 h in ice and oven-drying 37 °C was to solidify the gel. The experiment was repeated in quadruplicate with a higher concentration (450 mL/0.5 mL H_2O). To strengthen the gels using a copolymer, initially, a 90.3 mg/3 mL chitosan-acetic acid solution (CS-17) was dissolved with porcine gelatin (46.0 mg), before adding the β-GP-water crosslinker (414.5 mg/0.5 mL) before placing oven-drying the gel solution and adding a portion of it to PBS:

Table 25. Proportions of chitosan (LMM)-based hydrogels.

Hydrogel no.	Weight of chitosan (HMM) (mg)	Solvent	pH buffer	Primary crosslinker	Temperature (°C)
CS-12	89.3	0.1M Acetic acid (4 mL)	1M KOH	β-GP/water (96.4 mg/0.5 mL)	37
CS-13	90.6	0.1M Acetic acid (4 mL)	1M KOH	β-GP/water (450.5 mg/0.5 mL)	37
CS-14	90.4	0.1M Acetic acid (4 mL)	1M KOH	β-GP/water (450.8 mg/0.5 mL)	37
CS-15	90.6	0.1M Acetic acid (4 mL)	1M KOH	β-GP/water (450.8 mg/0.5 mL)	37
CS-16	90.4	0.1M Acetic acid (4 mL)	1M KOH	β-GP/water (450.8 mg/0.5 mL)	37

CS-17	90.3	0.1M Acetic acid (4 mL)	1M KOH	β-GP-Gelatin/water (414.5 mg, 46.0 mg/0.5 mL)	37

A new $NaHCO_3$ solution was prepared by dissolving 210.7 mg in 5 mL water. This solution would function as a co-crosslinking agent, with 0.5 mL of it added dropwise to the gel solution after β-GP (450.1 mg/0.5 mL H_2O) while stirring in ice, before being left to reach room temperature for 15 min. Its pH was measured as 7.4 and the gel was then oven-dried at 37°C. The repetitions of this method were performed in octuplicate, with half of the repetitions using 4 mL of 0.1M acetic acid instead of 3 mL, three repetitions using 340 mg/0.5 mL H_2O β-GP, five repetitions using 225 mg/0.5 mL H_2O β-GP, and three repetitions using half the dose of $NaHCO_3$. One was tested for injectability. Proportions are given below:

Table 26. Proportions of chitosan-based hydrogels featuring a co-crosslinker

Hydrogel no.	**Weight of chitosan (LMM) (mg)**	**Solvent**	**pH buffer**	**Primary crosslinker**	**Co-crosslinker**	**Temperature (°C)**
CS-19	90.4	0.1M Acetic acid (3 mL)	1M KOH	β-GP/water (450.1 mg/0.5 mL)	$NaHCO_3$ (0.5 mL)	37
CS-20	90.5	0.1M Acetic acid (3 mL)	1M KOH	β-GP/water (225.0 mg/0.5 mL)	$NaHCO_3$ (0.5 mL)	37
CS-21	90.6	0.1M Acetic acid (3 mL)	1M KOH	β-GP/water (340.1 mg/0.5 mL)	$NaHCO_3$ (0.5 mL)	37

CS-22	90.7	0.1M Acetic acid (3 mL)	1M KOH	β-GP/water (340.1 mg/0.5 mL)	$NaHCO_3$ (0.5 mL)	37
CS-23	90.8	0.1M Acetic acid (3 mL)	1M KOH	β-GP/water (225.0 mg/0.5 mL)	-	-
CS-24	90.3	0.1M Acetic acid (4 mL)	1M KOH	β-GP/water (225.3 mg/0.5 mL)	$NaHCO_3$ (0.25 mL)	37
CS-25	90.2	0.1M Acetic acid (4 mL)	1M KOH	β-GP/water (225.2 mg/0.5 mL)	$NaHCO_3$ (0.25 mL)	37
CS-26	90.5	0.1M Acetic acid (4 mL)	1M KOH	β-GP/water (225.7 mg/0.5 mL)	$NaHCO_3$ (0.5 mL)	37
CS-27	90.6	0.1M Acetic acid (4 mL)	1M KOH	β-GP/water (340.2 mg/0.5 mL)	$NaHCO_3$ (0.25 mL)	37

The procedure was later modified with $NaHCO_3$ was used as the solvent for β-GP instead of water. The new β-GP-$NaHCO_3$ (225.6 mg/0.5 mL) was added while the gel solution was stirred in in ice for 10 min. The gel solution was left to reach room temperature for 10 min and placed in the oven at 37 °C. The procedure was later repeated in triplicate, with lower doses of β-GP-$NaHCO_3$ (112 mg/0.5 mL) used in two of the repeats, shown below:

Table 27. Proportions of chitosan-based hydrogels with the first modification of the crosslinker/co-crosslinker configuration

Hydrogel no.	Weight of chitosan (LMM) (mg)	Solvent	pH buffer	Primary crosslinker	Co-crosslinker	Temperature (°C)
CS-28	90.1	0.1M Acetic acid (4 mL)	1M KOH	β-GP/$NaHCO_3$ (225.6 mg/0.5 mL)	$NaHCO_3$ (0.5 mL)	37
CS-29	90.3	0.1M Acetic acid (4 mL)	1M KOH	β-GP/$NaHCO_3$ (225.6 mg/0.5 mL)	$NaHCO_3$ (0.5 mL)	37
CS-30	90.8	0.1M Acetic acid (4 mL)	1M KOH	β-GP/$NaHCO_3$ (112.4 mg/0.5 mL) (0.165 mL for half, 0.335 mL for other half)	$NaHCO_3$ (0.5 mL)	37
CS-31	90.4	0.1M Acetic acid (4 mL)	1M KOH	β-GP/$NaHCO_3$ (112.3 mg/0.5 mL) (0.165 mL for half, 0.165 mL for other half)	$NaHCO_3$ (0.5 mL)	37

The experiment was later modified by combining GP-water/$NaHCO_3$ together into one vial, and adding the mixture dropwise to the chitosan-based gel solutions (CS-32, CS-33, CS-34, and CS-38 were tested for injectability), as per the table:

Table 28. Proportions of chitosan-based hydrogels with second modification to the crosslinker/co-crosslinker configuration

Hydrogel no.	Weight of chitosan (LMM) (mg)	Solvent	pH buffer	Primary crosslinker	Co-crosslinker	Temperature (°C)
CS-32	45.6	0.1M Acetic acid (2 mL)	1M KOH	β-GP-water/$NaHCO_3$ (66.5 mg/0.25 mL/0.25 mL)	$NaHCO_3$ (0.25 mL)	37
CS-33	45.1	0.1M Acetic acid (2 mL)	1M KOH	β-GP-water/$NaHCO_3$ (112.0 mg/0.25 mL/0.25 mL)	$NaHCO_3$ (0.25 mL)	37
CS-34	45.5	0.1M Acetic acid (2 mL)	1M KOH	β-GP-water/$NaHCO_3$ (170.4 mg/0.25 mL/0.125 mL)	$NaHCO_3$ (0.125 mL)	37
CS-35	45.4	0.1M Acetic acid (2 mL)	1M KOH	β-GP-water/$NaHCO_3$ (66.1 mg/0.25 mL/0.25 mL)	$NaHCO_3$ (0.25 mL)	37
CS-36	45.4	0.1M Acetic acid (2 mL)	1M KOH	β-GP-water/$NaHCO_3$ (112.8 mg/0.25 mL/0.25 mL)	$NaHCO_3$ (0.125 mL)	37

CS-37	45.6	0.1M Acetic acid (2 mL)	1M KOH	β-GP-water/$NaHCO_3$ (170.4 mg/0.25 mL/0.125 mL)	$NaHCO_3$ (0.125 mL)	37
CS-38	45.4	0.1M Acetic acid (2 mL)	1M KOH	β-GP-water/$NaHCO_3$ (112.4 mg/0.25 mL/0.25 mL)	$NaHCO_3$ (0.25 mL)	37

Another modification to the crosslinker/co-crosslinker configuration was the replacement of $NaHCO_3$ with a $CaCl_2.2H_2O$ solution (72.26 mg/mL), with three gels tested, per the table:

Table 29. Proportions of chitosan-based hydrogels with a calcium chloride dihydrate co-crosslinker

Hydrogel no.	**Weight of chitosan (LMM) (mg)**	**Solvent**	**pH buffer**	**Primary crosslinker**	**Co-crosslinker**	**Temperature (°C)**
CS-39	45.3	0.1M Acetic acid (2 mL)	1M KOH	β-GP-water/$CaCl_2.2H_2O$ (112.5 mg/0.25 mL/0.125 mL)	$CaCl_2.2H_2O$ (0.125 mL)	37
CS-40	45.2	0.1M Acetic acid (2 mL)	1M KOH	β-GP-water/$CaCl_2.2H_2O$ (112.5 mg/0.25 mL/0.125 mL)	$CaCl_2.2H_2O$ (0.125 mL)	37

CS-41	45.6	0.1M Acetic acid (2 mL)	1M KOH	β-GP-water/$CaCl_2.{}_2H_2O$ (112.1 mg/0.25 mL/0.125 mL)	$CaCl_2.{}_2H_2O$ (0.125 mL)	37

Addition of a tertiary crosslinker came in the form of $NaHCO_3$ and $MgCH_3COO_2$, with 0.125 mL of both added to a separate chitosan-acetic acid (45 mg/2mL) gel solution. Subsequently, two new chitosan portions (45 mg) were dissolved in 0.1M HCl (2 mL), after which the $NaHCO_3$ solution (0.125 mL) was added to the GP-water (112 mg/0.5 mL) solution in ice, left at room temperature for 3 hrs before being oven-dried for 6 min.

Table 30. Proportions of chitosan (HMM)-based hydrogels dissolved using HCl

Hydrogel no.	**Weight of chitosan (HMM) (mg)**	**Solvent**	**Primary crosslinker**	**Co-crosslinker**	**Temperature (°C)**
C-46	45.2	0.1M HCl (2 mL)	β-GP-water/$NaHCO_3$ (112.4 mg/0.25 mL/0.125 mL)	$NaHCO_3$ (0.125 mL)	37
C-47	45.4	0.1M HCl (2 mL)	β-GP/water/ $NaHCO_3$ (112.4 mg/0.25 mL/0.125 mL)	$NaHCO_3$ (0.125 mL)	37

Two new chitosan-acetic acid (45 mg/2 mL) solutions were dissolved in conjunction with methyl cellulose (45 mg), before administration of β-GP-water-$NaHCO_3$ (112 mg/0.25

mL/0.125 mL) crosslinkers and oven-drying at 37 °C. The experiment was repeated in quintuplicate: two repetitions used 10 mg of methyl cellulose, and three using 45 mg, 20 mg, and 15 mg, respectively. The β-GP-water-$NaHCO_3$ crosslinker proportions were also altered for 10 mg, 20 mg and 15 mg repetitions: 112 mg/0.125 mL/0.125 mL. Other modifications performed include replacing the β-GP-water-$NaHCO_3$ with $C_{11}H_{22}CaO_{14}.H_2O$ as the primary crosslinker, performed in triplicate.

3. Characterisation of chitosan hydrogels

To determine the correct solvent for chitosan-based hydrogels, chitosan (HMM) (59.5mg) was initially dispersed in a β-GP-water (96.1 mg/2 mL) solution for 1 hr before DMSO (0.2 mL) was added dropwise (numbered CS-1). A larger dose of chitosan (96.4 mg) was subsequently dispersed in β-GP-water solution, before a higher-concentration β-GP (192.1 mg/2 mL) solution was used to disperse chitosan, with its dose lowered to 60 mg. The crosslinker's concentration was increased to 384.3 mg/2 mL, then lowered to 96.6 mg/1 mL, as per the table:

Table 31. Early chitosan (HMM)-based hydrogels crosslinked with β-GP-water

Hydrogel no.	Weight of chitosan (HMM) (mg)	Solvent	Primary crosslinker	Temperature (°C)
CS-2	96.4	β-GP/water (96.1 mg/2 mL)	β-GP/water (96.1 mg/2 mL)	37
CS-3	60.3	β-GP/water (192.1 mg/2 mL)	β-GP/water (192.1 mg/2 mL)	37
CS-4	60.3	β-GP/water (384.3 mg/2 mL)	β-GP/water (384.3/2 mL)	37
CS-5	60.9	β-GP/water (96.6 mg/1 mL)	β-GP/water (96.6 mg/1 mL)	37

As a change of solvent, another dose of chitosan (60.9 mg) (CS-3) was dispersed in a dispersed 0.1M HCl (3 mL), before adding β-GP dropwise (96.6 mg/0.5 mL) to the solution in ice and oven-drying it at 37°C to solidify. Water was used to disperse two more chitosan (60 mg) (CS-4 and CS-5) portions in two volumes, first with 3 mL and then 6 mL, before the solutions were left at room temperature. Another dose of chitosan was dispersed in a 0.1M acetic acid solution (4.5 mL) buffered to pH 4 via dropwise addition of 1M KOH overnight before adding β-GP dropwise to the solution in ice and oven-drying it at 37 °C to solidify. The experiment was later repeated in duplicate in a higher concentration of crosslinker (450 mg/0.5 mL H_2O), with the proportions given in the table:

Table 32. Proportions of chitosan-based hydrogels featuring a pH buffer added to their solvent.

Hydrogel no.	Weight of chitosan (HMM) (mg)	Solvent	pH buffer	Primary crosslinker	Temperature (°C)
CS-9	60.9	0.1M Acetic acid (4.5 mL)	1M KOH	β-GP/water (96.5 mg/1 mL)	37
CS-10	90.7	0.1M Acetic acid (4 mL)	1M KOH	β-GP/water (450.5 mg/1 mL)	37
CS-11	90.5	0.1M Acetic acid (4 mL)	1M KOH	β-GP/water (450.6 mg/0.5 mL)	37

For better biocompatibility, a lower molecular mass (LMM) chitosan was used. CS-12 (89.3 mg/4 mL) was sonicated for 5 min and stirred for 30 min in quadruplicate and then stirred and sonicated for 10 min. The mixture was then cooled in ice for 10 min before adding β-GP dropwise while stirring. Further stirring for 1 hr in ice and oven-drying 37°C was to solidify the gel. The experiment was repeated in quadruplicate with a higher concentration (450

mL/0.5 mL H_2O). LMM chitosan was used on all chitosan-based hydrogels onwards, except CS-46 and CS-47. To strengthen chitosan-based hydrogels, the first attempt involved using a co-polymer: a 90.3 mg/3 mL chitosan-acetic acid solution (CS-17) was dissolved with porcine gelatin (46.0 mg), before adding the β-GP-water crosslinker (414.5 mg/0.5 mL) before placing oven-drying the gel solution and adding a portion of it to PBS:

Table 33. Proportions of chitosan (LMM)-based hydrogels.

Hydrogel no.	Weight of chitosan (HMM) (mg)	Solvent	pH buffer	Primary crosslinker	Temperature (°C)
CS-12	89.3	0.1M Acetic acid (4 mL)	1M KOH	β-GP/water (96.4 mg/0.5 mL)	37
CS-13	90.6	0.1M Acetic acid (4 mL)	1M KOH	β-GP/water (450.5 mg/0.5 mL)	37
CS-14	90.4	0.1M Acetic acid (4 mL)	1M KOH	β-GP/water (450.8 mg/0.5 mL)	37
CS-15	90.6	0.1M Acetic acid (4 mL)	1M KOH	β-GP/water (450.8 mg/0.5 mL)	37
CS-16	90.4	0.1M Acetic acid (4 mL)	1M KOH	β-GP/water (450.8 mg/0.5 mL)	37
CS-17	90.3	0.1M Acetic acid (4 mL)	1M KOH	β-GP-Gelatin/water (414.5 mg, 46.0 mg/0.5 mL)	37

Another approach to strengthening the gel was using a co-crosslinker, hence why a new $NaHCO_3$ solution was prepared by dissolving 210.7 mg in 5 mL water. This solution would function as a co-crosslinking agent, with 0.5 mL of it added dropwise to the gel solution after

β-GP (450.1 mg/0.5 mL H_2O) while stirring in ice, before being left to reach room temperature for 15 min. Its pH was measured as 7.4 and the gel was then oven-dried at 37 °C. The repetitions of this method were performed in octuplicate, with half of the repetitions using 4 mL of 0.1M acetic acid instead of 3 mL, three repetitions using 340 mg/0.5 mL H_2O β-GP, five repetitions using 225 mg/0.5 mL H_2O β-GP, and three repetitions using half the dose of $NaHCO_3$. One (CS-23) was tested for injectability. Proportions are given below:

Table 34. Proportions of chitosan-based hydrogels featuring $NaHCO_3$ as a co-crosslinker

Hydrogel no.	Weight of chitosan (LMM) (mg)	Solvent	pH buffer	Primary crosslinker	Co-crosslinker	Temperature (°C)
CS-19	90.4	0.1M Acetic acid (3 mL)	1M KOH	β-GP/water (450.1 mg/0.5 mL)	$NaHCO_3$ (0.5 mL)	37
CS-20	90.5	0.1M Acetic acid (3 mL)	1M KOH	β-GP/water (225.0 mg/0.5 mL)	$NaHCO_3$ (0.5 mL)	37
CS-21	90.6	0.1M Acetic acid (3 mL)	1M KOH	β-GP/water (340.1 mg/0.5 mL)	$NaHCO_3$ (0.5 mL)	37
CS-22	90.7	0.1M Acetic acid (3 mL)	1M KOH	β-GP/water (340.1 mg/0.5 mL)	$NaHCO_3$ (0.5 mL)	37
CS-23	90.8	0.1M Acetic acid (3 mL)	1M KOH	β-GP/water (225.0 mg/0.5 mL)	-	-

CS-24	90.3	0.1M Acetic acid (4 mL)	1M KOH	β-GP/water (225.3 mg/0.5 mL)	$NaHCO_3$ (0.25 mL)	37
CS-25	90.2	0.1M Acetic acid (4 mL)	1M KOH	β-GP/water (225.2 mg/0.5 mL)	$NaHCO_3$ (0.25 mL)	37
CS-26	90.5	0.1M Acetic acid (4 mL)	1M KOH	β-GP/water (225.7 mg/0.5 mL)	$NaHCO_3$ (0.5 mL)	37
CS-27	90.6	0.1M Acetic acid (4 mL)	1M KOH	β-GP/water (340.2 mg/0.5 mL)	$NaHCO_3$ (0.25 mL)	37

The first injectability test, using CS-23 (chitosan: 90.8 mg, acetic acid (0.1 M, buffered to pH4 with KOH): 4 mL) crosslinked by β-GP-water (225.0 mg/0.5 mL), but not solidified in the oven, drawing it in via a syringe and re retransferring it to its sample vial via syringe, first sans needle, and then with a needle attached. As it was not solidified it was not tested for stability in PBS.

The procedure was later modified with $NaHCO_3$ was used as the solvent for β-GP instead of water. The new β-GP-$NaHCO_3$ (225.6 mg/0.5 mL) was added while the gel solution was stirred in in ice for 10 min. The gel solution was left to reach room temperature for 10 min and placed in the oven at 37 °C. The procedure was later repeated in triplicate, with lower doses of β-GP-$NaHCO_3$ (112 mg/0.5 mL) used in two of the repeats (CS-30 and CS-31, both tested for injectability), shown below:

Table 35. Proportions of chitosan-based hydrogels with the first modification of the crosslinker/co-crosslinker configuration

Hydrogel no.	Weight of chitosan (LMM) (mg)	Solvent	pH buffer	Primary crosslinker	Co-crosslinker	Temperature (°C)
CS-28	90.1	0.1M Acetic acid (4 mL)	1M KOH	β-GP/$NaHCO_3$ (225.6 mg/0.5 mL)	$NaHCO_3$ (0.5 mL)	37
CS-29	90.3	0.1M Acetic acid (4 mL)	1M KOH	β-GP/$NaHCO_3$ (225.6 mg/0.5 mL)	$NaHCO_3$ (0.5 mL)	37
CS-30	90.8	0.1M Acetic acid (4 mL)	1M KOH	β-GP/$NaHCO_3$ (112.4 mg/0.5 mL) (0.165 mL for half, 0.335 mL for other half)	$NaHCO_3$ (0.5 mL)	37
CS-31	90.4	0.1M Acetic acid (4 mL)	1M KOH	β-GP/$NaHCO_3$ (112.3 mg/0.5 mL) (0.165 mL for half, 0.165 mL for other half)	$NaHCO_3$ (0.5 mL)	37

The crosslinkers were later modified by combining GP-water/$NaHCO_3$ together into one vial, and adding the mixture dropwise to the chitosan-based gel solutions (CS-32, CS-33, CS-34, and CS-38 were tested for injectability), as per the table:

Table 36. Proportions of chitosan-based hydrogels with second modification to the crosslinker/co-crosslinker configuration

Hydrogel no.	Weight of chitosan (LMM) (mg)	Solvent	pH buffer	Primary crosslinker	Co-crosslinker	Temperature (°C)
CS-32	45.6	0.1M Acetic acid (2 mL)	1M KOH	β-GP-water/$NaHCO_3$ (66.5 mg/0.25 mL/0.25 mL)	$NaHCO_3$ (0.25 mL)	37
CS-33	45.1	0.1M Acetic acid (2 mL)	1M KOH	β-GP-water/$NaHCO_3$ (112.0 mg/0.25 mL/0.25 mL)	$NaHCO_3$ (0.25 mL)	37
CS-34	45.5	0.1M Acetic acid (2 mL)	1M KOH	β-GP-water/$NaHCO_3$ (170.4 mg/0.25 mL/0.125 mL)	$NaHCO_3$ (0.125 mL)	37
CS-35	45.4	0.1M Acetic acid (2 mL)	1M KOH	β-GP-water/$NaHCO_3$ (66.1 mg/0.25 mL/0.25 mL)	$NaHCO_3$ (0.25 mL)	37
CS-36	45.4	0.1M Acetic acid (2 mL)	1M KOH	β-GP-water/$NaHCO_3$ (112.8 mg/0.25 mL/0.25 mL)	$NaHCO_3$ (0.125 mL)	37

CS-37	45.6	0.1M Acetic acid (2 mL)	1M KOH	β-GP-water/$NaHCO_3$ (170.4 mg/0.25 mL/0.125 mL)	$NaHCO_3$ (0.125 mL)	37
CS-38	45.4	0.1M Acetic acid (2 mL)	1M KOH	β-GP-water/$NaHCO_3$ (112.4 mg/0.25 mL/0.25 mL)	$NaHCO_3$ (0.25 mL)	37

The second injectability test used CS-30 (chitosan: 90.3 mg, 0.1M acetic acid pH 4: 4mL) with a GP-$NaHCO_3$ (112.4 mg/0.5 mL) prepared as the crosslinker was drawn in and out sans needle before being drawn in via needle. Due to resistance when attempting to draw in via needle, it was drawn in sans needle and injected into a vial of water via needle. The gel (1 mL) was transferred to an Eppendorf vial, the first addition of GP-$NaHCO_3$ (165 µL) to the solution followed, it was shaken and transferred to glass vial, and placed in the oven. The gel in the vial was then tested for stability in PBS by transferring a portion of it into a PBS vial with a spatula, and was left to cool to room temperature for 10 min or in the fridge for 1 h to determine its reversibility. The experiment was later repeated with CS-31 and CS-32, with a smaller dose of the chitosan and crosslinker: β-GP-water-$NaHCO_3$ (66.5 mg/0.25 mL/0.25 mL), as was the stability test in PBS and reversibility test cooling at room temperature for 10 min and 1 h in the fridge.

The third injectability test used a chitosan (45.1 mg) hydrogel (numbered CS-33), with a buffered acetic acid (4 mL) solvent, with β-GP-water-$NaHCO_3$ (112.4 mg/0.25 mL/ 0.25 mL) as its crosslinkers was drawn in via needle, with half of the contents of the syringe retransferred to the gel sample vial, and the remainder was left in the syringe for 1 h at room temperature before being returned to the vial. A repetition, CS-38, was performed with a slightly larger dose of crosslinkers (170.4 mg/0.25 mL/0.25 mL). The stability in PBS test and reversibility tests were repeated as before.

The fourth injectability test used a chitosan (45.5 mg) hydrogel (numbered CS-34), with a buffered acetic acid (4 mL) solvent, with β-GP-water-$NaHCO_3$ (112.4 mg/0.25 mL/ 0.125 mL) as its crosslinkers was drawn in via needle, with half of the contents of the syringe retransferred to the gel sample vial, and the remainder was left in the syringe for 1 h at room temperature before being returned to the vial.

Another modification to the crosslinker/co-crosslinker configuration was the replacement of $NaHCO_3$ with a $CaCl_2.2H_2O$ solution (72.26 mg/mL), with three gels tested, per the table:

Table 37. Proportions of chitosan-based hydrogels with a calcium chloride dihydrate co-crosslinker

Hydrogel no.	Weight of chitosan (LMM) (mg)	Solvent	pH buffer	Primary crosslinker	Co-crosslinker	Temperature (°C)
CS-39	45.3	0.1M Acetic acid (2 mL)	1M KOH	β-GP-water/$CaCl_2.2H_2O$ (112.5 mg/0.25 mL/0.125 mL)	$CaCl_2.2H_2O$ (0.125 mL)	37
CS-40	45.2	0.1M Acetic acid (2 mL)	1M KOH	β-GP-water/$CaCl_2.2H_2O$ (112.5 mg/0.25 mL/0.125 mL)	$CaCl_2.2H_2O$ (0.125 mL)	37

CS-41	45.6	0.1M Acetic acid (2 mL)	1M KOH	β-GP-water/$CaCl_2.{}_2H_2O$ (112.1 mg/0.25 mL/0.125 mL)	$CaCl_2.{}_2H_2O$ (0.125 mL)	37

Addition of a tertiary crosslinker came in the form of $NaHCO_3$ and $MgCH_3COO_2$, with 0.125 mL of both added to a separate chitosan-acetic acid (45 mg/2 mL) gel solution. Subsequently, two new chitosan portions (45 mg) were dissolved in 0.1M HCl (2 mL), after which the $NaHCO_3$ solution (0.125 mL) was added to the GP-water (112 mg/0.5 mL) solution in ice, left at room temperature for 3 h before being oven-dried for 6 min.

Table 38. Proportions of chitosan (HMM)-based hydrogels dissolved using HCl

Hydrogel no.	**Weight of chitosan (HMM) (mg)**	**Solvent**	**Primary crosslinker**	**Co-crosslinker**	**Temperature (°C)**
C-46	45.2	0.1M HCl (2 mL)	β-GP-water/$NaHCO_3$ (112.4 mg/0.25 mL/0.125 mL)	$NaHCO_3$ (0.125 mL)	37
C-47	45.4	0.1M HCl (2 mL)	β-GP/water/ $NaHCO_3$ (112.4 mg/0.25 mL/0.125 mL)	$NaHCO_3$ (0.125 mL)	37

4. Preparation of PF-127-based hydrogels

A new Pluronic F-127 (200.6 mg)-based hydrogel was prepared using a water solvent and hydroxypropyl cellulose (20.4 mg) crosslinker/co-polymer, all of which was added to the solvent over 10 min, from one weighing boat, and stirred until fully dissolved, and oven-dried at 40 °C. Six more samples were prepared with 500, 400, and 300 mg of PF-127, respectively with 20 mg of hydroxypropyl cellulose with the first three, and 40 mg doses of hydroxypropyl cellulose with the other three, with one of the latter oven-dried at 37 °C, while the rest were oven-dried at 40 °C.

5. Characterisation of PF-127-based hydrogels

A new Pluronic F-127 (200.4 mg) (PF-1) based hydrogel was initially prepared using 20.4 mg of cellulose, with both the polymer and co-polymer/crosslinker weighed out in one boat and added to the stirring 2 mL of water over the course of 10 min. The procedure was repeated using PF-127 mg (200.4 mg)-and hydroxypropyl cellulose (20.5 mg) as the crosslinker/co-polymer, all of which was added to the solvent over 10 min, from one weighing boat, and stirred until fully dissolved, and oven-dried at 40 °C. Six more samples were prepared with 500, 400, and 300 mg of PF-127, respectively with 20 mg of hydroxypropyl cellulose with the first three, and 40 mg doses of hydroxypropyl cellulose with the other three, with one of the latter oven-dried at 37 °C, while the rest were oven-dried at 40 °C.

Table 39. Proportions of PF-127-based hydrogels with varying doses of hydroxypropyl cellulose.

Hydrogel no.	Weight of PF-127 (mg)	Solvent	Co-polymer	Temperature (°C)
PF-1	200.6	Water (2 mL)	Cellulose (20.4 mg)	-
PF-2	200.4	Water (2 mL)	Hydroxypropyl cellulose (20.5 mg)	40
PF-3	500.9	Water (2 mL)	Hydroxypropyl cellulose (20.7 mg)	40
PF-4	400.5	Water (2 mL)	Hydroxypropyl cellulose (19.96 mg)	40
PF-5	300.5	Water (2 mL)	Hydroxypropyl cellulose (20.1 mg)	40
PF-6	500.1	Water (2 mL)	Hydroxypropyl cellulose (40.1 mg)	40
PF-7	400.0	Water (2 mL)	Hydroxypropyl cellulose (40.1 mg)	40
PF-8	300.8	Water (2 mL)	Hydroxypropyl cellulose (40.3 mg)	40

Table 40. Proportions of PF-127-based saccharin-loaded (PF-10-PF-12) and amoxicillin hydrogels (PF-14 and PF-15) with varying doses of hydroxypropyl cellulose.

Hydrogel no.	Weight of PF-127 (mg)	Solvent	Co-polymer	Temperature (°C)
PF-10	500.9	Saccharin-water (2 mL)	Hydroxypropyl cellulose (40.0 mg)	37
PF-11	500.3	Saccharin-water (2 mL)	Hydroxypropyl cellulose (20.5 mg)	37
PF-12	500.3	Saccharin-water (2 mL)	Hydroxypropyl cellulose (40.3 mg)	37
PF-14	500.4	Amoxicillin trihydrate (2 mL)	Hydroxypropyl cellulose (20.2 mg)	37
PF-15	500.4	Amoxicillin trihydrate (2 mL)	Hydroxypropyl cellulose (20.1 mg)	37

Two PF-127 (500 mg) (labelled PF-3 and PF-6) based hydrogel with a water (2 mL) solvent, with hydroxypropyl cellulose (20.7 mg for PF-2, and 40.1 mg for PF-5) as co-polymers and crosslinkers were drawn in via syringe and out to a centrifuge tube for drug release tests. The same procedure was repeated with six more types of PF-127-based hydrogels (400.5 mg, 300.8 mg, and 500 mg) with hydroxypropyl cellulose (20 mg and 40 mg doses) as co-polymer. Seven hydrogels loaded with test drugs like saccharin and amoxicillin trihydrate in the water solvent were also tested for injectability, being drawn into a syringe sans and via needle and retransferred to the vial, in the case of PF-10-PF-15 were easily transferred to a dialysis tube and centrifuge tube. All parameters are listed below:

Table 41. All proportions of the PF-127-based hydrogel components and their injectabilities

Hydrogel no.	Weight of PF-127 (mg)	Solvent	Co-polymer	Temperature (°C)
PF-3	500.9	Water (2 mL)	Hydroxypropyl cellulose (20.7 mg)	40
PF-4	400.5	Water (2 mL)	Hydroxypropyl cellulose (19.96 mg)	40
PF-5	300.5	Water (2 mL)	Hydroxypropyl cellulose (20.1 mg)	40
PF-6	500.1	Water (2 mL)	Hydroxypropyl cellulose (40.1 mg)	40
PF-7	400.0	Water (2 mL)	Hydroxypropyl cellulose (40.1 mg)	40
PF-8	300.8	Water (2 mL)	Hydroxypropyl	40

			cellulose (40.3 mg)	
PF-10	500.9	Saccharin-water (2 mL)	Hydroxypropyl cellulose (40.0 mg)	37
PF-11	500.3	Saccharin-water (2 mL)	Hydroxypropyl cellulose (20.5 mg)	37
PF-12	500.3	Saccharin-water (2 mL)	Hydroxypropyl cellulose (40.3 mg)	37
PF-13	400.87	4-nitrophenol-water (2 mL)	Hydroxypropyl cellulose (20.42 mg)	40
PF-14	500.4	Amoxicillin trihydrate-PBS (2 mL)	Hydroxypropyl cellulose (20.2 mg)	37
PF-15	500.4	Amoxicillin trihydrate-PBS (2 mL)	Hydroxypropyl cellulose (20.2 mg)	37

6. Release studies.

Chitosan-based gels

To test the release of the membrane method, and see if any molecules prevent sustained release, a nicotinamide-PBS stock (50 mg in 50 mL) solution was prepared and 5 mL of it was transferred to a dialysis tube and placed in a beaker. Twelve 50 µL samples were collected in 12 time marks over the course of 5 h, before being diluted to 5 ml with PBS and UV/Vis analysed at 251 nm (Timespan: 5 hrs, % Release: 87.23%).

PF-127 based gels

To determine if PF-127-based gels interfere with the UV/Vis spectrum, a PF-127-based hydrogel (500.46 mg of PF-127, 21.32 mg of hydroxypropyl cellulose) loaded with water (acting as the solvent), was solidified in the oven at 37 °C (weighed out to be 2201.9 mg). The

gel was weighed out (2201.9 mg) in a centrifuge tube after being transferred from the sample vial. Subsequently 25 mL of PBS was added directly to the gel in the centrifuge tube, before the stopwatch was started and another 10 mL of PBS was added. Seven 0.5 mL extractions were made over the course of 23.5 hours, with the absorbance values recorded at 225 nm

Subsequently, a saccharin-water stock solution prepared (2.5 mg/mL) and 2 mL of it was used and as the solvent for PF-127 (500.9 mg) and hydroxypropyl cellulose (40.0 mg), which solidified at 37 °C, and was transferred to a centrifuge tube in a beaker and weighed out. The experiment was repeated in duplicate with a 500 mg dose of PF-127, 20 mg and 40 mg doses of hydroxypropyl cellulose.

The PF-127-based hydrogel (yield: 2053.2 mg), containing 40.0 mg of hydroxypropyl cellulose (numbered PF-10) (used: 1831.4 mg, oven-dried at 37°C), was immersed in PBS, had four 0.5 mL samples extracted at four time marks over the course of 5 hrs. Subsequent dilution to 5 mL with PBS and UV/Vis analysis at 223 nm followed. An absorbance of 0.655318 was collected after 3 days. (Timespan: 72 h, % Release: 567.38%). The procedure was later repeated with another PF-127 hydrogel (numbered PF-11) with 2 mL of saccharin as the solvent and analyte (yield: 2189.6 mg) was transferred to an empty centrifuge tube, its weight obtained as 2073.0 mg, before being oven-dried at 37 °C. Once solidified 35 mL of pre-heated PBS were pipetted carefully to the gel, with the stopwatch started after the first 25 mL portion. The solution was then left in the oven at 37 °C with 0.5 mL extractions made at seven time marks over the course of 22.5 h, which were diluted to 5 mL with PBS and UV/Vis analysed at 223 nm (Timespan: 22.5 h, % Release: 552.0%). The procedure was later repeated (numbered PF-12) (yield: 2181.7 mg) under the same conditions with 1615.5 mg of the gel oven-dried at 37°C, and 35 mL of pre-heated PBS added to it, with 0.5 mL extractions at the same time marks over 22.75 h (Timespan: 22.75 h, % Release: 473.41%)

An amoxicillin trihydrate-PBS stock (0.2512 mg/mL) solution was prepared and pipetted in increasing aliquots (from 0.04 to 0.4 mL) into 7 sample vials, which were diluted to 5 mL with PBS and UV/Vis analysed at 225 nm and 235 nm.

Table 42: Compositions of the amoxicillin trihydrate-PBS standards.

Standard no.	Vol. stock (µL)	Vol. PBS (mL)
1	40	4.960
2	80	4.920
3	120	4.880
4	160	4.840
5	200	4.800
6	300	4.700
7	400	4.600

Table 43. Table of the time intervals, absorbance values, system type and analyte of the amoxicillin trihydrate calibration plot.

Composition	Crosslinker(s)	Analyte	Concentration (mg/mL)	Absorbance @ 225 nm	Absorbance @ 235 nm	Aliquot extracted (mL)	Dilution volume (mL)
Amoxicillin trihydrate-PBS stock solution (62.5 mg/mL) dissolved in seven 5 mL aliquots	-	1.034944 mg amoxicillin trihydrate	0.0020096	0.066226	0.04366	0.04	5
			0.0040192	0.112705	0.08122	0.08	5
			0.0060288	0.148867	0.113154	0.120	5
			0.0080384	0.189603	0.134579	0.160	5
			0.010048	0.241815	0.182402	0.200	5
			0.015072	0.337344	0.245734	0.300	5
			0.020096	0.442751	0.323446	0.400	5

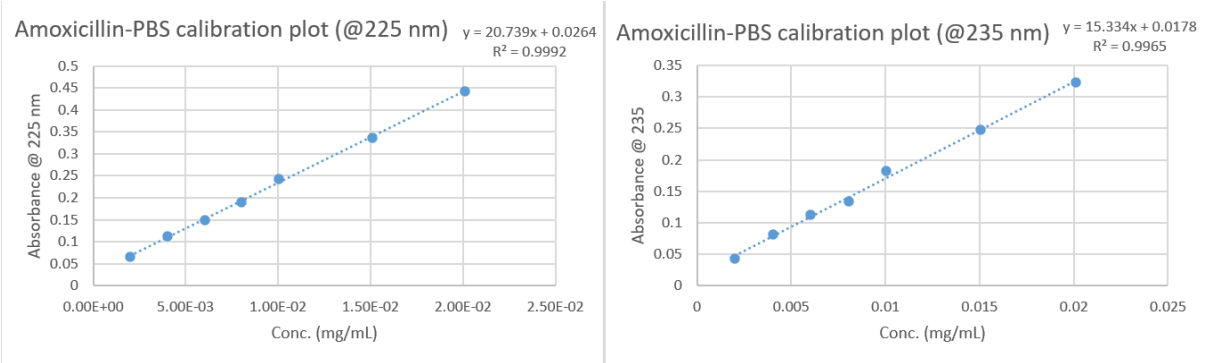

Fig.9: Amoxicillin trihydrate calibration plot

The plots showed better linearity at 225 nm, indicating it is the best wavelength at which to measure the release of amoxicillin trihydrate from PF-127-based hydrogels.

Subsequently, a new amoxicillin trihydrate-PBS (2.512 mg/mL) stock was prepared and 2 mL of this stock served as the solvent and analyte of the PF-127 hydrogel (numbered PF-14) (yield: 2388.1 mg, 2243.6 mg used). Seven 0.5 mL extractions over 8 h were diluted to 5 mL with PBS and UV/Vis analysed at 225 nm (Timespan: 8 h, % Release: 57.63%). The procedure was repeated, with 1817.4 mg of the PF-127-amoxicillin trihydrate gel (numbered PF-15) (yield: 2089.3 mg) in 35 mL of PBS (Timespan: 8 h, % Release: 56.98%)

4.Conclusion

4.1 Synthesis of MSNs and development of protective coating

Regarding the synthesis of MSNs, Method 3 resulted in excess precipitate, most likely resulting from an insufficient number of the precursor in the immediacy of its addition, as it was added 0.1 mL per minute. Method 5 of synthesizing them did not produce any yield.

Aminofunctionalisation by post-synthetic grafting was successful, as shown by IR spectroscopy. Aminofunctionalisation by co-condensation of TEOS and APTES was also successful (Fig.12), shown by the IR spectrum. Extraction from the surfactant has been successful, confirmed by (Fig.13).

Gelatin coating by adding a dialdehyde linker was unsuccessful, as the FTIR spectrum didn't show functionalisation: there was a lack of a characteristic peak of aldehyde groups at 1716 cm^{-1}, for two possible reasons: the low number of amino groups present in them, meaning that there was an insufficient number to form reactions with aldehydes. clearly indicated that the MSNs' aldehyde functionalisation was unsuccessful. Gelatin coating by electrostatic attraction, followed by linking the attached molecules to each other via a dialdehyde linker was only partially successful. Gelatin coating by electrostatic attraction, followed by linking

the attached molecules to each other via a dialdehyde linker by coating the MSNs via electrostatic interaction, and then attempting to cross-link the gelatin with aldehyde functional groups via an imine bond showed partial functionality, as the gelatin coating of the MSNs was verified by the pronounced peak at 1536.12 cm^{-1}, corresponding to the gelatin's N-H stretching vibration. Crosslinking was partially successful.

The concentration values obtained using the absorbance values were much different than those calculated using the composition of the analyte, meaning that MSNs did interfere with the UV/Vis spectrum.

UV/Vis spectroscopy proved unsuitable for analysis of drug loading, as the nanoparticles could not be completely removed by centrifugation and interfered with the analysis. HPLC would be a more accurate and more efficient method of drug loading analysis but could not be utilized due to time constraints.

4.2 Hydrogel synthesis and drug release tests.

Synthesis and characterisation of the gels showed that chitosan-based gels were irreversible: after solidifying at 37 °C, they did not reliquefy. Using a less acidic solvent (0.1M acetic acid buffered to pH 4 using 1M KOH) was the most reliable solvent for the CS-based gels than a more acidic solvent (0.1M HCl), as the latter weakened the gel structure. Use of a co-crosslinking agent ($NaHCO_3$) proved to significantly enhance the strength of the CS-based gels. Lack of reliquification after leaving the gels in the fridge for 1 hr confirmed not only their irreversibility, but that CS-based gels were only stable as gels at low temperatures. The methods were not reproducible as some gels did not gelate, even after being oven-dried at 37 °C for 16-30 min, subsequently gelating at room temperature. In addition, chitosan-based hydrogels, when exposed to excess moisture were shown to develop fungal-like growths after being left at room temperature for 4-5 days.

CS-based hydrogels, with no co-cross-linking agents were not injectable. The increased levels of a co-crosslinker and its role in strengthening the gels inhibited the gels from filling the

syringe through the needle. This observation established a rule of thumb that increase in strength for CS-based hydrogels has a detrimental effect on their injectability.

The method of monitoring drug release through a semi-permeable membrane proved to be insufficient, allowing only for 45.95% release in one hour.

Synthesis of PF-127 based hydrogels, crosslinked using hydroxypropyl cellulose (which also acted as a co-polymer) showed better reproducibility in synthesis, had overall shorter gelation times (less than 10 minutes), and were shown to be reversible, reliquefying 5 min after being left at room temperature after solidifying at 37 °C. They had, however, a shorter storage time than CS-based gels. When exposed to moisture while stored in the oven, they began to decompose after 3 days.

The PF-127 based hydrogels also demonstrated high injectability in liquid form, easily filling the syringe through the needle.

In terms of release studies, PF-127-based hydrogels, saccharin (showing abnormal percentage releases due to contamination of PBS solution), and amoxicillin trihydrate, with 57% released in a span of 8 hrs in PF-14 and 56.98% release in the same timespan by PF-15, were slow-releasing gels. Fluctuations in % released only occurred in tests involving amoxicillin trihydrate.

PF-127-based hydrogels, crosslinked with hydroxypropyl cellulose, despite having higher % of model substances released over the course of 1-3 days than CS-based hydrogels and a shorter storage life, they have much better injectability and reversibility and reproducibility in synthesis, seem to be the better-suited hydrogel systems for drug delivery.

5. Materials.

5.1: Synthesis of MSNs and development of protective coating.

- *Chemicals*: 0.1-1.12g of Hexadecyltrimethylammonium bromide (CTAB) (*TCI Chemicals*), 0.5 mL Tetraethyl orthosilicate (TEOS) (*Millipore Corporation (Merck)*),

0.35 mL sodium hydroxide solution (2M NaOH) (*Fisher Scientific*), 6.6 mL ethanol (absolute, 99%, EtOH) (*Fisher Scientific*), 5.7 mL triethanolamine (TEA) (*Sigma-Aldrich*), 0.08-0.7 mL 3-aminopropyltriethoxysilane (APTES) (*TCI Chemicals*), 0.171-2.018g of sodium chloride (NaCl), 21-240 mL methanol (99.9%, MeOH) (*Fisher Scientific*), 2.0-4.950 mL phosphate-buffered saline (PBS) composed of:

- ~4g sodium chloride (NaCl), ~0.1g potassium chloride (KCl) (Glentham Life Sciences), 0.7g dibasic disodium phosphate (Na_2HPO_4) (*Sigma-Aldrich*), 0.12g monobasic potassium dihydrogen phosphate (KH_2PO_4) (*Sigma-Aldrich*), 500 mL water.

pH buffer 8 composed of:

- 8.141g of dibasic potassium phosphate (K_2HPO_4) (*Sigma-Aldrich*), 0.44g of monobasic potassium dihydrogen phosphate (KH_2PO_4) (*Sigma-Aldrich*), 500 mL of water.

5 mL dimethylformamide (DMF) (*TCI Chemicals*), 5 mL dimethyl sulfoxide (DMSO) (*TCI Chemicals*), 0.02-0.03 mL glutaraldehyde (*TCI Chemicals*), 20.8 g of porcine gelatin (*Sigma-Aldrich*), 0.261-1.004g of 4-nitrobenzaldehyde (*TCI Chemicals*), 0.025-0.031g acetazolamide (50%) (*TCI Chemicals*), 8.140g of dibasic potassium phosphate (K_2HPO_4) (*Sigma-Aldrich*), 0.195g of N-hydroxysuccinimide (*TCI Chemicals*), 0.020g of 4-phenylbutyric acid (*TCI Chemicals*), 0.12g of (3-Dimethylamino-propyl)-ethyl-carbodiimide hydrochloride (EDC HCl) (*TCI Chemicals*), 0.031g of saccharin (*Sigma-Aldrich*), 0.05 mL acetone (*Fisher Scientific*).

- UV/Vis spectra recorded on a Cary-Varian 50 Scan UV/Vis spectrometer

-FTIR analysis performed with a Perkin-Elmer Spectrum 400 FT-IR/FT-FIR spectrometer.

-Centrifugations performed with a:

- (@ 5500 rpm) Thermo Scientific Heraeus Megafuge 16 centrifuge.

- (@ 14400 rpm) Sigma 1-14 microcentrifuge.

Analytical instruments:

- Centrifugation at 5500 rpm: The MSNs were separated from their solvents with a ThermoScientific Heraeus Megafuge 16. The MSNs were placed in a 50 mL centrifuge tube and were balanced by weight using a second tube filled with water. The centrifuge comprised of a stainless-steel chamber with 9 acceleration and 10 braking curves, a rotor for 2 steel buckets, which could either contain one 50 mL tube or four 12 mL tubes. The centrifugation speed (ranging from 300-6000 for the rotor used) and time (unlimited range) was adjusted with the arrow keys on the control panel for the microprocessor to control the centrifugation apparatus, thanks to automatic rotor recognition. The lid was locked automatically, and locking was started from an initial hold position[62].
- Centrifugation at 14400 rpm: The aminated, CTAB-free MSNs had their amino groups quantified via separation of their supernatant with a Sigma 1-14 microcentrifuge. The centrifuge comprised of a fixed-angle polypropylene rotor 12094, with a capacity of twenty four 2 mL Eppendorf tubes. The rotor had its own plastic lid, locked in place at the centre was microprocessor-controlled, responding to and controlling centrifugation speed and time values adjusted with the arrow keys on the control panel. The centrifuge featured an automatic a motorized lid locking mechanism, started from an initial hold position[63].
- FTIR analysis: The characterisation of MSNs was carried out on a Perkin-Elmer Spectrum 400 FTIR spectrometer. The sample was placed on the ATR crystal, with sufficient force applied on the sample by the presser. The ATR module information, after going through a source screen and doubling mirror (to maximise signal-to-noise ratio) is stabilized by an interferometer for better reproducibility. After being relayed by focusing optics, it was obtained by the electronically temperature stabilized DTGS detectors[64].

- UV/Vis analysis: The analysis of the supernatant and standards for calibration plots with 4-nitrobenzaldehyde, acetazolamide were performed using a Cary-Varian 50 UV/Vis spectrometer. The samples were transferred to a UV/Vis cuvette ~4 mL, which was placed in the sample compartment, the lid closed. The Xe source's UV/Vis rays were reflected before passing through a monochromator (which selects wavelength), and a diffraction grating before passing through the sample and to the detector, relaying the information to the computer. The cuvette's clear side always had to face the detector and be kept clean[65].

5.2: Hydrogel synthesis and drug release tests

- Chemicals: ~4g of potassium hydroxide (KOH) (*Millipore Corporation (Merck)*), glacial acetic acid (*Fisher Scientific*), 0.045-0.450g of β-glycerophosphate (β-GP) (*Sigma-Aldrich*), 0.045-0.112g of chitosan (HMM: *Sigma-Aldrich*, LMM: *Glentham Life Sciences*), 0.2 mL dimethylsulfoxide (DMSO) (*TCI Chemicals*), 0.001-saccharin (*Sigma-Aldrich*), phosphate-buffered saline (PBS) composed of:

    - potassium chloride (KCl) (Glentham Life Sciences), dibasic disodium phosphate (Na_2HPO_4) (*Sigma-Aldrich*), monobasic potassium dihydrogen phosphate (KH_2PO_4) (*Sigma-Aldrich*), 500 mL of water.

0.21g of sodium hydrogen carbonate ($NaHCO_3$) (*Fisher Scientific*), 0.025g of calcium chloride dihydrate $CaCl_2.2H_2O$ (*TCI Chemicals*), 0.05g of nicotinamide (*Sigma-Aldrich*), 0.01-0.1g hyaluronic acid (TCI Chemicals), magnesium acetate ($(CH_3COO)_2.4H_2O$) (Sigma-Aldrich), calcium gluconate monohydrate (TCI Chemicals), 0.03-0.5g of Pluronic F-127 (*Sigma-Aldrich*), 0.01-5.0096 g methyl cellulose (*TCI Chemicals*), 0.06g of 4-nitrophenol (*Alfa Aesar*), 0.06g of amoxicillin trihydrate (*TCI Chemicals*).

-UV/Vis spectra recorded on a Cary-Varian 50 Scan UV/Vis spectrometer

Analytical instruments:

- UV/Vis analysis: The nicotinamide, saccharin, and amoxicillin trihydrate calibration plots and drug release tests were analysed using the Cary-Varian 50 UV/Vis spectrometer. The UV/Vis cuvette ~4 mL, containing the analyte was placed in the sample compartment, with the lid closed. The Xe source's UV/Vis rays were reflected before passing through a monochromator (which selects wavelength), a diffraction grating before passing through the sample and to the detector, relaying the information to the computer[66].

6. References.

Named in order of reference:

1. "Drug delivery systems: What are drug delivery systems" can be found under 'https://www.nibib.nih.gov/science-education/science-topics/drug-delivery-systems-getting-drugs-their-targets-controlled-manner#pid-1236', **2022**, (accessed 09/12/2022)

2. Haesun Park, Andrew Otte, Kinam Park, *J. Control. Release* **2022**, *342*, 53-65.

3. Rukkumani Rajagopalan, Jatinder V. Jakhmi, *N. Cancer Therapy Micro. Nano Technologies* **2017**, *8*, 211-240

4. Helena Gavilán, Sahitya Kumar Avugadda, Tamara Fernández-Cabada, Nisarg Soni, Marco Cassani, Binh T. Mai, Roy Chantrell, Teresa Pellegrino, *Chem. Soc. Rev.* **2021**, *50*, 11614-11667.

5. "Cancer statistics: Cancer mortality in Ireland" can be found under 'https://www.cancer.ie/cancer-information-and-support/cancer-information/about-cancer/cancer-statistics', **2023**, (accessed 02/01/2023)

6. "Cancer" can be found under 'https://ourworldindata.org/cancer', **2015**, (accessed 09/01/2023)

7. Vincent T. DeVita, Jr., Edward Chu, *A history of cancer chemotherapy*, Cancer Res **2008**, *68*, 8643-8653

8. "Happy 50th anniversary to cisplatin, the drug that changed cancer treatment: the history of cisplatin" can be found under 'https://theconversation.com/happy-50th-anniversary-to-cisplatin-the-drug-that-changed-cancer-treatment-38382', **2015**, (accessed 09/01/2023)

9. Roger Y. Tsang, Turki Al-Fayea, Heather-Jane, *Drug Saf.* **2009**, *32*, 1109-1122

10. “The "Accidental" Cure—Platinum-based Treatment for Cancer: The Discovery of Cisplatin” can be found under ‘https://www.cancer.gov/research/progress/discovery/cisplatin’, **2014**, (accessed 10/01/2023)

11. Roger Y. Tsang, Turki Al-Fayea, Heather-Jane, *Drug Saf.* **2009**, *32*, 1109-1122

12. “40th Anniversary of First FDA Approved, Pt-Based Anti-Cancer Drug” can be found under ‘https://www.strem.com/catalog/product_blog/156/7/40th_anniversary_of_first_fda_approved_pt-based_anti-cancer_drug’, **2018**, (accessed 13/01/2023)

13. Pavan, S.R., Prabhu, *J. Mater. Sci.* **2022**, *57*, 16192–16227

14. G.P. Stathopoulos and T. Boulikas, *J. Drug Deliv.* **2012**, *2012*, Article No. 581363.

15. Qianjun He, Jianlin Shi, Feng Chen, Min Zhu, Lingxia Zhang, *Biomaterials* **2010**, *31*, 3335–3346

16. Wei Zhang, Jianliang Sheng, Hua Su, Ge Mu, Jing-Hua Sun, Cai-Ping Tan, Xing-Jie Liang, Liang-Nian Ji, Zong-Wan Mao, *ACS Appl. Mater. Interfaces* **2016**, *8*, 13332−13340

17. Xinxiang Yang, Wai-Ho Oscar Yeung, Kel Vin Tan, Tak-Pan Kevin Ng, Li Pang, Jie Zhou, Jinyang Li, Changxian Li, Xiangcheng Li, Chung Mau Lo, Weiyuan John Kao, Kwan Man, *Drug delivery* **2021**, *28*, 520–529

18. Reema Narayan, Usha Y. Nayak, Ashok M. Raichur, Sanhay Garg, *Pharmaceutics* **2018**, *10*, Article No. 118

19. “Process for producing low-bulk silica”, can be found under ‘https://patentimages.storage.googleapis.com/b5/01/74/fbab3b310d0e5d/US3556725.pdf’, **1971**, (accessed 13/01/2023)

20. “Porous silica particles containing a crystallized phase and method” can be found under ‘https://patentimages.storage.googleapis.com/e1/4f/b8/4f7d34b37259dd/US3493341.pdf’, **1967**, (accessed 14/01/2023)

21. Yanagisawa Tsuneo, Shimizu Toshio, Kuroda Kazuyuki, Kato Chuzo, *Bull. Chem. Soci. Jpn.* **1990**, *63*, 988-992

22. Reema Narayan, Usha Y. Nayak, Ashok M. Raichur, Sanhay Garg, *Pharmaceutics* **2018**, *10*, Article No. 118

23. Reema Narayan, Usha Y. Nayak, Ashok M. Raichur, Sanhay Garg, *Pharmaceutics* **2018**, *10*, Article No. 118

24. Qianjun He, Jiamin Zhang, Jianlin Shi, Ziyan Zhu, Linxia Zhang, Wenbo Bu, Limin Guo, Yu Chen, *Biomaterials* **2010**, *31*, 1085–1092

25. Anna Watermann, Juergen Brieger, *Nanomaterials* **2017**, *7*, Article No. 189

26. "An Introduction to Hydrogels and Some Recent Applications" can be found under 'https://www.intechopen.com/chapters/51535', **2016**, (accessed 12/02/2023)

27. Yongqiang Lu, Liufang Chen, Chuanfu Li, Lin Lin, Zhibo Yan, Junming Liu, *Gels* **2022**, *8*, Article No. 409

28. Sang Cheon Lee, Il Keun Kwon, Kinam Park, *Advanced Drug Delivery Reviews* **2013**, *65*, 17–20

29. Shahid Bashir, Maryam Hina, Javed Iqbal, A. H. Rajpar, M.A. Mujtaba, N.A. Alghamdi, S. Wageh, K. Ramesh, S. Ramesh, *Polymers (Basel)* **2020**, *12*, Article No. 2702

30. Oluwadamilola M. Kolawole, Wing Man Lau, Vitaliy V. Khutoryanskiy, *International Journal of Pharmaceutics: X* **2019**, *1*, Article No. 100007

31. F. Ahmadi, Z. Oveisi, S. Mohammad Samani, Z. Amoozgar, *Res. Pharm. Sci.* **2015**, *10*, 1–16.

32. "Chitosan-Based Hydrogels: Preparation, Properties, and Applications; Hydrogel formation via crosslinking of chitosan" can be found under 'https://link.springer.com/referenceworkentry/10.1007/978-3-319-77830-3_55#citeas', **2018**, (accessed 20/02/2023)

33. Jianyu Li, David J. Mooney, *Nat. Rev. Mater.* **2016**, *1*, Article No. 16071

34. Jianyu Li, David J. Mooney, *Nat. Rev. Mater.* **2016**, *1*, Article No. 16071

35. Xiaoliang Cheng, Houli Li, Xuemei Ge, Lijuan Chen, Yao Liu, Wenwei Mao, Bo Zhao, Wei-En Yuan, *Front. Mol. Biosci.* **2020**, *7*, Article No. 576420

36. Xianchao Jiang, Zhen Du, Xinran Zhang, Fakhar Zaman, Zihao Song, Yuepeng Guan, Tengfei Yu, Yaqin Huang, *Front. Bioeng. Biotechnol.* **2023**, *11*, Article No. 1158749

37. Jyh-Ping Chen, Yann-Lii Leu, Chia-Lang Fang, Chao-Huang Chen, Jia-You Fang, Journal of *Pharmaceutical Sciences* **2011**, *100*, 655-665

38. Federica Rizzi, Rachele Castaldo, Tiziana Latronico, Pierluigi Lasala, Gennaro Gentile, Marino Lavorgna, Marinella Striccoli, Angela Agostiano, Roberto Comparelli, Nicoletta Depalo, Maria Lucia Curri, Elisabetta Fanizza, *Molecules* **2021**, *26*, Article No. 4247

39. Panayiotis Bilalis, Leto-A. Tziveka, Spyridon Varlas, Hermis Iatrou, *Polym. Chem.* **2016**, *7*, 1475-1485

40. “Aminofunctionalised mesoporous silica loaded with 5-fluorouracil” can be found under ‘http://journalijcar.org/sites/default/files/issue-files/1341-A-2017.pdf, **2017**, (accessed 07/03/2023)

41. Parasuraman Paramanantham, Asha P. Anthony, S.B. Sruthil Lal, Alok Sharan, Asad Syed, Mukhtar Ahmed, Abdullah A. Alarfaj, Siddhardha Busi, M. Maaza, K. Kaviyarasu, *Scientific African* **2018**, *1*, Article No. e00007

42. Hosein Ghaedi, Ming Zhao, *Energy Fuels* **2022**, *36*, 2424–2446

43. Ying Sun, Filip Kunc, Vinod Balhara, Brian Coleman, Oltion Kodra, Mohammad Raza, Maohui Chen, Andreas Brinkmann, Gregory P. Lopinski, *Nanoscale Adv.* **2019**, *1*, 1598-1607

44. Nicolás Jackson, Andrea C. Ortiz, Alejandro Jerez, Javier Morales, Francisco Arriagada, *Pharmaceutics* **2023**, *15*, 1590

45. Xuanjun Wu, Liu Yang, Wu Shuqi, J. Mater. Chem. **2012**, 22, 17121-17127

46. Zhen Zou, Dinggeng He, Xiaoxiao He, Kemin Wang, Zhihe Qing, Quan Zhou, *Langmuir* **2013**, *29*, 12804–12810

47. Anjali Pal, Jaya Bajpai, A.K. Bajpai, *Polym. Bull.* **2018**, *75*, 4691–4711

48. Anjali Pal, Jaya Bajpai, A.K. Bajpai, *Polym. Bull.* **2018**, *75*, 4691–4711

49. “Carbonic anhydrase inhibitors as emerging agents for the treatment and imaging of hypoxic tumours” can be found under ‘https://www-tandfonline-com.nuigalway.idm.oclc.org/doi/abs/10.1080/13543784.2018.1548608’, **2018**, (accessed 07/06/2023)

50. Nikola Ž. Knežević, Nebojša Ilić, Veljko Đokić, Rada Petrović, Đorđe Janaćković, *ACS Appl. Mater. Interfaces* **2018**, *10*, 20231–20236

51. Oluwadamilola M. Kolawole, Wing Man Lau, Vitality V. Kutoryanskiy, *International Journal of Pharmaceutics* **2019**, *1*, No.100007

52. “Elaboration, synthesis and characterisation by the viscosimetric study of chitosan materials in dimethyl sulfoxide hydrochloric acid” can be found under ‘https://www.tandfonline.com/doi/abs/10.1080/00319104.2023.2249578?src=’, **2023**, (accessed 08/07/2023)

53. Julia Vaz Ernesto, Isis de Macedo Gasparini, Fulvio Gabriel Corazza, Monica Beatriz Mathor, Classius Ferreira da Silva, Vania Rodrigues Leite-Silva, Newton Andreo-Filho, Patricia Santos Lopes, *Materials Chemistry and Physics* **2023**, *301*, Article No. 127636

54. Maria José Tavera-Quiroz, Jhon Jairo Feria Díaz, Adranna Pinotti, *International Journal of Applied Engineering Research* **2018**, *13*, 13302-13307

55. "21102 Calcium chloride dihydrate" can be found under 'https://www.sigmaaldrich.com/IE/en/product/sial/21102', **2023**, (accessed 08/07/2023)

56. Xin Li, Chuanai Cao, Dongxue Yuan, Qian Liu, Jinhai Zao, *Foods* **2022**, *11*, Article No. 278

57. JinFeng Jiao, BeiYu Wang, YiXing Huang, Ying Qu, JinRong Peng, ZhiYong Qian, *ACS Omega* **2017**, *2*, 443-454

58. Ivana M. A. Diniz, Chider Chen, Xingtian Xu, Sahar Ansari, Homayoun H. Zadeh, Marcia M. Marques, Songtao Shi, Alireza Moshaverinia, *J. Mater. Sci: Mater. Med* **2015** *26*, Article No. 153

59. "Amoxicillin: 1. About amoxicillin" can be found under 'https://www.nhs.uk/medicines/amoxicillin/', **n.d.**, (accessed 08/08/2023)

60. "Amoxicillin trihydrate: Description" can be found under 'https://pubchem.ncbi.nlm.nih.gov/compound/Amoxicillin-trihydrate', **n.d.**, (accessed 09/08/2023)

61. Carolina Righetti Grizotto, Koey Yu, Calibration plot of nicotinamide, performed 7th July 2023 at University of Galway

62. "ThermoScientific Megafuge 10 Instruction Manual" can be found under 'https://assets.thermofisher.com/TFS-Assets/LED/manuals/50156024-c-Thermo%20Scientific%20Megafuge%2016-en.pdf', **2020**, (accessed 24/08/2023)

63. "Sigma 1-14 microcentrifuge instruction manual" can be found under 'https://www.sigma-zentrifugen.de/fileadmin/user_upload/sigma/produkte/pdf/broschueren/EN/Sigma_1-14_1-14K_E.pdf', **n.d.**, (accessed 24/08/2023)

64. "Introducing the PerkinElmer Spectrum 400 FT-IR and FT-NIR Spectrometer", can be found under 'https://resources.perkinelmer.com/corporate/content/relatedmaterials/brochures/bro_spectrum400intl.pdf', **2007**, (accessed 24/08/2023)

65. "Ultraviolet/visible spectroscopy: Varian Cary 50" can be found under 'https://www.kutztown.edu/academics/colleges-and-departments/liberal-arts-and-sciences/departments/physical-sciences/chemistry-and-biochemistry/instrumentation/uv-vis-spectroscopy.html', **2023**, (accessed 24/08/2023)

66. "Ultraviolet/visible spectroscopy: Varian Cary 50", can be found under 'https://www.kutztown.edu/academics/colleges-and-departments/liberal-arts-and-

sciences/departments/physical-sciences/chemistry-and-biochemistry/instrumentation/uv-vis-spectroscopy.html', **2023**, (accessed 24/08/2023)

7. Appendix.

7.1 Synthesis of MSNs

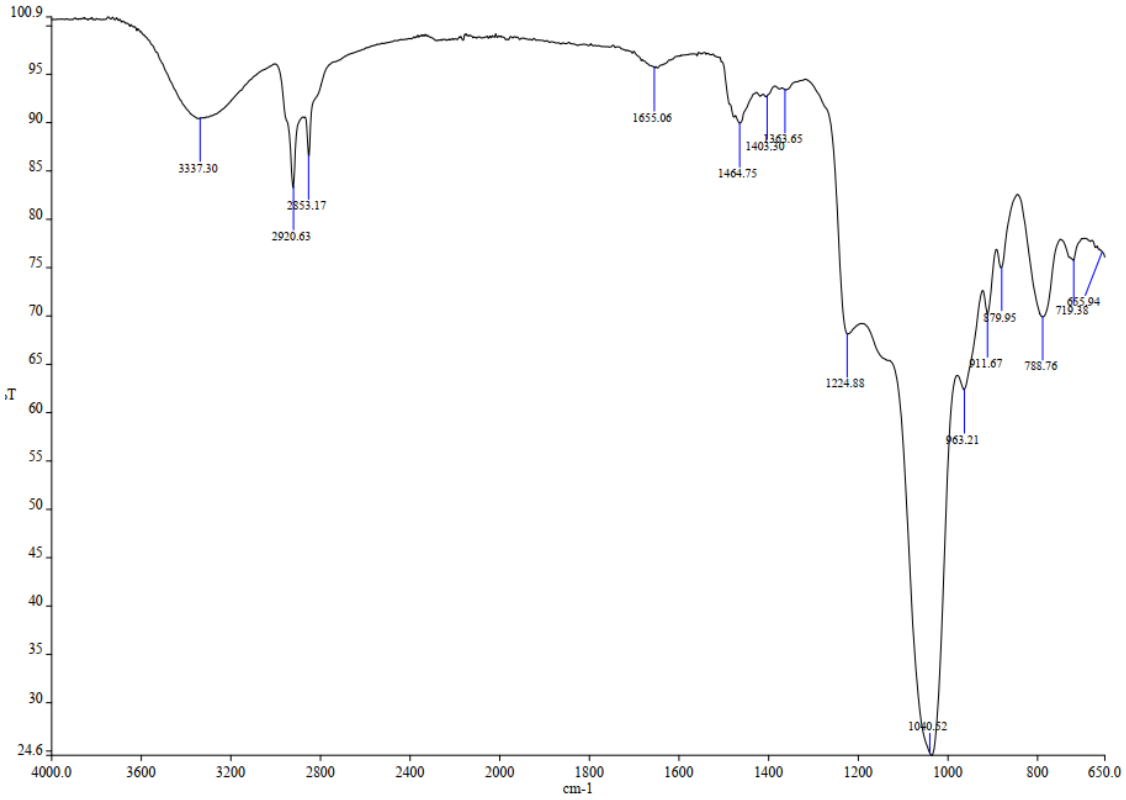

Fig.10: The unmodified MSNs containing CTAB.

C-H bond of CTAB: 2920.63 cm-1, 2853.17 cm-1.

Si-O-Si bend: 1040.52 cm-1.

Si-O stretch: 788.6 cm-1.

Si-OH stretch: 3337 cm-1.

7.2 Aminofunctionalisation of MSNs:

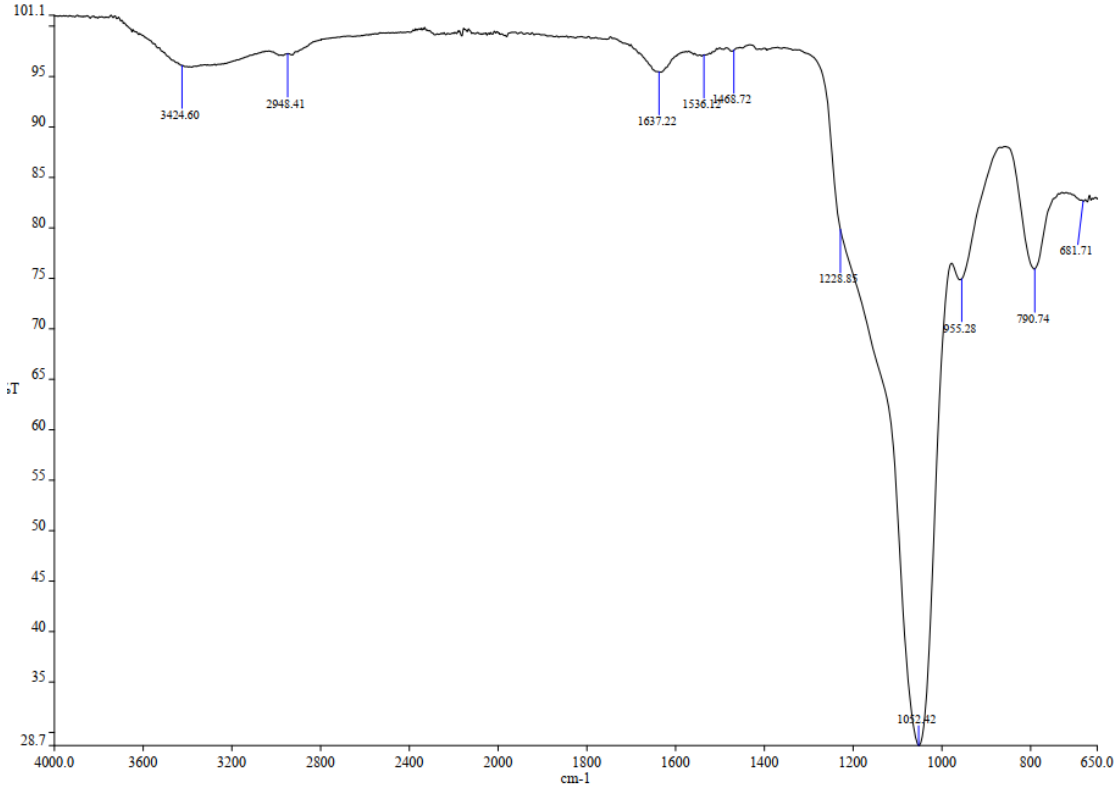

Fig.11: Aminofunctionalised MSNs by post-synthetic grafting.

N-H stretch: 1637.22 cm-1

NH_2 stretch: 3424.60 cm-1

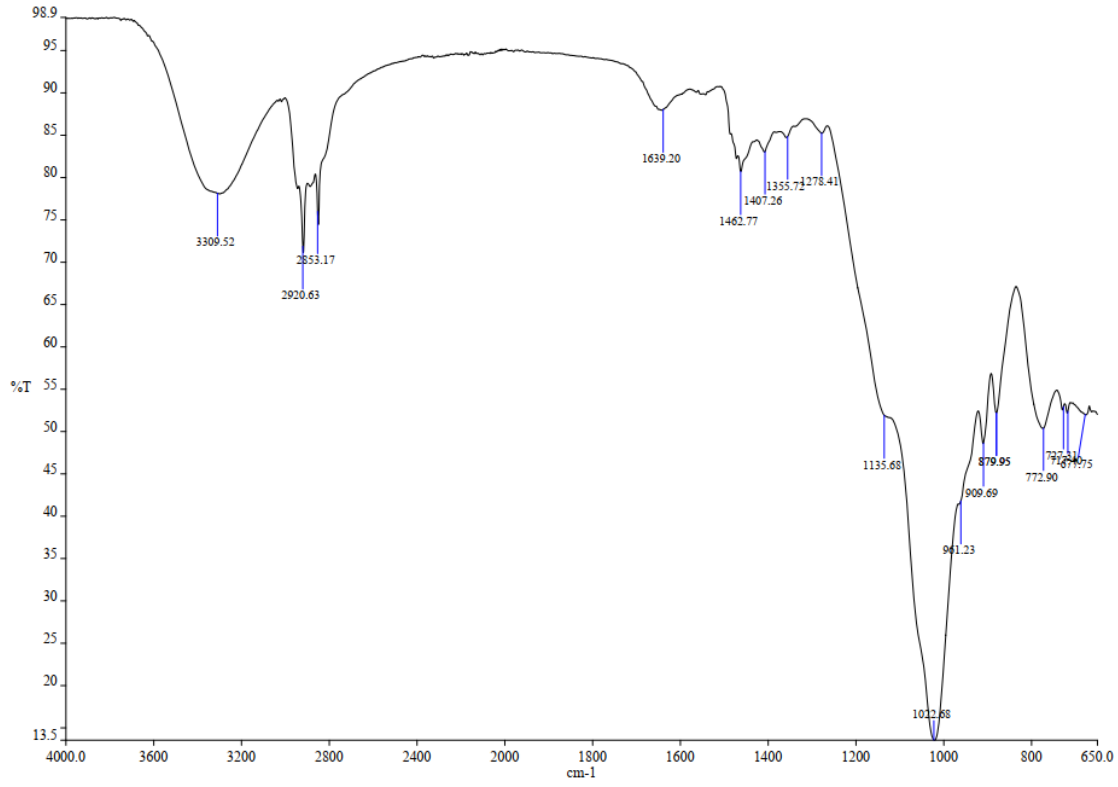

Fig.12: Aminofunctionalised MSNs by co-condensation of TEOS and APES

N-H stretch: 1639.20 cm-1

NH_2 stretch: 3309.52 cm-1

7.3 Removal of surfactant

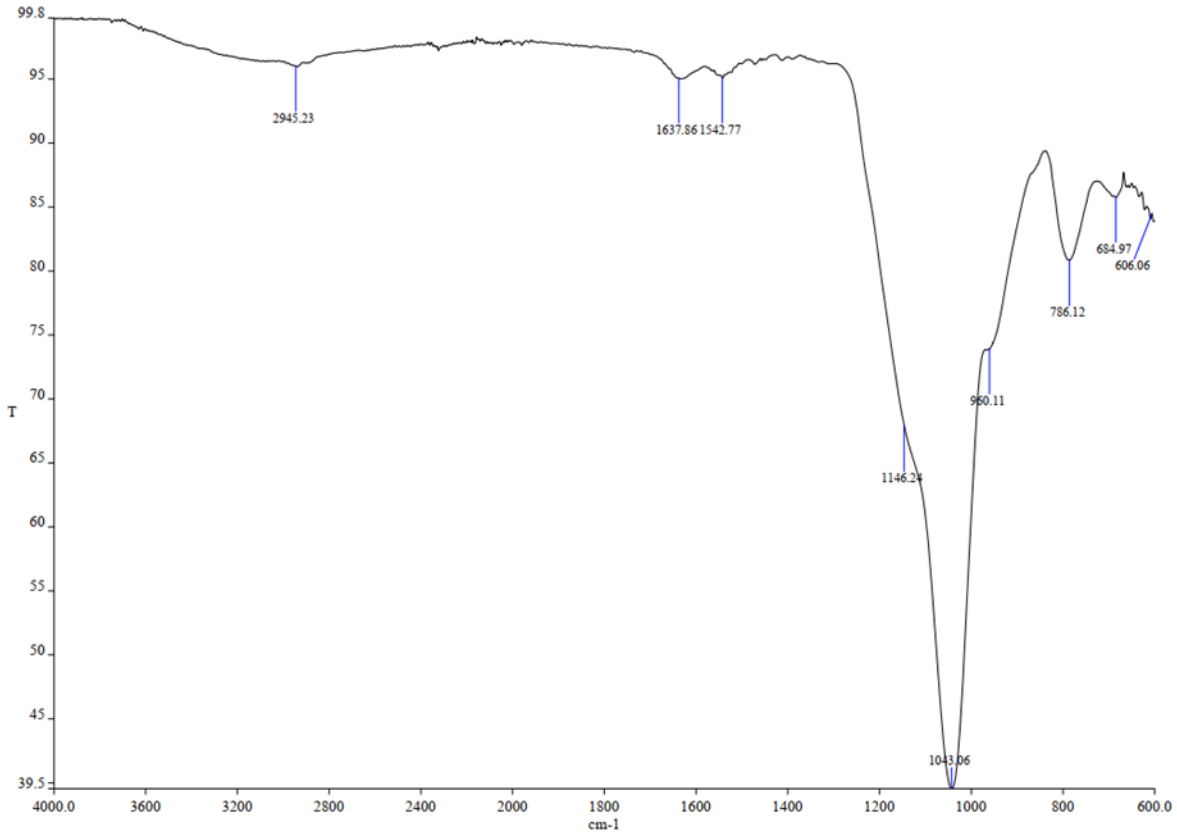

Fig.13: MSNs with removed surfactant.

Note the absence of strong peaks at 2920.63 cm-1 and 2853.17 cm-1, corresponding to C-H bond of CTAB

7.4 Quantification of amino groups

The aminofunctionalised MSNs and have three supernatants extracted and combined for UV/Vis analysis. Before the analysis of MSNs, the solubility of 4-nitrobenzaldehyde had to be ascertained and a calibration plot had to graphed on Excel and subsequently validated. The steps in this analysis, followed per the literature procedure[43] had to modify the following conditions: change in stock solution concentration, change in PBS volume. preparation of a parallel 4-nitrobenzaldehyde standard, incorporation of the MSNs into the 4-nitrobenzaldehyde stock solution. Overall, the method was very accurate, culminating in a linear graph with an R^2 value higher than 0.99. The parallel standard gave an

absorbance of 0.446253 and a concentration of 0.0422 mg/ml. The absorbance of the supernatant was 0.350011 subbed in for y = 9.9137x + 0.0475, with the concentration calculated to be 0.0305 mg/mL.

Quantification calculations:

$$0.350011 = 9.9137x + 0.0475$$

$$0.350011 - 0.0475 = 9.9137x, 0.302511 = 9.9137x$$

$$\frac{0.302511}{9.9137} = x = 0.0305\ mg\ ml^{-1}$$

Another 4-nitrobenzaldehyde sample had an absorbance of 0.011735, and first, subbed into the equation y = 9.9137x + 0.0475, gave a concentration of -3.60763388x10^{-3} mg/mL

$$0.011735 = 9.9137x + 0.0475$$

$$0.011735 - 0.0475 = 9.9137x, -0.035765 = 9.9137x$$

$$-\frac{0.035765}{9.9137} = x = -3.60763388\ x\ 10^{-3}\ mg/ml$$

After the equation had its intercept set to 0, its values were y = 10.828x, it gave a concentration of 1.08376 x 10^{-3} mg/mL:

$$0.01175 = 10.828x$$

$$\frac{0.01175}{10.828} = x = 1.08376\ x\ 10^{-3}\frac{mg}{ml} or\ 1.08376\ x\ 10^{-3}\ g/L$$

$$\frac{1.08376\ x\ 10^{-3}}{151.12\ g\ mol^{-1}} = 7.171519322\ x\ 10^{-6}\frac{mol}{L}, 7.171519322\ x\ 10^{-6}\ x\ 1000$$

$$= 7.171519322\ x\ 10^{-3}\ \mu mol$$

$$7.171519322\ x\ 10^{-3}\ x\ 0.006 = 4.302911593\ x\ 10^{-5}\ \mu mol\ in\ 6\ ml$$

$$\frac{4.302911593\ x\ 10^{-5}}{40.2\ mg} = 1.0704\ x\ 10^{-6}\ \mu mol/mg$$

Further calculations gave the amount of amino groups as 0.0513 µmol/mg:

$$Weight\ of\ 4-nitrobenzaldehyde = 1039.2\ mg, concentration = \frac{1039.2}{20\ mL}$$

$$= 51.96\frac{mg}{mL} or\ 51.96\ g/L$$

$$\frac{51.96}{151.12\ g\ mol^{-1}} = 0.3438327157\frac{mol}{L}, 0.3438327157\ x\ 1000 = 343.827157\ \mu mol$$

$$343.827157\ x\ 0.006 = 2.062962942\ \mu mol\ in\ 6\ ml$$

$$\frac{2.062962942}{40.2\ mg} = 0.0513\ \mu mol/mg$$

7.5 Gelatin coating and aldehyde functionalisation.

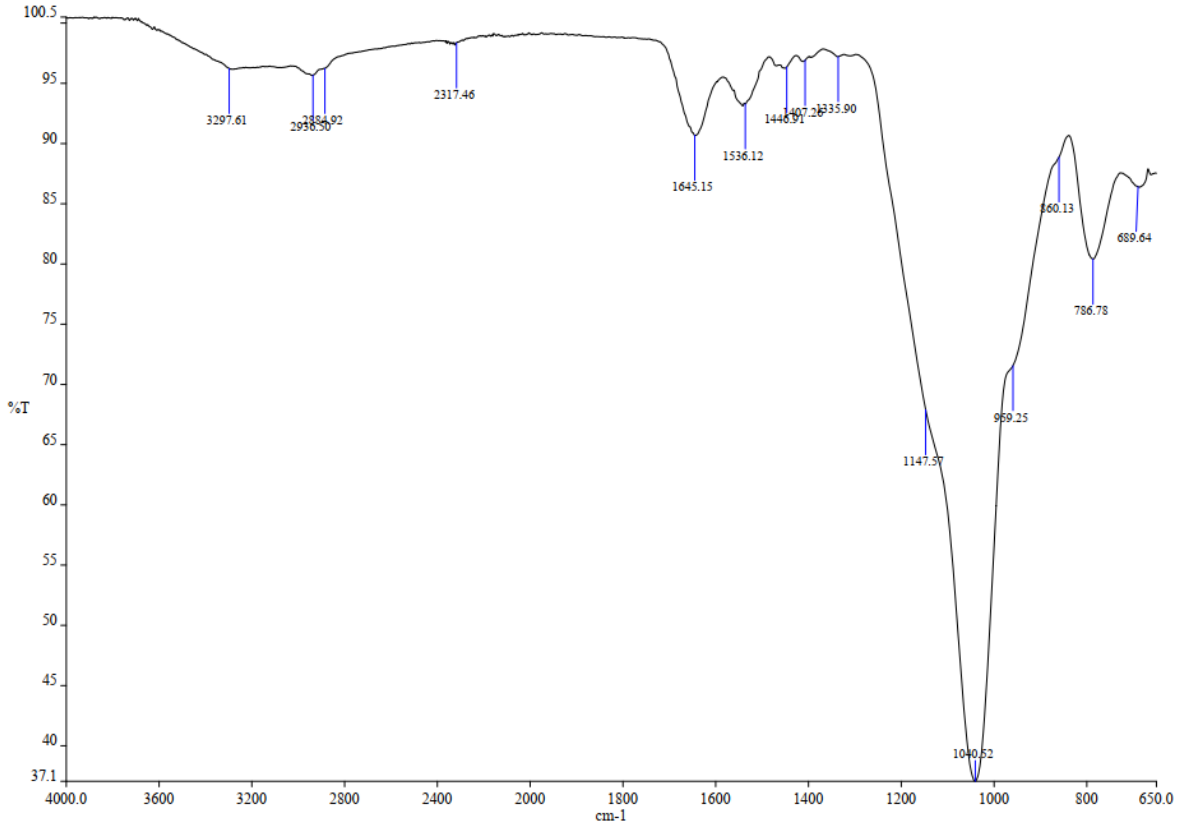

Fig.14: Gelatin-coated MSNs.

Note the pronounced peak at 1536.12 cm-1, corresponding to the gelatin's N-H stretching vibration and the less-pronounced signals of 2936.50 cm-1 and 2884.92 cm-1 correspond to the gelatin's C-H stretching vibrations.

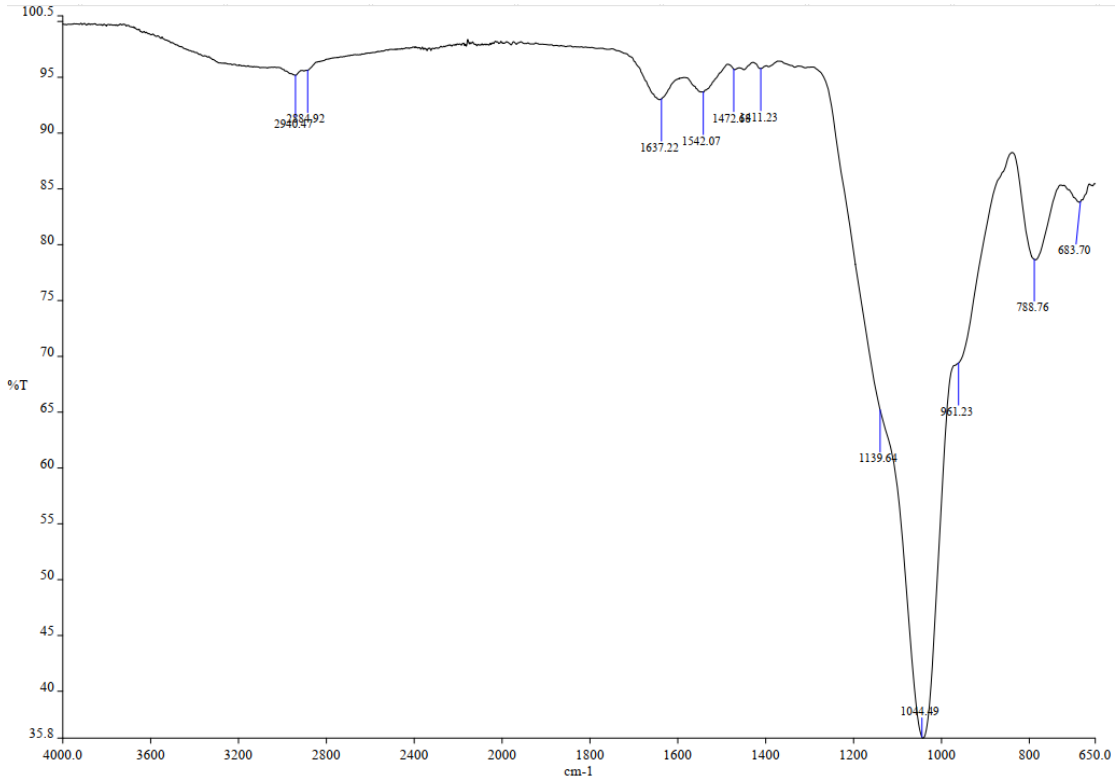

Fig.15: Gelatin cross-linked MSNs.

Note the slight peak at 1472.68 cm-1, corresponding to the aldimine linkage ($N=CH-(CH_2)_3-CH=N$) with gelatin chains, while lacking a strong peak 1244 cm-1, which corresponds to a strong C-O vibration, showing partial crosslinking

7.6 Drug loading

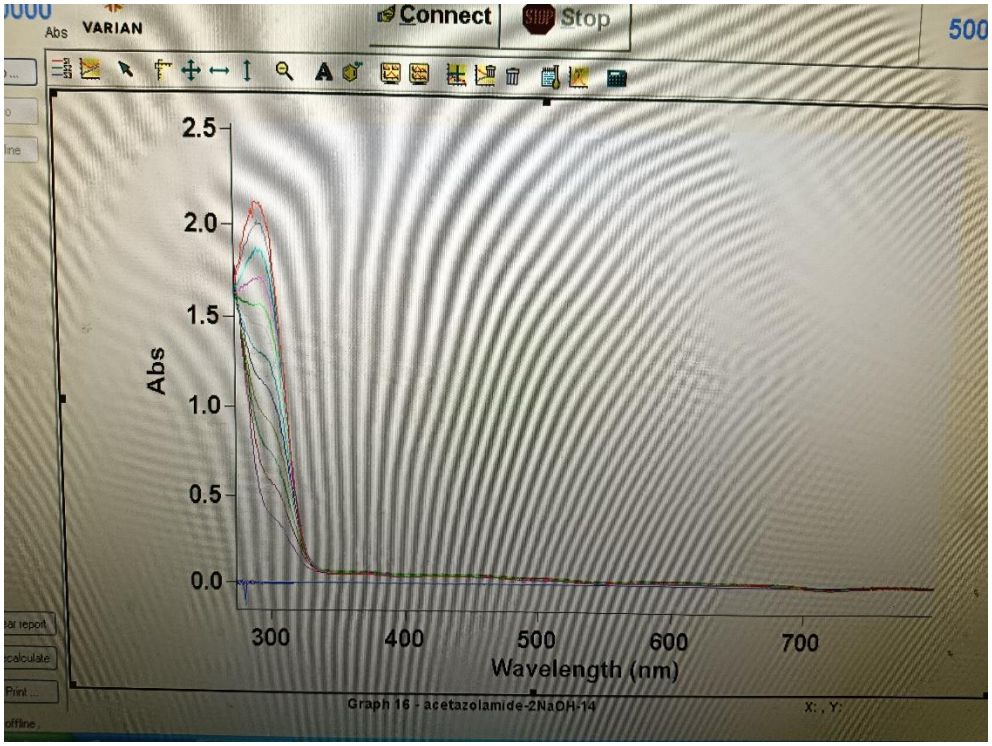

Fig.16: UV/Vis spectra for NaOH standards, the first half of the pH test.

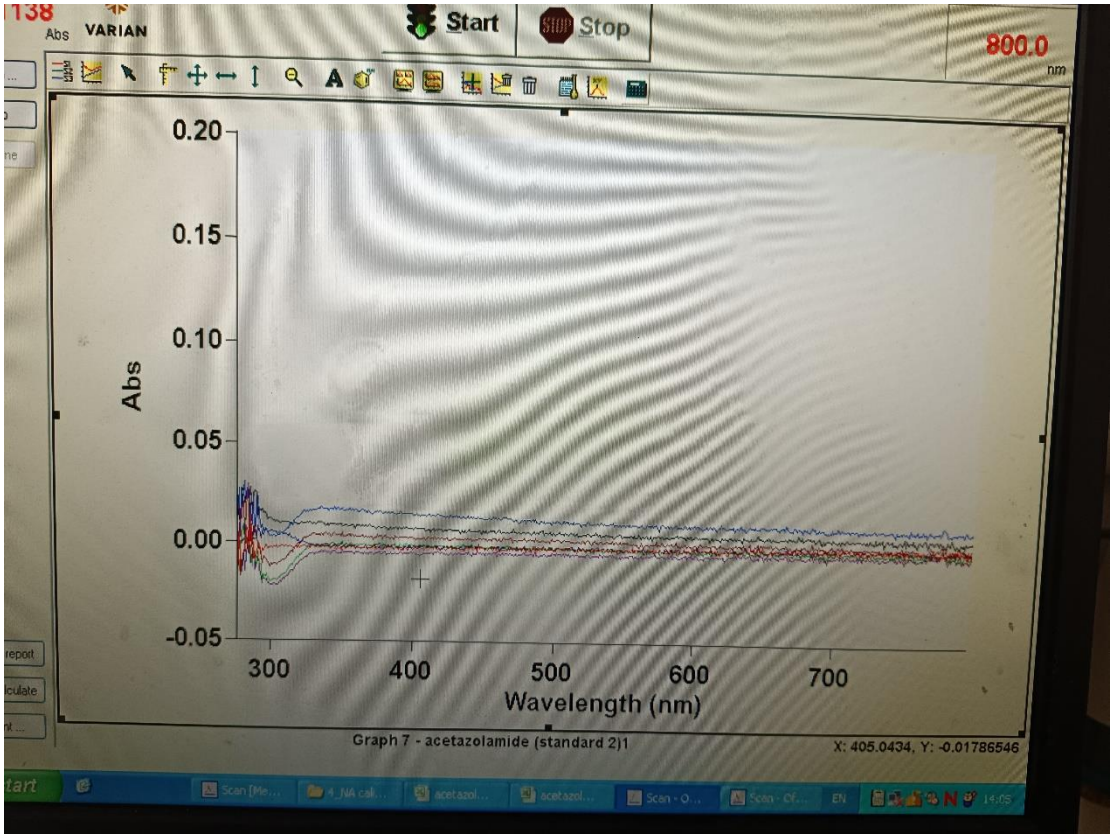

Fig.17: UV/Vis spectra for HCl standards, the second half of the pH test.

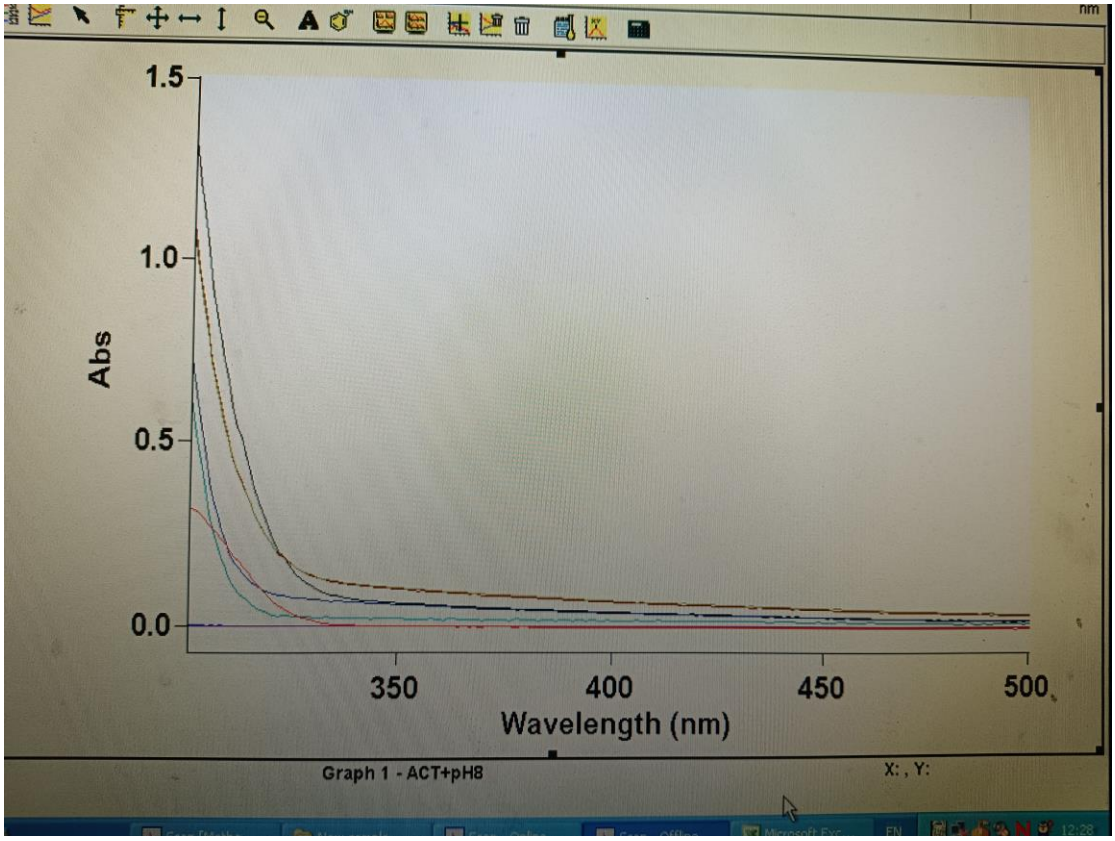

Fig.18: UV/Vis spectra of MSNs tested for interference

7.7 Release tests of hydrogels

Chitosan-based hydrogels

Table 44. Table of the time intervals, absorbance values, of the nicotinamide control experiment

Composition	Crosslinker (s)	Analyte	Time (min)	Absorbance @ 251 nm	Aliquot extracted (mL)	Dilution volume (mL)
Nicotinamide- (1 mg/mL) PBS (5 mL)	-	50 mg nicotinamide	2	-0.00598	0.5	5
			5	0.00133	0.5	5
			10	0.022239	0.5	5
			20	0.038255	0.5	5
			30	0.044376	0.5	5
			45	0.070402	0.5	5
			60	0.089209	0.5	5
			90	0.112695	0.5	5
			120	0.183321	0.5	5

			180	0.141162	0.5	5
			240	0.176102	0.5	5
			300	0.169363	0.5	5

Release calculations I:

Nicotinamide control release test

Nicotinamide in stock solution (50.0 mg/50 ml)

Nicotinamide used as analyte, 5 ml transferred to a dialysis tube

50.0 mg/50 ml (1 mg/ml) x 5 = 5 mg

Table 45. Table of the masses of nicotinamide per aliquot and corresponding percentage releases of the control experiment

PBS-Nicotinamide sample	Time (min)	Absorbance @ 251 nm	Weight in aliquot (mg)	% Release
S1	2	-0.00598	-0.1540	-3.08%
S2	5	0.00133	0.0343	0.69%
S3	10	0.022239	0.5727	11.45%
S4	20	0.038255	0.9852	19.70%
S5	30	0.044376	1.1428	22.86%
S6	45	0.070402	1.8131	36.26%
S7	60	0.089209	2.2974	45.95%
S8	90	0.112695	2.9023	58.05%
S9	120	0.183321	4.7211	94.42%
S10	180	0.141162	3.6354	72.71%
S11	240	0.176102	4.5352	90.70%
S12	300	0.169363	4.3617	87.23%

Absorbance at t = 60 min: 0.089209, equation y = 19.415x

0.089209/19.415 = x = 0.0046 mg/ml

Percentage release: (0.089209/19.415) x 500 = 2.2974

2.2974/5 x 100/1 = 45.95%

PF-127 based hydrogels

PF-10 (Abbreviation: PF = Pluronic F127)

Table 46. Table of the time intervals, absorbance values, and composition of the third PF-127-based hydrogel release test.

Composition	Crosslinker(s)	Analyte	Time (min)	Absorbance @ 223 nm	Aliquot extracted (mL)	Dilution volume (mL)
PF-127-saccharin hydrogel (500.9 mg PF-127. 40.0 mg hydroxypropyl cellulose, 2 mL saccharin)	Hydroxypropyl cellulose (40.0 mg)	5 mg saccharin	60	0.369031	0.5	5
			120	0.393735	0.5	5
			180	0.462904	0.5	5
			300	0.475297	0.5	5
			4320	0.655318	0.5	5

Release calculations II:

PF-10

Saccharin in stock solution (62.5 mg/ml)

Gel prepared using 2 ml of stock

Saccharin conc. in gel 62.5/25 mL x 2 = 5 mg, gel weight: 2053.2 mg

Gel used: 1831.4 mg

5 mg/2053.2 mg x 1831.4 mg = 4.46 mg of saccharin in gel

PF-11

Table 47. Table of the time intervals, absorbance values, system type and composition of the fourth PF-127-based hydrogel release test.

Composition	Crosslinker(s)	Analyte	Time (min)	Absorbance @ 223 nm	Aliquot extracted (mL)	Dilution volume (mL)
PF-127-saccharin hydrogel (500.3 mg PF-127. 20.5 mg hydroxypropyl	Hydroxypropyl cellulose (20.5 mg)	5 mg saccharin	30	0.122639	0.5	5
			60	0.171192	0.5	5
			90	0.266369	0.5	5
			120	0.370878	0.5	5

cellulose, 2 mL saccharin)			180	0.437199	0.5	5
			300	0.535247	0.5	5
			1350	0.63755	0.5	5

Release calculations III:

PF-11

Saccharin in stock solution (62.5 mg/ml)

Gel prepared using 2 ml of stock

Saccharin conc. in gel 62.5/25 mL x 2 = 5 mg, gel weight: 2189.6 mg

Gel used: 2073.0 mg

5 mg/2189.6 mg x 2073.0 mg = 4.73 mg saccharin in gel

PF-12

Table 48. Table of the time intervals, absorbance values, system type and composition of the fourth PF-127-based hydrogel release test.

Composition	Crosslinker(s)	Analyte	Time (min)	Absorbance @ 223 nm	Aliquot extracted (mL)	Dilution volume (mL)
PF-127-saccharin hydrogel (500.3 mg PF-127. 40.3 mg hydroxypropyl cellulose, 2 mL saccharin)	Hydroxypropyl cellulose (40.3 mg)	5 mg saccharin	30	0145261	0.5	5
			60	0.205637	0.5	5
			90	0.251564	0.5	5
			120	0.337029	0.5	5
			180	0.403601	0.5	5
			300	0.513416	0.5	5
			1350	0.546785	0.5	5

Release calculations IV:

PF-12

Saccharin in stock solution (62.5 mg/ml)

Gel prepared using 2 ml of stock

Saccharin conc. in gel 62.5/25 mL x 2 = 5 mg, gel weight: 2181.7 mg

Gel used: 1615.5 mg

5 mg/2181.7 mg x 1615.5 mg = 3.70 mg saccharin in gel

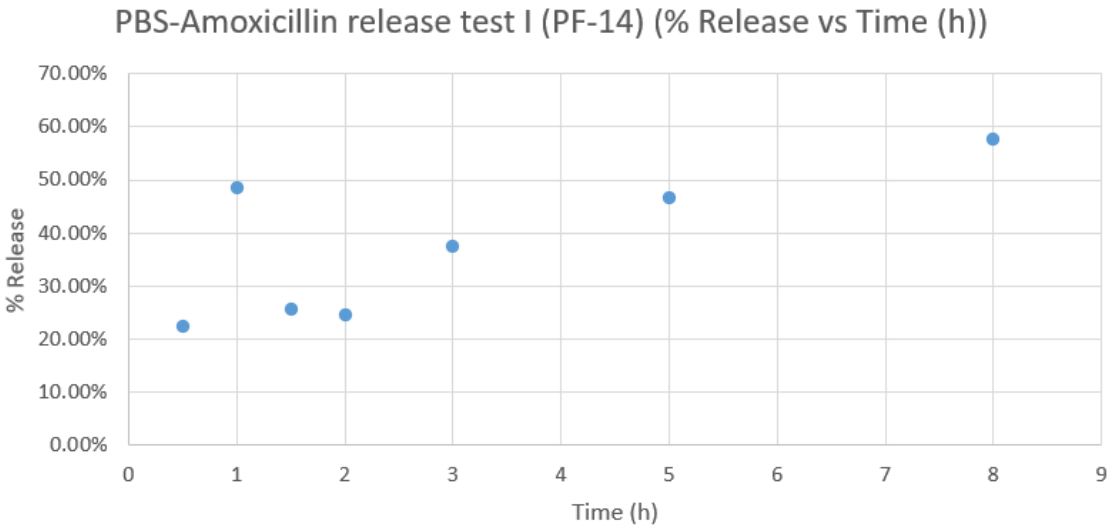

Fig.19: First release test of amoxicillin trihydrate out of PF-127-based hydrogel (500.4 mg of PF-127 & 20.2 mg hydroxypropyl cellulose (PF-14)

PF-14

Table 49. Table of the time intervals, absorbance values, system type and analyte of the fifth PF-127-based hydrogel release test.

Composition	Crosslinker(s)	Analyte	Time (min)	Absorbance @ 225 nm	Aliquot extracted (mL)	Dilution volume (mL)
PF-127-amoxicillin trihydrate hydrogel (500.4 mg PF-127. 20.2 mg hydroxypropyl cellulose, 2 mL amoxycillin trihydrate)	Hydroxypropyl cellulose (20.2 mg)	0.5024 mg amoxicillin trihydrate	30	0.09315	0.5	5
			60	0.170948	0.5	5
			90	0.102885	0.5	5
			120	0.099399	0.5	5
			180	0.138302	0.5	5
			300	0.165711	0.5	5
			480	0.197968	0.5	5

Release calculations V:

PF-14

Amoxicillin trihydrate in stock solution (62.8 mg/25 ml)

Gel prepared using 2 mL of stock

Amoxicillin trihydrate conc. in gel 62.8 mg/25 mL x 2 = 5.024 mg, gel weight: 2388.1 mg

Gel used: 2243.6 mg

5.024 mg/2388.1 mg x 2243.6 mg = 4.72 mg of amoxicillin trihydrate

Table 50. Table of the masses of amoxicillin trihydrate per aliquot and corresponding percentage releases of PF-14

Sample	Time (h)	Absorbance @ 225 nm	Weight of aliquot (mg)	% Release
S1	0.5	0.09315	1.126500796	22.42%
S2	1	0.170948	2.43945224	48.56%
S3	1.5	0.102885	1.290792709	25.69%
S4	2	0.099999	1.242087372	24.72%
S5	3	0.138302	1.88850475	37.59%
S6	5	0.165711	2.351070447	46.80%
S7	8	0.197968	2.895453011	57.63%

Absorbance at 1 h: 0.170948, equation y = 20.739x + 0.0264

0.170948-0.0264/20.739 = x = 0.0070 mg/ml

Percentage release: (0.170948-0.0264/20.739)*(350) = 1.1265 mg

1.1265/5.024 x 100/1 = 48.56%

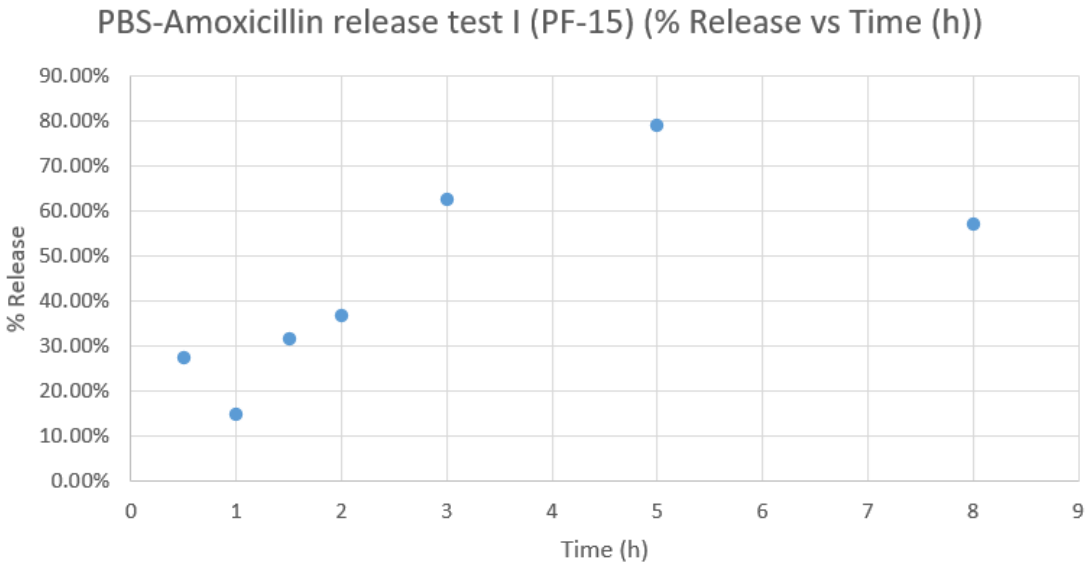

Fig.20: Second release test of amoxicillin trihydrate out of PF-127-based hydrogel (500.4 mg of PF-127 & 20.1 mg hydroxypropyl cellulose) (PF-15)

PF-15

Table 51. Table of the time intervals, absorbance values, system type and analyte of the sixth PF-127-based hydrogel release test.

Composition	Crosslinker(s)	Analyte	Time (min)	Absorbance @ 225 nm	Aliquot extracted (mL)	Dilution volume (mL)
PF-127-amoxicillin trihydrate hydrogel (500.4 mg PF-127. 20.1 mg hydroxypropyl cellulose, 2 mL amoxycillin trihydrate)	Hydroxypropyl cellulose (20.1 mg)	0.5024 mg amoxicillin trihydrate	30	0.108131	0.5	5
			60	0.071166	0.5	5
			90	0.120974	0.5	5
			120	0.13032	0.5	5
			180	0.212968	0.5	5
			300	0.261993	0.5	5
			480	0.196037	0.5	5

Release calculations VI:

PF-15

Amoxicillin trihydrate in stock solution (62.8 mg/25 ml)

Gel prepared using 2 mL of stock

Amoxicillin trihydrate conc. in gel 62.8 mg/25 mL x 2 = 5.024 mg, gel weight: 2089.3 mg

Gel used: 1817.4 mg

5.024 mg/2089.3 mg x 1817.4 mg = 4.37 mg of amoxicillin trihydrate

Table 52. Table of the masses of amoxicillin trihydrate per aliquot and corresponding percentage releases of PF-15

Sample	Time (h)	Absorbance @ 225 nm	Weight in aliquot (mg)	% Release
S1	0.5	0.108131	1.37932639	27.45%
S2	1	0.071166	0.755489657	15.04%

S3	1.5	0.120974	1.596070206	31.77%
S4	2	0.13632	1.855055692	36.92%
S5	3	0.212968	3.148599257	62.67%
S6	5	0.261993	3.975965572	79.14%
S7	8	0.196037	2.862864651	56.98%

Absorbance at 1 h: 0.07116, equation y = 20.739x + 0.0264

0.07116-0.0264/20.739 = x = 0.0022 mg/ml

Percentage release: (0.07116-0.0264/20.739) x 350 = 0.7554 mg

0.7554/5.024 x 100/1 = 15.04%